Megakaryocyte localization in the bone marrow depending on the knock-out of small Rho GTPases

• • •

Megakaryozytenlokalisation im Knochenmark in Abhängigkeit der Defizienz von kleinen Rho GTPasen

Aus dem Institut für experimentelle Biomedizin, Lehrstuhl I des Rudolf-Virchow-Zentrums und Universitätsklinikums Würzburg
Vorstand: Prof. Dr. rer. nat. Bernhard Nieswandt

Inaugural – Dissertation

zur Erlangung der Doktorwürde der

Medizinischen Fakultät

der

Julius-Maximilians-Universität Würzburg

vorgelegt von

Philipp Huber

aus Hof

Würzburg, Februar 2019

Mitglieder des *Promotionskomittees*

Referent: Univ-Prof. Dr. rer. nat. Bernhard Nieswandt

Korreferent: Priv.-Doz. Dr. Heike Hermanns

Berichterstatter: Univ.-Prof. Dr. rer. nat. Philip Tovote

Dekan: Prof. Dr. Matthias Frosch

Tag der mündlichen Prüfung: 04.03.2020

Der Promovend ist Arzt.

1. Introduction

1.1 Megakaryocyte development & maturation in the bone marrow and platelet production

Platelets are small, anucleate, discoid-shaped cell fragments, usually ranging from 1 to 3 µm in diameter and the essential cellular mediator of hemostasis. They are released into the circulation from the cytoplasm of megakaryocytes (MKs), their progenitors, which mature in the bone marrow (BM) and are produced from hematopoietic stem cells (HSCs). While MKs are the largest cells encountered in the BM by size (50-100 µm), they represent less than 1% of total nucleate cells within the BM[1]. A hallmark event in MK differentiation and maturation is endomitosis yielding polyploid MKs which is postulated to be necessary for the assembly of the large quantity of granules and organelles required in the later platelets.

For platelet formation, the cytoplasm of the MK is reorganized into long processes, designated proplatelets, and finally the multilobulated nucleus of the MK is extruded. MKs exhibit roughly 10-20 proplatelets which branch repeatedly and therefore allow the generation of estimated 10^3 platelets per MK[2]. Proplatelets protrude into the blood stream and via intermediate formation of preplatelets the mature platelet comes into existence.

The journey from the early MK to the final platelet can also be divided by time length. MK maturation and migration within the BM compartment takes several days, whereas the process of proplatelet formation and platelet shedding is completed within hours.

Given the experimental importance of murine models in hemato- and megakaryopoiesis it is important to note that platelet production takes approximately 5 days in humans, while rodents accomplish platelet production within 2-3 days. Platelet lifetime though is longer in humans with 7-10 days, whereas it does not surpass 4-5 days in rodents[3].

1.1.1 From the hematopoietic stem cell to the mature MK

Like all other hematopoietic cells, MKs develop from multipotent HSCs. MK and erythroid lineages are closely related, sharing a common progenitor the MK/erythroid-progenitor (ME-P)[4]. Differentiation from HSCs to MKs is mainly driven by thrombopoietin (TPO) and its corresponding MK receptor c-Mpl[5]. It was further shown that differentiation of the ME-P towards the erythroid or megakaryocytic lineage downstream of the TPO/Mpl axis is driven by the balanced antagonism of the transcription factors FLI1 toward megakaryopoiesis and KLF1 toward erythropoiesis[6]. Recent work, however, suggests that megakaryopoiesis can bypass the ME-P stage, when HSCs give rise to MK-progenitors directly(MK-P)[7]. In this context, the Bmi1/Runx1 axis is of notable interest, as Runx1 is responsible for the epigenetic inactivation of KLF1[8] and Runx1 activation leads to platelet-producing MKs from MK-Ps in vitro[9].

After successful lineage restriction, the MK precursor or promegakaryoblast initializes the synthesis of platelet proteins and also increases its ploidy by endomitosis. Usually a response to stress in other nucleated cells, polyploidy is regularly encountered in MKs with genomic content ranging from 2 to 64N with the modal being 16N. It has been speculated that polyploidy facilitates production of the huge quantities of mRNA and protein needed in platelets without mitotic and cytokinetic stress and helps increase cytoplasm volume more efficiently than in mitosis[10]. Theoretically, it also provides a salvage pathway in case of one-allelic mutation of a MK key gene[4].

Although many aspects of endomitosis remain unsolved, it is now believed that defects in late cytokinesis are responsible[3]. For mitosis, formation of a complete cleavage furrow is necessary, forming a contractile ring consisting of nonmuscle myosin (NM) IIA, NMIIB and F-actin, to effectively separate cells[11,12,13]. In MKs, both the required nonmuscle myosins IIA and IIB are expressed. A recent study from Roy et al. showed that basal RhoA/ROCK activity is required for NMIIB localization to the cleavage furrow[13] and that inhibition of RhoA lead to loss of the same, promoting polyploidization. In an earlier study on NMIIB, it was already found out that early occurrences of endomitosis (2N – 4N) rely on inactivation of the myosin heavy chain (MYH)10 gene-encoded NMIIB in the contractile ring by

Runx1[14], fostering Roy's results. The authors could also demonstrate that RhoA/ROCK signaling affects NMIIA/B localization most likely through increased actin turnover and somewhat independently of the classical RhoA/ROCK pathway revolving around myosin light chain (MLC) phosphorylation[13,15]. Additionally, RhoA activity-related proteins GEF-H1 and ECT2 were identified to play a role in endomitosis and polyploidization in a third study[16]. GEF-H1 needs to be downregulated during the first endomitotic event from 2N to 4N and ECT2 ever thereafter[17], probably signifying a close relationship to RhoA/ROCK and NMIIA/B signaling. These results might possibly constitute the molecular basis of findings in $RhoA^{-/-}$ mice of increased MK polyploidization, macrothrombocytopenia and impaired integrin $\alpha IIb\beta3$ outside-in signaling[18], as deficiency of NMIIA by MYH9 inactivation yielded comparable results. Firstly, decreased NMIIA function led to slower MK migration towards the vascular niche[19]. Moreover, MYH9 inactivation was accompanied by defective integrin $\alpha IIb\beta3$ outside-in signaling and impaired thrombus formation under flow and lastly, macrothrombocytopenia as a sign of defective megakaryopoiesis was also reported[20].

Maturation of MKs is also connected to their localization in the BM. MKs form in the endosteal niche[21,22] of the BM and migrate toward the vascular niche[23,24,25], where they release their platelets[2,26]. Therefore, MK migration and maturation is linked to one another. Attraction of MKs to the vascular niche is mediated by chemokines produced by surrounding endothelial and perivascular mesenchymal cells[27]. Of major importance in that journey is the cytokine CXCL12 or previously referred to as SDF-1. The corresponding MK receptor CXCR4 is increasingly expressed during maturation and administration/stabilization of CXCL12 leads to a higher percentage of MKs neighboring BM sinusoids[28]. By expression of high levels of CXCL12 and FGF-4, even TPO/Mpl axis-deficient MKs could be recruited to the vascular niche – VCAM-1 and VLA-4-mediated – and shed functional platelets[29]. Adult MKs become unresponsive to CXCL12, however, as overexpression of RGS16 attenuates CXCR4 function, hereby reducing retention forces and enabling egress of the MK from the BM[30,31]. It was also shown that the Wiskott-Aldrich syndrome protein (WASP) is a crucial player in actin

polymerization in hematopoietic cells. Lack of WASP leads to premature proplatelet formation as early as in the endosteal niche and the development of podosomes which hinder MK migration towards the BM sinus[32,33], although this migration concept has been contested by recent imaging studies[34].

Another purpose of endomitosis is the generation of the invaginated membrane system (IMS), or previously referred to as demarcation membrane system (DMS). It has been described as an extensive complex of tubules and cisternae permeating the cytoplasm of the MK and primarily functions as a membrane reservoir for proplatelet formation[3,35,36]. Invagination relies on actin-driven cytoskeletal remodeling via the WASP/WAVE pathway, downstream of PI-4,5-P$_2$ signaling[37]. Membrane cytoskeleton-bridging proteins like CIP4 are also crucial in formation of the IMS, as loss of CIP4 results in impaired plasma membrane stiffening and reduced proplatelet development, because of aberrant IMS formation[33,38,39]. A recent study was able to show that a 'pre-IMS' structure exists in immature MKs, thereby proposing a new model for IMS formation which starts with focal membrane assembly at one peripheral region of the MK, subsequent invagination and finally expansion through lipid transfer from both the golgi network and the endoplasmatic reticulum[40].

1.1.2 Proplatelet formation and platelet release

Mature MKs extend long branching protrusions called proplatelets through junctions in the lining of blood sinuses of the BM[3,41]. Only MKs which are able to form proplatelets have been shown to successfully produce platelets[42,43]. The process of proplatelet development starts with one membrane region of the MK to erode by giving rise to pseudopodial-like structures which begin to elongate, branch and taper. Branching is repetitive which helps create the great number of proplatelet tips required. In the proplatelet tip, a single microtubule forms a loop and reenters the proplatelet shaft. It will later constitute the microtubule coil defining the platelet size and its discoid shape[41]. Studies demonstrated that microtubules are the main force driving proplatelet elongation, as drugs effecting disrupting microtubule assembly, e.g. colchicine, vincristine or nocodazole prevent proplatelet synthesis[44]. Visualization of microtubule arrangements

4

throughout one MK life cycle showed significant remodeling. Immature MKs possess a microtubule arrangement in a starburst pattern with microtubules starting from centrosomes. When proplatelet formation begins, cortical microtubules are arranged into thick bundles parallel to the plasma membrane and later form an array lining the entire length of the proplatelet. Tapering takes place, as microtubule bundles are thick near the proplatelet shaft, whereas only 5-10 microtubules can be found near the proplatelet tip. Further visualization studies using EB3 – binding to the nucleating plus end of microtubules – found that proplatelet growth and microtubule assembly rates are not the same, indicating a certain amount of independency of one another, and that polymerization occurs in both directions, meaning bundles have mixed polarity[45,46,47]. Furthermore, the net plus end oriented motor protein kinesin which traffics organelles and cargo, was seen to change direction during its migration, supporting the notion of mixed microtubule polarity[41]. Additionally, when a certain degree of proplatelet formation has taken place, blockade of microtubule assembly does not attenuate proplatelet growth rates, proposing the parallel-oriented microtubules bundles possess a sliding mechanism by which they mediate elongation. The minus end-oriented motor protein dynein is hypothesized to facilitate that sliding, as disruption of its dynactin complex inhibits proplatelet elongation which can be recovered in permeabilized MKs by addition of excessive amounts of ATP[46]. Branching of proplatelet processes, with the proplatelet usually making a U-turn and the daughter proplatelet emerging from the vertex, was shown to be driven by the actin cytoskeleton, as inhibition with cytochalasin or latrunculin leads to a failure of proplatelets to bifurcate and branch[43].

Rho GTPases as general modifiers and effectors of actin-related cytoskeletal remodeling were shown to be closely connected to proplatelet formation. RhoA for example is hypothesized to regulate thrombopoiesis in late-stage MKs[48]. Knock-out of RhoA produced stiff membranes in the studied MKs and premature platelet clearance, suggesting involvement also in proplatelet formation, although no observable defect was perceived[49]. Other researchers addressed RhoA

through one of its effector kinases, PKCε. Downregulation of PKCε was accompanied by reduced proplatelet length in cultured murine MKs which was alleviated by RhoA inhibition[50]. Substantiating this report is a study which showed that constitutively active RhoA also decreases proplatelet length[51]. Juxtaposition of these findings illustrate that RhoA regulation is most likely complex and intricately regulated from both a temporal and spatial perspective[45].

A murine double knock-out of Rac1 and Cdc42, two major contributors in lamellipodia and filopodia development respectively, showed surprising findings and potential redundancy of these two Rho GTPases. Unlike previously believed, double deletion of these proteins had minor impact on actin dynamics, whereas microtubule formation was severely disrupted, including the marginal platelet microtubule coil, yielding morphologically altered proplatelets and larger platelets[52].

Research showed that MKs release a heterogeneous cytoplasm mix into the circulation, most abundantly proplatelet fractions which form dumbbell-like structures[3]. Recently added as an intermediary stage of platelet production was the preplatelet, an immature platelet with dimensions of 3-10 µm in diameter, probably either the reason of a still higher mRNA content, 'young (reticulated) platelet', or as the result of conditions with few and large platelets, i.e. macrothrombocytopenia[45]. Preplatelets were found to interconvert into aforementioned dumbbell proplatelets and finally convert to mature platelets through microtubule polymerization and subsequent abscission[53,54].

The lung has emerged as a potential organ for the terminal stages of platelet maturation, as an early study already found the platelet concentration in postpulmonary vessels to be higher than elsewhere in the circulation[55] and rat models displayed lower platelet counts after lung injury[56]. Interestingly and supporting this thesis is that infused MKs from fetal liver-cell and BM cultures predominantly localize to the lung where they release platelets within 2h[57].

1.2 The Rho family of small GTPases

The Rho family of small GTPases was discovered in the wake of the search for

Ras-like genes, as Ras had been found to be commonly mutated in human carcinomas[58] and was identified early on in this effort[59,60]. With additional discoveries made over time, five distinct subfamilies of the Ras-related small GTPase superfamily could be established: Ras – constituting its own subfamily –, Rho, Rab, Ran and Arf[61,62].

Regarding the Rho (sub)family, three members came into the spotlight, namely RhoA, Rac1 and Cdc42, because of their importance for the actin cytoskeleton and dynamical rearrangement processes[63,64]. It could further be shown that RhoA, Rac1 and Cdc42 also take part in signaling events concerning cell cycle entry and survival, as well as gene expression[61,64,65]. Not surprisingly, these 3 GTPases are among the most highly conserved across all eukaryotes, including plants and fungi as well[66]. Research conducted by Hall, Ridley and Nobes yielded landmark findings helping understand the roles of the aforementioned proteins[67]. The Rho GTPase Rac was shown to be the major contributor in lamellipodia formation[68], whereas Rho is necessary in the development of contractile actomyosin fibers or so-called stress fibers and focal adhesions[69]. Cdc42 in turn takes part in the formation of filopodia, as was found out in cell experiments[70].

As of recently, also other members within the Rho family – yet again comprising 8 subgroups with 20 proteins in total[71,72] – come into focus. Eight members were described as 'atypical' owing to their natural GTP-bound state, being the result of nucleotide exchange or amino-acid substitutions[73]. Most commonly, Rho GTPases cycle between an active GTP-bound and an inactive GDP-bound form. Guanine nucleotide exchange factors (GEFs), guanine nucleotide-dissociation inhibitors (GDIs) and GTPase-activating proteins (GAPs) are the main group of regulators in this setting[74,75,76]. Activity of atypical Rho GTPases, however, is modulated by protein stability, phosphorylation state and gene expression[77].

Anucleate platelets serve as a prototype of a minimal cell for the study of the actin cytoskeleton and microtubule system lacking compensation mechanisms at the DNA level[78,79]. Though there is mounting evidence that platelets possess an intact spliceosome, transcriptional factors working in a non-genomic way and miRNA indicative of complex post-translational processes which might be necessary to maintain the platelet proteome during its life time[80,81].

1.2.1 RhoA

RhoA is the most abundantly expressed isoform of the highly homologous Rho GTPase proteins RhoA, RhoB and RhoC in human platelets and the sole representative in murine platelets[16,82,83,84]. Studies showed that the clostridium botulinum C3 transferase leads to inactivation of Rho GTPases through ADP ribosylation which was used to gain insight into their function[85,86]. RhoA is activated by the α-subunits of G-protein coupled receptors (GPCRs) $G_{12/13}$ and G_q in platelets and mediates e.g. platelet shape change, spreading and clot retraction[18,79,87].

Due to the fact that platelet shape change occurs also in the absence of $G\alpha_q$, a $G\alpha_{13}$-Rho/Rho-kinase-dependent pathway via myosin light chain (MLC) phosphorylation was established[88].

Upon activation with thrombin, $G\alpha_{13}$ binds to p115RhoGEF which leads to nucleotide exchange from GDP to GTP in RhoA, hence activation of the GTPase[89]. The effector protein of RhoA is the Rho-associated protein kinase (ROCK) which drives MLC phosphorylation and is ultimately responsible for shape change and granule release[90,91,92,93]. After initial stages of platelet activation, the $G\alpha_{13}$ subunit associates with integrin $\alpha IIb\beta3$ which activates c-Src. c-Src then activates p190RhoGAP converting RhoA into a GDP-bound inactive state to allow for platelet spreading. By the time clot retraction occurs, platelet calcium signaling enhances Calpain protease activity which cleaves the cytosolic domain of integrin $\beta3$, resulting in promotion of the $G\alpha_{13}$-RhoGEF association and activation of RhoA another time for clot retraction[79,94,95]. These processes illustrate the complex spatiotemporal regulation of the GTPase.

Murine models deficient of RhoA exhibited that RhoA is indispensable for platelet adhesion under high shear conditions[82]. Regarding thrombosis and hemostasis, RhoA deficiency protects from arterial thrombus formation and ischemic stroke, whereas hemostasis is defective, as mouse tail-bleeding assays showed. A moderate aggregation defect downstream of both $G\alpha_{13}$ and $G\alpha_q$ was seen, too. Spreading was not found to be altered on fibrinogen – a substrate of integrin

$\alpha IIb\beta3$[18].

In the light of megakaryopoiesis, RhoA-deficient mice display macrothrombocytopenia which is accompanied by an in increase in BM MKs stipulating a need for RhoA in later stages of platelet production[18,19,51].

1.2.2 Rac1

First discovered as another substrate of the clostridial C3 enzyme[96], Rac has emerged as an important player in actin rearrangement processes. The Rac family with Rac1, Rac2, Rac3 and RhoG as members, based on homology analysis[97], was shown to drive lamellipodium and membrane-ruffle formation, as well as membrane extension in phagocytosis in nucleated cells[98]. Several Rac GEFs have been shown to mediate Rac activity, including TIAM1, β-PIX and DOCK180[66,99,100], although the most intensively studied Rac GEFs with regard to platelets are the Vav proteins and P-Rex1. Rac then interacts with its predominant effector proteins WAVE/Scar, formin protein mDia2 and PAKs which in turn activate actin-nucleating proteins, e.g. Arp2/3[66,101,102], or related regulators ,e.g. cortactin and cofilin[103,104]. Most interestingly, Rho/ROCK activation is believed to negatively inhibit lamellipodium formation, as RhoA inhibition leads to multiple and larger lamellipodia[105], demonstrating the need of a balanced activity of pro-migratory proteins and cellular adhesion mediating ones[66].

In platelets, only Rac1 is expressed in significant amounts[106]. Activation of Rac1 may occur analogous to Cdc42, i.e. by release of 14-3-3ζ from the GPIb-IX-V complex[107], when the GPIb receptor is activated by vWF[87]. Signaling through G_i coupled platelet receptors such as P2Y1 alone cannot activate Rac1 sufficiently, whereas their signaling is required for full activation[108,109]. In case platelet activation occurs through receptor GPVI or integrin $\alpha IIb\beta3$, Rac1 activation is mediated through the Src family kinase, SFK[106,110,111] and Rac1 then activates PLCγ2. Platelet activation through $G\alpha_q$ coupled GPCRs occurs via agonists ADP, thrombin and TxA2 and has been shown to activate PLCβ which also activates Rac1 [112]. As PLCs regulate calcium release through IP_3 and DAG, it becomes

visible that Rac1 modulates calcium-mediated signaling at different stages, finding itself up- and downstream of PLCs. Exemplary of this observation is that while PI3K activation is needed for Rac1 to become fully active, it is also a reported activator of PI3K at the same time[113].

In platelet function, Rac1 is required for lamellipodia formation which was learned from spreading experiments on fibrinogen-, vWF-, laminin- and collagen-coated surfaces[106,114]. Aggregation and platelet activation exhibited defects in the setting of collagen and CRP activation, too, strengthening the importance of Rac1 in the GPVI-ITAM-Src pathway of platelet activation[115]. Rac1-deficient mice also lack stable thrombus formation[106,115]. It is not clear, however, if this is due to defective lamellipodia formation or because of a lack of platelet activation and consecutive scarcity of secondary messengers with the latter explanation being substantiated by two works so far[115,116]. This supports a role for Rac1 in platelet granule release which is backed by studies on nucleated cells which exhibit secretion and exocytosis deficits, when Rac1 is absent[117,118].

Rac1-deficient mice do not exhibit thrombocytopenia, indicating potential dispensability of the GTPase in light of megakaryopoiesis and platelet biogenesis[115].

1.2.3 Cdc42

The third extensively studied Rho GTPase, Cdc42 was first described by researchers studying cell polarity in yeast[119,120]. While several small Rho GTPases, including RhoD, RhoF, RhoQ and RhoU have been characterized with regard to filopodia formation[58,72,121,122], Cdc42 probably remains the most important one in nucleated cells[70,123,124], as well as platelets[125,126]. Development of filopodia can also occur in settings void of Cdc42 which is then attributed to the small GTPase Rif or RhoF[127,128,129].

It might be possible that two distinct entities of filopodia exist[101], because cultured cells expressing Rif display long, thin and flexible filopodia[58,130], whereas those of Cdc42 are shorter and thicker, at the same time being restricted to the cell periphery[131].

Additional roles for Cdc42 have been outlined regarding secretion and

exocytosis[132,133], too. Cdc42 can be activated through soluble agonists, e.g. TRAP and ADP, by activation of PARs which leads to relocalization of the GTPase from the membrane to the cytosol[134,135]. Another activation pathway is through 14-3-3ζ which is released from the GPIb-IX-V complex upon exposure to vWF[107].

No specific GEFs for Cdc42 have been reported so far[79]. Vav proteins, although preferentially working through Rac1, also mediate Cdc42 activity[79]. Noteworthy effector proteins of the small GTPase include WASP and N-WASP which induce branching of actin via Arp2/3[136,137,138], however, this pathway was later proven redundant regarding overall filopodia formation ability[139]. Further well-established links between Cdc42 and actin rearrangement processes and dynamics are through effector proteins mDia2 and PAKs[140,141]. PAK in turn activates LIMK which phosphorylates cofilin and renders the protein inactive[72]. Contradicting this activation pattern are findings that Cdc42-deficient neurons also show increased cofilin phosphorylation which adds to the complexity of the Cdc42/cofilin relationship[142,143]. Further studies established additional effectors, e.g. IRSp53 to convey filopodia formation[144]. By now more than 70 Rho GAPs have been discovered – usually inactivating RhoGTPases – but few have been extensively characterized unfortunately[76]. Regarding Cdc42 and Rac1, IQGAP2, OPHN1 and Nadrin have been shown to regulate GTPase activity[145,146,147,148].

Study of Cdc42 in the light of platelet function generated mixed results, maybe due to differences in methodical approaches[125,126,149]. Generation of filopodia was diminished downstream of GPIb, but neither GPVI nor integrin αIIbβ3. Granule release was also upregulated in this study[149]. Another group found filopodia formation also to be impaired on fibrinogen and CRP, at the same time reporting reduced secretion in Cdc42-deficient platelets[125]. Due to these results, further studies seem warranted to clarify Cdc42 function in platelet activation.

With regard to MK maturation and HSC differentiation, Cdc42 is not dispensable, as deletion leads to defective differentiation and homing/lodging of MKs[150,151]. Cdc42 deficiency is even accompanied with a reduction of Rac1 activity[127,152], whereas upregulation of Cdc42 leads to faster migration in HSC/progenitor cells[153]. Apparently, Cdc42 positively influences Rac activity and therefore

lamellipodia formation[72]. Concerning MK development, early stages of MK development do not seem to rely on both Cdc42 and Rac1, as ploidy does not deviate from wild-type (wt) MKs, indicating endomitosis is not impaired[52]. However, at later stages when the focus shifts towards the ability of the MK to produce platelets, it was reported that proplatelet formation is diminished in Cdc42-deficient mice, as well as structural integrity of MKs is reduced[52]. This observation might explain in part, the reported macrothrombocytopenia found in an earlier study[149].

1.2.4 G protein coupled receptors G_{12} and G_{13}

The G_{12} and G_{13} receptor couple to heterotrimeric G proteins on their cytosolic end[154]. Both receptors are interaction partners of protease-activated receptors (PARs) upon stimulation. G_{12}-deficient mice are phenotypically normal. In case of G_{13}, its effect is mediated through the α-subunit of the G protein which regulates signaling in the RhoA/ROCK pathway by binding to RhoGEF and subsequent activation of the GTPase RhoA. Lack of G_{13}, but not G_{12} is accompanied by defective shape change and aggregation at low and intermediate concentrations of PAR4 receptor agonists like thrombin, U46 or TxA2. This effect can be overcome by use of high agonist concentrations yielding unaffected platelet shape change. Additionally, in double knock-out $G_{12/13}^{-/-}$ mice, there is no aggravation of the phenotype observed in G_{13}-deficient mice. At high levels, TxA2 and thrombin couple to G_q receptors which can also activate the RhoA/ROCK axis. On the other hand, elaborate platelet functions such as degranulation or aggregation requiring a higher degree of platelet activation cannot be mediated by activation of the G_{13} axis alone, as G_q-deficient platelets are impaired in these regards[79,154,155].

Signaling through both pathways ultimately leads to a net increase of myosin light chain (MLC) phosphorylation, yet through different mechanisms. G_{13} signaling works through the RhoA/ROCK axis and results in reduced MLC phosphatase activity by phosphorylation. G_q signaling on the other hand elevates intracellular Ca^{2+} levels fostering MLC kinase and hence MLC phosphorylation[155].

1.2.5 RhoF

A more recent addition to the small GTPase family was RhoF or Rif[101]. It is most closely related to RhoD within the family, but only shares low overall homology[156]. It is not ubiquitously expressed, unlike RhoA, Rac1 and Cdc42, but can be found in MKs and platelets[84,97,157] and has been shown to also drive filopodia formation[58,130]. High expression levels have also been found in malignant B-cell lymphoma and were hypothesized to promote malignant transformation[158].

To date, no specific GEFs, GAPs or GDIs for RhoF have been established, when compared to a list of the most prevalent aforementioned proteins, compiled by Goggs et al[101]. The same group is in the process of identifying potential interaction partners, but their observations have not been published yet. Regarding potential effector proteins of RhoF, observations confirmed interaction with mDia1, mDia2 and mDia3, proposing a function similar to those of RhoA (mDia1) and Rac1 and Cdc42 (mDia2, mDia3)[159].

Filopodia development triggered by RhoF lead to longer and thinner protrusions, than those produced by Cdc42, as mentioned before[131]. This might be due to the influence of mDia1 which is not known to activate Cdc42 and therefore might explain the discrepancy between the observed phenotypes[128,129]. Supporting its link to mDia1 activity is stress fibre formation – usually the domain of RhoA – in HeLa cells[160].

Generation of RhoF-deficient mice was helpful to assess potential effects of a knock-out of the GTPase in platelet function and consequently hemostasis and thrombosis[161]. Hematologic indices, activation patterns, integrin signaling and, most importantly, adhesion assays were unaltered though, in line with the redundant activation patterns of the so far established interaction partners, i.e. mDia proteins. It seems likely more effector pathways for RhoF exist, as mDia1-deficient mice were comparable to wt, especially regarding filopodia formation[162], indicating the differences in RhoF- and Cdc42-induced filopodia might be explained by other pathways than mDia1.

1.4 Platelet activation and signaling in thrombus formation

Platelets are the cellular mediators of hemostasis and essential in forming a primary plug at sites of vascular injury to prevent further blood loss of the organism[163]. Dysregulation of this intricate balance of pro- and anti-coagulant factors including platelets may result in arterial or venous thrombosis and can lead to cardiovascular diseases, e.g. myocardial infarction and stroke.

Upon contact with components of the extracellular matrix (ECM), platelet receptors GPIb-IX-V and GPVI are activated, leading to primary cellular responses which are upheld by subsequent signaling of GPCRs and autocrine self-activation by platelet-released pro-coagulatory molecules. These events lead to transformation of the fragile initial platelet plug to a firmly-adhered blood clot, allowing appropriate thrombus growth[87].

1.4.1 Overview of involved platelet receptors and signaling pathways

After binding of circulating von Willebrand factor (vWF) to the exposed ECM, platelet deceleration and tethering takes place by binding of platelet glycoprotein (GP) receptor GPIb-IX-V to the vWF multimers. These rolling platelets are able to interact with collagen via platelet receptor GPVI, initiating shape change from a discoid to a spherical shape and cellular activation. One part of the following intracellular events comprises the exocytosis of preformed cytoplasmic vesicles, so-called α- and dense granules which serve as potentiators of the platelet coagulant response and lead to the generation of thromboxane A2 (TxA2). With respect to α-granules, pro-coagulatory molecules vWF and fibrinogen are released which recruit additional platelets to the injured site, whereas in dense granules, e.g. ADP, ATP, TxA2 and serotonin can be found which are termed second wave mediators because of their autocrine signaling effects which further sustain platelet activation. These signaling pathways converge in transformation of platelet integrins from an inactive low-affinity to a functional high-affinity state securing firm adhesion of platelets to the ECM and platelet-platelet binding for a stable thrombus[87,90,155,163], see also Fig. 1.
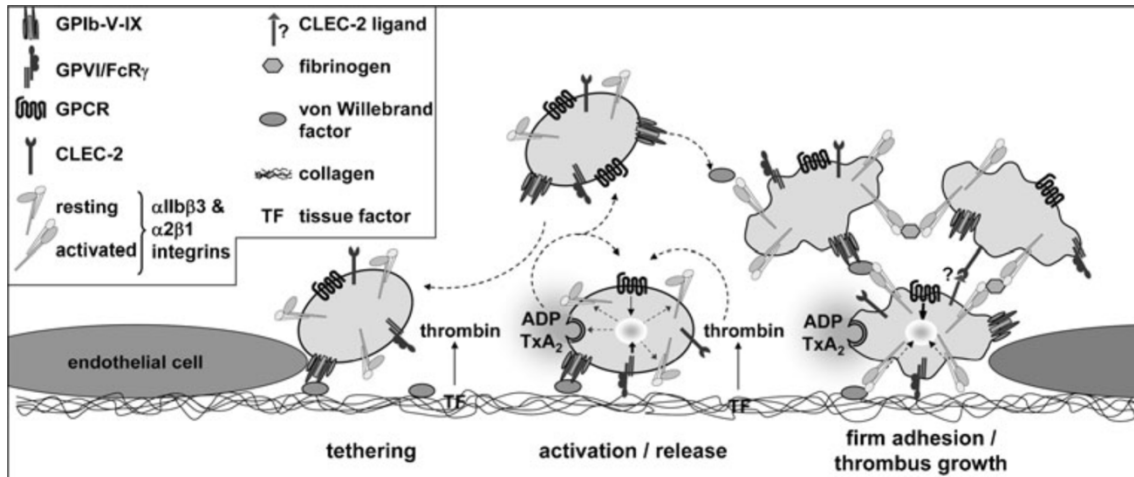
Fig. 1. Platelet activation model. Damage to the endothelial lining results in exposure of subendothelial ECM proteins with binding of vWF and exposure of collagen. Platelet tethering is then mediated by platelet vWF receptor GPIb which in turn allows binding of the platelet GPVI receptor to collagen, effectuating platelet activation, exocytosis of stored granule content, thromboxane A_2 generation and integrin transformation. Likewise exposed tissue factor initiates the plasmatic coagulation cascade resulting in thrombin generation, additionally serving as a strong platelet activator. Finally, integrins $\alpha2\beta1$ and $\alpha IIb\beta3$ secure the platelet plug at the injured site and allow for thrombus growth by interconnecting platelets. Taken from Stegner et al.[87].

Two major activation pathways in platelets exist: one involves signaling through platelet GPCRs with ADP, thrombin and TxA_2 as agonists, while the other is based on tyrosine phosphorylation of respective receptors GPVI or C-type lectin receptor 2 (Clec-2) via the associated immunoreceptor tyrosine activation motif (ITAM) or (hem)ITAM[87].

Soluble agonists activate either G_q proteins and hence PLCβ, yielding inositol-1.4.5-triphosphate (IP_3) and diacylglycerol (DAG)[112] which helps elevate intracellular calcium levels required for full platelet activation and granule release or $G_{12/13}$ proteins which signal through the RhoA/ROCK axis, leading to platelet shape change[89].

1.4.2 The role of platelet receptor GPIb-IX-V in hemostasis and thrombosis

Platelets rapidly decelerate upon exposure and binding of vWF to their GPIb-IX-V receptor complex, enabling a first contact with the ECM which is mandatory for any further platelet activation to occur[164,165].

Recent models suggest that additionally, a high shear force-driven GPIb

activation pathway, e.g. in stenosed arteries exists[166,167], but not contradicting the GPIb-mediated adhesion model.

GPIb signaling in general leads to downstream activation of 14-3-3ζ which induces mainly PI3K- and Src-related signaling and PLCγ[163] activity, leading to mild direct activation of the main platelet integrin αIIbβ3[87], see also Fig. 2. However, amplification pathways through TxA_2, ADP and PLD are further initiated[163]. Most interestingly, mice deficient of PLD isoform D1 displayed an activation defect on vWF at high shear rates, but not in tail bleeding assays, making it an interesting antithrombotic target [168]. Furthermore, mouse models deficient of either the GPIbα or GPIbβ subunit reproduced a congenital bleeding disorder seen in humans named Bernard-Soulier syndrome, suggesting an essential role for the receptor in thrombus formation[169,170]. At the same time, blockade of GPIbα has been proposed as an antithrombotic target, as skin bleeding time in baboons was not significantly prolonged[171] and mice were profoundly protected from secondary infarct growth in a stroke model[172,173].

1.4.3 The role of platelet receptor GPVI in hemostasis and thrombosis

The collagen receptor GPVI contains an ITAM domain, itself bearing Fc receptor (FcR)γ-chain dimers and is exclusive to MKs and platelets[174]. Once activated, Src family kinases (SFK) mediate further phosphorylation with the help of adaptor proteins linker of activated T-cells (LAT) and SLP-76, leading to calcium elevation, integrin activation and granule release via PLCγ2 and PI3K pathways[174,175], see also Fig. 2. GPVI is responsible to mediate firm adhesion to ECM components, but requires the help of integrins αIIbβ3 and α2β1 which undergo a conformational change upon GPVI-induced signaling[176], resulting in stable and shear-independent adhesion. Studies using GPVI/FcRγ-chain-depleted mice showed marked protection from arterial thrombosis in ischemic stroke models[172,177,178]. Moreover, a knock-out model of integrin α2β1 alone did not find observable defects in hemostasis, whereas combined integrin α2β1 and GPVI deficiency resulted in drastically impaired hemostatic function[179,180].
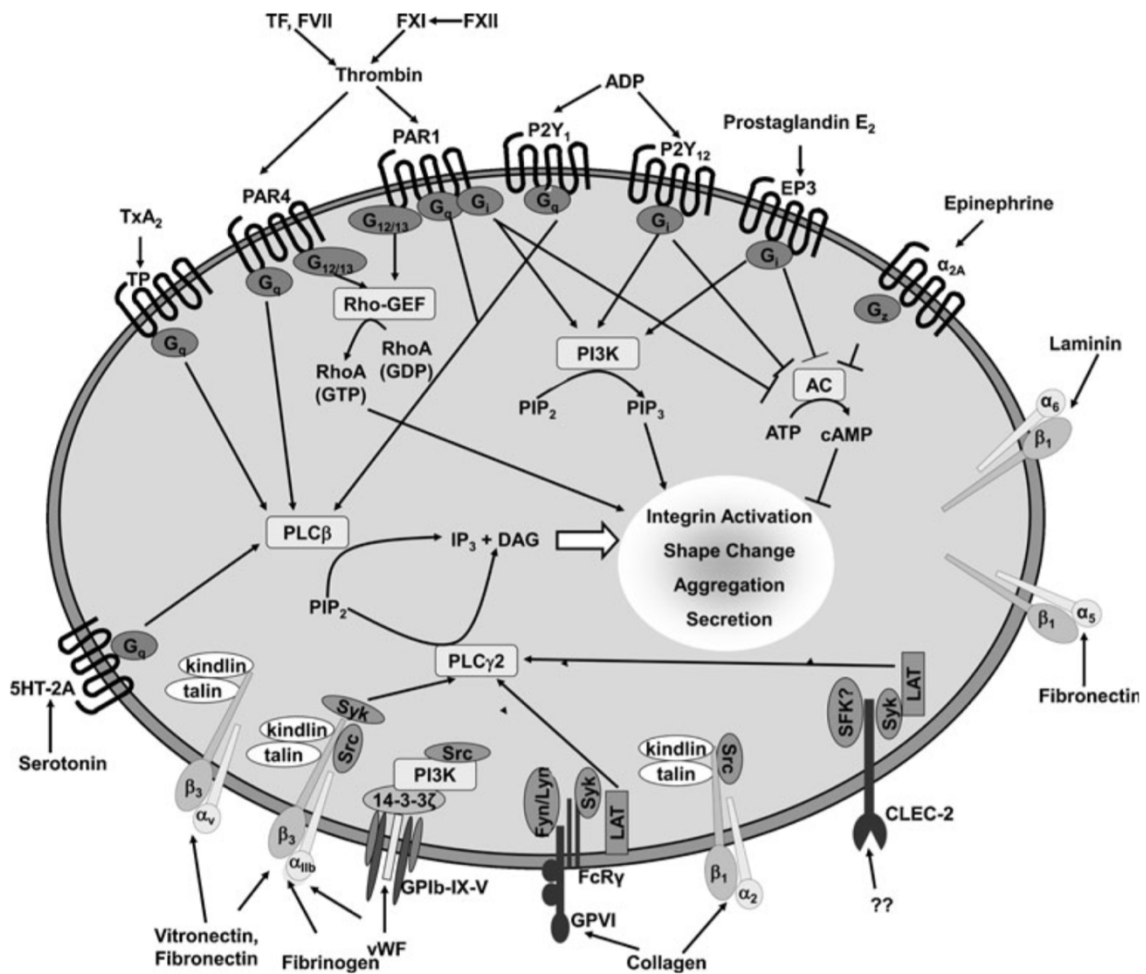
Fig. 2. Overview of platelet receptors and major signaling pathways. Soluble agonists and ECM components couple to a multitude of platelet receptors which are linked on their cytoplasmic ends to either G-proteins or ITAM or (hem)ITAM domains. Downstream, phospholipase signaling and small molecules lead to increases in intracellular calcium levels for farther platelet activation or directly influence the platelet cytoskeleton to induce shape change, aggregation, secretion and integrin activation. Phospholipase (PL) Cγ2 and β. TF tissue factor, TxA2 thromboxane A2, TP TxA2 receptor, PAR protease-activated receptor, RhoGEF Rho-specific guanine nucleotide exchange factor, PI3K phosphoinositide-3- kinase, AC adenylyl cyclase, PIP2 phosphatidylinositol-4,5- bisphosphate, PIP3 phosphatidylinositol-3,4,5- trisphosphate, IP3 inositol-1,4,5-trisphosphate, DAG diacylglycerol. Taken from Stegner et al.[87].

1.4.4 Platelet receptor Clec-2 and GPCRs in hemostasis and thrombosis

Similarly functioning receptor Clec-2 was a more recent addition to the canon of platelet receptors. Originally discovered as a receptor for the snake venom rhodocytin[181], the endogenous ligand remains unknown, although shown to be present on activated platelets[182]. Observations of both antibody-treated and Clec-2 knock-out mice showed reduced thrombus formation in arterial and venous

models, indicative of its involvement and importance in hemostatic processes. So far, it is known that regulation and inhibition of Clec-2 signaling is subject to immunoreceptor tyrosine-based inhibition motif (ITIM) bearing receptors such as PECAM-1 or G6b-B, but their role in hemostasis and thrombosis remains poorly understood up to now[87,183,184].

GPCR-mediated signaling is the other main pillar of platelet activation. Most notable receptors in this regard are $P2Y_1$ and $P2Y_{12}$ which are activated by ADP and signal through G_q and $G_{i2/3}$ respectively[185]. Main effect of their signaling is intracellular calcium release which is in turn required for shape change and aggregation [186]. $P2Y_1$ knock-out leads to ubiquitous response defects upon activation with all major platelet agonists and to increased bleeding times in vivo[187]. Another receptor in this context is $P2X_1$ which is an ATP-gated cation channel, guiding mainly calcium into the platelet, thereby also facilitating calcium-dependent shape change. Deficiency of $P2X_1$ results in partial protection against thromboembolism, whereas overexpression promotes thromboembolism[188,189].

TxA_2 is a so-called second wave mediator, being released from dense granules[190] and activates thromboxane-prostanoid (TP) receptors TPα and TPβ[87]. Both receptors are coupled to $G_{12/13}$ and G_q, but signaling is considerably weaker than through thrombin receptors which share the same effector pathway[155]. This is also illustrated by the limited activation potential of the TxA_2 analogue U46619 (U46) itself and mainly enhances effects of other agonists[163]. Patients with mutated TP receptors exhibit a mild bleeding phenotype[32] which is mirrored in mouse TP receptor knock-out studies[191].

The most potent soluble platelet activator, however, is thrombin, a serine protease which is the final end point of both the plasmatic extrinsic and intrinsic coagulation pathway and next to platelet activation also converts fibrinogen into fibrin[87]. Isoform expression of thrombin receptors varies among mammals with humans expressing protease-activated receptor (PAR)1 and PAR4, whereas mice express PAR3 and PAR4. In both species, studies revealed that PAR1/3 function as a co-activator of PAR4 which is usually activated only by high concentrations of thrombin[192,193,194,195]. Deficiency of PAR4 abolished thrombin

signaling in platelets and protects mice from thrombosis, at the cost of increased bleeding propensity[196,197].

1.4.5 Downstream signaling, autocrine self-activation and final stages of activation

Activation pathways in platelets are numerous and comprise a vast variety of kinases, nucleotides and effector proteins. Among them, PI3K, cAMP, cGMP, MAPK and PLA_2 are comprehensively described in the literature[198,199,200]. Ultimately, platelet activation and signaling leads to an increase of intracellular calcium which is the prerequisite to many subsequent events[87]. As this work will later focus on attachment of platelets and spreading on immobilized surfaces, platelet glycoprotein and integrin signaling will be discussed in more detail.

Four isoforms of type I phosphoinositide 3-kinases (PI3K) exist, i.e. $p110\alpha$, $p110\beta$, $p110\delta$ and $p110\gamma$[198]. $p110\beta$ and $p110\gamma$ appear as promising antithrombotic targets, as their deficiency is not paired with a bleeding propensity[201,202]. Deletion of the catalytic p85 subunit leads to a combined reduction of expression levels of $p110\alpha$, $p110\beta$ and $p110\gamma$ at the same time which makes it a useful tool to investigate the overall function of PI3Ks[198]. Despite being responsive to basically all common platelet activators, p85-deficient platelets are defective in platelet aggregation, spreading and in response to collagen, establishing PI3Ks as effector molecules in GPVI signaling. Furthermore $p110\delta$ deficiency studies showed impaired lamellipodia formation on CRP and collagen suggesting their involvement in cytoskeleton processes as well[203,204].

Cyclic nucleotides (cAMP, cGMP) on the other hand have been shown to negatively regulate platelet activation. Platelet antagonists like PGE_1 or PGI_2 couple to stimulatory G proteins on the platelet membrane and sustain adenylyl and guanylyl cyclase function, thereby increasing available cAMP and cGMP levels leading to stabilization of the actin cytoskeleton and inhibition of the fibrinogen receptor activation. cAMP and cGMP effectors include mainly their respective protein kinases cAMP-PK and cGMP-PK[200]. Vasodilator-activated phosphoprotein (VASP) finds itself downstream of both cAMP-PK and cGMP-PK.

Its phosphorylation goes in hand with diminished actin polymerization and inhibition of the fibrinogen receptor αIIbβ3[205,206]. Phosphorylation of ABP, a downstream protein of cGMP has also been linked to impaired fibrinogen binding in a ADP-induced setting of activation[207] and increased cytoskeletal stability[208]. Additionally, phosphorylation of GPIb of the GPIb-IX-V complex by PGE$_1$ was accompanied with reduced collagen-mediated actin polymerization[209]. Together these studies illustrate how rises in cAMP and cGMP levels negatively influence platelet adherence or spreading upon contact with components of the ECM like fibrinogen or vWF.

Also at the level of transcription factors, signaling through collagen and vWF receptors GPVI and GPIb can be impaired as deficiency of GATA1 shows[32,210].

Integrin adhesion receptors or integrins mediate shear-resistant and sustained adhesion to the ECM and various isoforms are expressed in platelets. Integrins are heterodimers composed of a transmembranous α- and β-chain respectively. Three β1-isoforms can be found in platelets with α5β1 constituting a fibronectin receptor, α6β1 a laminin receptor and α2β1 a collagen receptor[87]. β1-isoforms are believed to play only a supportive role in platelet adhesion, as knock-out models of integrin α2β1 failed to exhibit major hemostatic deficiencies[179,211,212]. This is most likely due to the fact that the most abundant platelet integrin αIIbβ3 is compensating for the loss, enabling the platelet to attach to the ECM also under high shear stress[212]. The other β3-isoform is integrin αVβ3, binding partner of fibronectin, osteopontin and vitronectin. Low expression levels, however, precluded it from extensive scientific interest which is why its function is not well characterized[87]. On the other hand, αIIbβ3 has always been in the focus of platelet research. Lack of integrin αIIbβ3 in humans leads to Glanzmann thrombasthenia, exhibiting severe activation defects upon stimulation with major agonists and resulting in mucocutaneous bleeding[213]. In mouse models, similar results can be gained by deletion of the αIIb- or β3-subunit with absence of platelet aggregation, lack of thrombus formation and even spontaneous bleeding[87]. Integrin αIIbβ3 has several ligands, the most important being fibrinogen by bridging platelets to one another in the developing clot. Its protease-

cleaved form fibrin secures the clot at the site of the vascular injury. Fibrinogen deficiency analogously leads to spontaneous bleeding and a failure of platelets to aggregate[214]. Certain mutations of integrin $\alpha IIb\beta 3$ involving Arg995 and Asp723 of the respective subunits were shown to correlate with an increased activation state of the integrin resulting in down-regulation of RhoA and impaired megakaryopoiesis[215].

The multimer vWF is an additional ligand of integrin $\alpha IIb\beta 3$ and required for platelet bridges at high shear rates[216]. Another interaction partner is CD40 ligand whose role has been addressed in knock-out studies. Lack of CD40 ligand is accompanied with impaired integrin $\alpha IIb\beta 3$ outside-in signaling in arterial flow and therefore high shear settings. Once integration of the thrombus is mediated by integrin $\alpha IIb\beta 3$, other proteins, including ephrin kinases, Gas6 and ESAM take over and affect thrombus stability[217].

Upon activation, integrins undergo conformational changes from a low- to a high-affinity state which coined the term inside-out signaling in platelet research. This remodeling is necessary for integrins to bind to their ligands and mediate their effects. As soon as ligands have bound, integrins activate cellular response pathways which was in turn named outside-in signaling[218].

Important interaction partners of integrins comprise talin1 and kindlin3. Actin-binding protein talin1 associates with Rap1-interacting adaptor molecule (RIAM)[219] to mediate its effect on integrin $\alpha IIb\beta 3$. Studies on knock-out mice lacking talin1 found abrogation of inside-out integrin activation, spreading defects on fibrinogen – substantiating also impaired outside-in signaling – and total insufficiency of primary hemostasis in vivo[220,221]. Talin1 relies on phospholipid PIP_2[222] for integrin binding which might be the link to how PLD1 modulates integrin activity, as it enhances PIP_2 concentrations through respective kinases.

Kindlin3, sometimes termed Fermt3, also influences integrin β-chain activity, as deficiency of the integrin adaptor molecule mimics the above described phenotype of talin1-deficient mice and talin1 cannot operate alone in integrin activation, either, indicative of the existence of other regulators like kindlin3[223]. Recently, mutations of kindlin3 were first observed in humans[224,225] with patients suffering from recurrent clinical bleeding, hence exhibiting features already seen

in kindlin3-deficient mice[226].

1.5 Aim of the study

With the establishment of MK and platelet-specific knock-out mouse models for the small Rho GTPases RhoA, Rac1 and Cdc42 insight into their function in platelet biology could be gained. RhoA and Cdc42 deficiency were shown to be accompanied by defects and alterations in granule secretion, as well as more and less pronounced macrothrombocytopenia respectively. With regard to Cdc42 deficiency, impaired filopodia formation downstream of GPIb signaling was observed, too[18,149].

This study wants to address the functions of predominantly RhoA and Cdc42 in megakaryopoiesis and involved signaling pathways in formation, maturation and migration of MKs in the BM to supplement our understanding of these GTPases in the field of platelet and MK biology.

Therefore, appropriate knock-outs and double knock-outs of RhoA and Cdc42 were generated and studied with respect to MK numbers in the BM, as well as their localization. In a second step, pathways potentially involved in migration and MK localization in the bone marrow of RhoA knock-out mice were examined by antibody treatment of mice.

A smaller part of this work is directed at a more recent addition to the small GTPase family, namely RhoF and its role in filopodia formation. RhoF, next to Cdc42 has been hypothesized to play a role in filopodia development and for this reason a MK and platelet-specific knock-out mouse was generated in order to study the effects of RhoF loss in the setting of platelet activation, degranulation and most importantly spreading on immobilized surfaces downstream of GPIb and fibrinogen signaling[129,160,161].

2. Materials and Methods

2.1 Materials

2.1.1 Chemicals and reagents

acetic acid	Roth (Karlsruhe, Germany)
ADP	Sigma (Schnelldorf, Germany)
agarose	Roth (Karlsruhe, Germany)
agarose, low melting	Euromedex (Souffelweyersheim, France)
ammonium peroxodisulfate (APS)	Roth (Karlsruhe, Germany)
apyrase (grade III)	Sigma (Schnelldorf, Germany)
Aquatex	Merck (Darmstadt, Germany)
bovine serum albumin (BSA)	AppliChem (Darmstadt, Germany)
calcium chloride	Roth (Karlsruhe, Germany)
Complete mini protease inhibitors (+EDTA)	Roche Diagnostics (Mannheim, Germany)
convulxin	Alexis Biochemicals (San Diego, USA)
dNTP mix	Fermentas (St. Leon-Rot, Germany)
EDTA	AppliChem (Darmstadt, Germany)
eosin	Roth (Karlsruhe, Germany)
epinephrine	Sigma (Schnelldorf, Germany)
ethanol	Roth (Karlsruhe, Germany)
Eukitt mounting medium	Sigma (Schnelldorf, Germany)
fluorescein-isothiocyanate (FITC)	Molecular Probes (Oregon, USA)
Forene® (isoflurane)	Abott (Wiesbaden, Germany)

Fura-2 acetoxymethyl ester (AM)	Molecular Probes (Oregon, USA)
gelatine capsules	Agar scientific (Stansted, England)
GeneRuler 1kb DNA Ladder	Fermentas (St. Leon-Rot, Germany)
glucose	Roth (Karlsruhe, Germany)
hematoxylin	Sigma (Schnelldorf, Germany)
HEPES	Roth (Karlsruhe, Germany)
high molecular weight heparin	Sigma (Schnelldorf, Germany)
human fibrinogen	Sigma (Schnelldorf, Germany)
human vWF	CSL Behring (Hattersheim, Germany)
igepal CA-630	Sigma (Schnelldorf, Germany)
integrilin	GlaxoSmithKline (Germany)
isopropanol	Roth (Karlsruhe, Germany)
6x Loading Dye Solution	Fermentas (St. Leon-Rot, Germany)
magnesium chloride	Roth (Karlsruhe, Germany)
paraformaldehyde	Roth (Karlsruhe, Germany)
phenol/chloroform/isoamylalcohol	AppliChem (Darmstadt, Germany)
potassium acetate	Roth (Karlsruhe, Germany)
prostacyclin	Calbiochem (Bad Soden, Germany)
R-phycoerythrin (PE)	EUROPA (Cambridge, UK)
Rotiphorese Gel 30 (PAA)	Roth (Karlsruhe, Germany)
sodium azide	Roth (Karlsruhe, Germany)
sodium chloride	AppliChem (Darmstadt, Germany)
sodium cacodylate	Roth (Karlsruhe, Germany)
tannic acid	Merck (Darmstadt, Germany)
Taq polymerase	Fermentas (St. Leon-Rot, Germany)

Taq polymerase buffer (10x)	Fermentas (St. Leon-Rot, Germany)
TEMED	Roth (Karlsruhe, Germany)
3,3,5,5-tetramethylbenzidine (TMB)	EUROPA (Cambridge, UK)
thrombin	Roche Diagnostics (Mannheim, Germany)
U-46619	Alexis Biochemicals (San Diego, USA)

Botrocetin was procured from Francoi Lanza (EFS Alsace, Strasbourg, France). S.P. Watson (University of Birmingham, UK) generously provided collagen-related peptide (CRP). Rhodocytin was kindly donated by Johannes Eble (University Hospital Frankfurt, Germany). All other non-listed chemicals were obtained from either AppliChem (Darmstadt, Germany), Sigma (Schnelldorf, Germany) or Roth (Karlsruhe, Germany).

2.1.2 Kits

PCR

PCR Extender System	5 PRIME (Hamburg, Germany)
GeneAmp XL PCR Kit	Applied Biosystems (New Jersey, US)
Triple Master PCR System	Eppendorf (Hamburg, Germany

Immunohistochemistry

Peroxidase Labeling Kit	Roche (Mannheim, Germany)

2.1.3 Antibodies

Polyclonal and monoclonal antibodies that were used in this thesis can be found in the following subsections.

2.1.3.1 Purchased primary and secondary antibodies

rabbit anti-human vWF antibody	DAKO (Hamburg, Germany)
anti-integrin β1chain (CD29) 9EG7	BD Pharmingen
rat anti-mouse GPIbα antibody	Emfret Analytics (Wuerzburg, Germany)
rat anti-mouse IgG-HRP	DAKO (Hamburg, Germany)

2.1.3.2 In-lab generated and modified monoclonal antibodies

antibody name	clone	isotype	antigen	description
JAQ1	98A3	IgG2a	GPVI	[227]
DOM1	89F12	IgG2a	GPV	[228]
DOM2	89H11	IgG1	GPV	[228]
JON/A	4H5	IgG2b	GPIIb/IIIa	[229]
LEN1	12C6	IgG2b	α2 integrin	[230]
WUG1.9	5C8	IgG1	P-Selectin	unpublished
ULF1	97H1	IgG2a	CD9	unpublished
p0p4	15E2	IgG2b	GPIbα	[228]
p0p6	56F8	IgG2b	GPIX	[168]
JON6	14A3	IgG2b	α2bβ3 integrin	unpublished
INU1	11E9	IgG1	Clec-2	[182]
p0p5	13G12	IgG1	GPIbα	[228]
p0p3	7A9	IgG2a	GPIbα	[231]

2.1.4 Buffers and solutions

Buffers were prepared and diluted according to protocol using aqua ad iniectabilia (DeltaSelect Pfullingen, Germany) or deionized water obtained from a MilliQ Water Purification System (Millipore, Schwalbach, Germany). pH adjustment was

performed with HCl or NaOH.

Acid-citrate-dextrose (ACD) buffer, pH 4.5

citric acid anhydrous	65 mM
glucose anhydrous	110 mM
trisodium citrate dehydrate	85 mM

Blocking solution for immunohistochemistry

BSA	3%
rat serum	0,3%
TBS-T	

Decalcification buffer

EDTA	10%
PBS	

FACS buffer

BSA	0,1%
NaN_3	0,02%
PBS	

Lysis buffer for DNA sampling from mouse tissue

EDTA (0,5 M)	5 mM
NaCl	200 mM
SDS	0,2%
TRIS base	100 mM
add Proteinase K (20 mg/ml)	100 µg/ml

Phosphate buffered saline (PBS), pH 7.14

KCl	2,7 mM
KH_2PO_4	1,5 mM
NaCl	137 mM

$Na_2HPO_4 \times 2H_2O$	8 mM

Tris-buffered saline (TBS), pH 7.3

NaCl	137 mM
TRIS/HCl	20 mM

TE buffer, pH 8

EDTA	1 mM
TRIS base	10 mM

Tyrode's buffer, pH 7.3

BSA	0,35%
$CaCl_2$	1 mM
glucose	0,1%
HEPES	5 mM
KCl	2.7 mM
$MgCl_2$	1 mM
NaCl	137 mM
$NaHCO_3$	12 mM
NaH_2PO_4	0.34 mM

2.2 Methods

2.2.1 Creation of ko and dko mouse strains

All knock-out (ko) and double-knock-out (dko) mouse strains studied in this thesis, i.e. RhoA, RhoA/Cdc42, $G_{12/13}$ and RhoF were created using a loxP/PF-4 Cre gene deletion approach. Hereby, the gene in question is introduced to flanking loxP sites and mice were accordingly labeled, e.g. *RhoF*^{fl/fl} [232]. Floxed (fl) mice were crossed with mice containing the MK- and platelet specific promoter platelet factor 4 (PF4) Cre recombinase. This Cre recombinase is located downstream of PF-4 which gets activated during MK maturation and hence provides a lineage specific knock-out[233] with combined labeling being, e.g. *RhoA*^{fl/fl,PF-4Cre +/-}. The Cre

recombinase excises the loxP flanked regions, leading to loss of the gene product and resulting in the respective knock-out.

RhoA and Cdc42 floxed mice were generously provided by Cord Brakebusch (Copenhagen, Denmark). Mice containing the PF-4 Cre recombinase were a gift from Radek Skoda (Basel, Switzerland). RhoF floxed mice were generated by ordering targeted ES cells from KOMP.

Mice were maintained on a SV/129/C57/Bl-6 background. 8- to 13-week-old mice of mixed gender were used for all experiments, if not stated otherwise.

2.2.2 Genotyping of mice

2.2.2.1 Mouse DNA sample isolation

For DNA sampling, a 5mm^2 area of ear tissue was obtained. Dissolved in 500 μL DNA lysis buffer, samples were incubated overnight at 56°C and shaken at 900 rpm. After addition and mixing of 500 μL phenol/chloroform, samples were centrifuged at 14000 rpm for 10 min at room temperature (RT). The upper phase was transferred into a new tube containing isopropanol (1:1 vol). Samples were subsequently centrifuged at 14000 rpm for 10 min at 4°C. The resulting DNA pellet was then resuspended in 70% ethanol and centrifuged as before. This washing step was repeated and the resulting DNA pellet was ultimately resuspended in 100 μl TE buffer. Genotyping by PCR was performed using 2 μl DNA solution. Following the PCR reaction, separation on agarose gels for ko/wt analysis was conducted. Sampling was kindly performed by Sebastian Dütting, Deya Cherpokova, Michael Popp or Ina Thielmann depending on the respective mouse strain.

2.2.2.2 Sample preparation for PCR

The following pipetting scheme was used for all knock-out and double knock-out mouse strains described in this thesis for determination of genotype by PCR,

5µl	10x Taq buffer
2µl	DNA solution
2µl	dNTP solution (10µM)
31.5µl	H_2O
5µl	$MgCl_2$ (25mM)
2µl	primer 1 1:10 (stock: 1µg/µl)
2µl	primer 2 1:10 (stock: 1µg/µl)
0.5µl	Taq polymerase

thus creating a final volume of 50µl for 1 sample. Genotyping was again kindly performed by Sebastian Dütting, Deya Cherpokova, Michael Popp, Ina Thielmann and lab technician Sylvia Hengst.

2.2.2.3 Cdc42 floxed allele detection

Primers

Cdc42_for	5' ATG TAG TGT CTG TCC ATT GG 3'
Cdc42_rev	5' TCT GCC ATC TAC ACA TAC AC 3'

PCR program

95°C	2:00 min	
95°C	0:30 min	
63°C	0:30 min	10x
(-1°C each cycle)		
72°C	0:45 min	
95°C	0:30 min	35x
53°C	0:30 min	

72°C	0:45 min	
72°C	4:00 min	
4°C	storage	

Band sizes

wt allele	: 200 bp
floxed allele	: 300 bp

2.2.2.4 PF4-Cre transgene detection

Primers

PF4-Cre_for   5' CCC ATA CAG CAC ACC TTT TG 3'
PF4-Cre_rev   5' TGC ACA GTC AGC AGG TT 3'

PCR program

96°C	3:00 min	
94°C	0:30 min	
58°C	0:30 min	35x
72°C	0:45 min	
72°C	3:00 min	
4°C	storage	

Band sizes

wt	: missing
PF-4 Cre+	: 450 bp

2.2.2.5 G_{12} and G_{13} knock-out floxed allele detection

Primers G_{12} floxed allele

12INC   5' GTG CTC ATC CTT CCT GGT TTC C
1092R   5' CGG GTC GCC CTT GAA ATC TGG
Neo B   5' GGC TGC TAA AGC GCA TGC TCC

PCR program

94°C	5:00 min	
94°C	1:00 min	
65°C	1:00 min	36x
72°C	2:00 min	
72°C	10:00 min	
4°C	storage	

Band sizes

wt allele	: 441 bp (12INC + 1092R)
floxed allele	: 314 bp (12INC + NeoB)

Primers G_{13} floxed allele

13Seq1   5' GCA CTC TTA CAG ACT CCC AC
Lox3.2   5' GCC ACA GAG GGA TTC AGC AC

PCR program

95°C	5:00 min	
95°C	0:15 min	
56°C	0:15 min	39x
72°C	2:30 min	
72°C	10:00 min	
4°C	storage	

Band sizes

wt allele	: 400 bp
floxed allele	: 470 bp

2.2.2.6 RhoF floxed allele detection

Primers

RhoF_for   5' CGC GAT CCT CGA ACA TCT AT 3'
RhoF_rev   5' GCC CTG GAA CTC ACT TTG TC 3'

PCR program

95°C	5:00 min	
95°C	0:30 min	
58°C	0:30 min	35x
72°C	0:45 min	

72°C	5:00 min	
4°C	storage	

Band sizes

wt allele	: 199 bp
floxed allele	: 242 bp

2.2.2.7 RhoA floxed allele detection

Primers

JVH11_for   5' AGC CAG CCT CTT GAC CGA TTT A
JVH15_rev   5' TGT GGG ATA CCG TTT GAG CAT

PCR program

94°C	2:00 min	
94°C	0:30 min	
55°C	0:30 min	35x
72°C	0:30 min	
72°C	10:00 min	
4°C	storage	

Band sizes

wt allele	: 297 bp
floxed allele	: 393 bp

2.2.3 Histology

2.2.3.1 Organ dissection, processing and preservation

Mice were quickly and deeply anesthetized with maximum concentrations of isoflurane under high flow and humanely euthanized by prompt cervical dislocation. Dead mice were pinned onto a polystyrene board in supine position for sectioning and femura were retrieved by longitudinal incision below the iliac crest. Femura were cleaned from soft tissue and immersed in 4% paraformaldehyde (PFA) in phosphate buffered saline (PBS) overnight. Femura were then put into a decalcifying buffer of 10% ethylenediaminetetraacetic acid (EDTA) in PBS for 1 week with the buffer being changed 3 times. Mice spleens were obtained by lateral incision below the edge of the left ribcage (Kocher's incision). Spleens were left to incubate at 4% PFA in PBS as well. Subsequently, all organs were embedded in paraffin and cutting was performed using a Microm cool cut microtome (Thermo Scientific, Braunschweig, Germany), creating 3 µm thin sections. Sections were left to dry overnight and stored in histology boxes.

2.2.3.2 Hematoxylin and eosin staining, read-out

Dried sections were immersed in Xylol for 10 min twice, before being rehydrated in a descending alcohol dilution series of 100%, 90%, 80% and 70% for 30 sec respectively. Sections rested in deionized water for 2 min and were subsequently put in hematoxylin (Sigma, Schnelldorf, Germany) solution for 15 sec and left to stain under running tab water for 7 min. Eosin was prepared using a 1:10 dilution of Eosin G 0.5% (Roth, Karlsruhe, Germany) in ddH_2O and one drop of 100% acetic acid. Sections were counterstained in the eosin solution for 90 sec and washed shortly in deionized water. Rehydration was carried out in an ascending alcohol series, compare above for concentrations and time length. Two final steps of Xylol immersion for 10 min followed and glass cover slips were mounted using Eukitt. Stained sections were left to dry overnight and stored appropriately. Two bone marrow/spleen sections and 20 visual fields per section were analyzed at

40x magnification, if not stated otherwise.

2.2.4 Measurement of spleen weight

Mice were anesthetized and put on a precision balance for measurement of total body weight. After dissection of spleens described in 2.2.3.1, spleens were carefully examined to exclude artificial tissue damage and loss by sectioning. Remaining adjoining tissue was removed by tweezers and spleens were likewise measured on a precision balance and related to respective body weight.

2.2.5 Glycoprotein inhibition

Antibodies used for GP blockade experiments were kindly adjusted to 1 mg/ml antibody in PBS with 0.2% BSA by lab technicians.
For GPIIb/IIIa and GPV blockade, RhoA deficient mice were injected into the retroorbital plexus with 100 µg 4H5-Fab-fragments or 100 µg 89F12 antibody respectively on three consecutive days with femura being retrieved on day 5. Regarding Clec-2 and GPVI blockade, 100 µg 11E9 antibody was used for Clec-2 and 100 µg of 98A3 antibody for GPVI inhibition. Injection was performed twice on day 1 and 3; dissection of bones followed on day 5.

2.2.6 Platelet depletion

Platelet depletion was performed by one-time injection of 100µg rat anti-mouse GPIbα into the retroorbital plexus of mice. Circulating platelet counts were monitored by consecutive blood drawing (vol 50µl) for 10 days after treatment by a Sysmex KX-21N automated hematology analyzer (Sysmex Corp., Kobe, Japan). Bones were explanted 1 day or 10 days after antibody injection.

2.2.7 Determination of platelet count and size

Anesthetized mice were bled from the retroorbital plexus using microcapillaries (vol 50µl) and blood was collected into an Eppendorf tube containing 300µl

heparin (20 U/ml) in Tris-buffered saline (TBS). Platelet counts and sizes were established using a Sysmex KX-21N.

2.2.8 Platelet preparation and washing

Blood was drawn under isoflurane anesthesia by insertion of a heparinized microcapillary into the retroorbital plexus. At least 700µl of blood was collected into a tube containing 300µl heparin in TBS. Platelet rich plasma (prp) was obtained by twice centrifugation at 800 rpm for 5 min with the buffy coat and supernatant being transferred to a new tube each time. Washing of prp was performed by centrifugation at 2,800 rpm for 5 min in the presence of apyrase (0.02 U/ml) and prostacyclin (PGI$_2$, 0.01 µg/ml). The platelet pellet was resuspended in Tyrode's buffer without Ca^{2+} and washed a second time under equal conditions. After incubation of platelets at 37°C for 5 min, another washing step concluded platelet preparation and the final platelet pellet was resuspended in Tyrode's buffer with Ca^{2+} and left to incubate at 37°C for 30 min before fluorescence activated cell sorting (FACS) analysis.

2.2.9 Flow cytometry

Basal surface glycoprotein (GP) expression levels were determined by staining samples whole blood with fluorophore-conjugated antibodies (see section 2.1.3.) for 15 min at room temperature (RT). The reaction was stopped by addition of 500µl PBS. For GPIIb/IIIa and P-Selectin activation studies, the respective agonists were added to the washed-platelet suspension and left to incubate for 6 min at 37°C and 6 min at RT, before halting the reaction by addition of 500µl PBS. FACS measurement was performed directly after using a FACSCalibur (Becton Dickinson, Heidelberg, Germany). For two-color stainings, the following listing provides an overview of settings:

Detectors/Amps

Parameter	Detector	Voltage
P1	FSC	E01

P2	SSC	380
P3	FI1	650
P4	FI2	580
P5	FI3	150

Threshold

Value	Parameter
253	FSC-H
52	SSC-H
52	FI1-H
52	FI2-H
52	FI3-H

Compensation

FI1	2.4% of FI2
FI2	7.0% of FI1
FI2	0% of FI3
FI3	0% of FI2

2.2.10 Platelet spreading assay

2.2.10.1 Platelet spreading on fibrinogen

100 µl of human fibrinogen (Sigma) diluted in PBS (100µg/ml) was pipetted onto glass cover slips and slides were left to incubate in a damp chamber overnight at 4°C. Cover slips were rinsed with sterile PBS and blocked with PBS 1% BSA at 37°C for 2h. Washed platelets were obtained as described in 2.2.8 and aliquots of $0{,}3 \times 10^6$ plts/µl were produced. Platelets were left to incubate at 37°C for 30 min.

Glass cover slips were rinsed with sterile PBS multiple times before being ultimately washed with Ca^{2+}-containing Tyrode's buffer. Platelets were then activated by addition of Thrombin (0.01 U/ml) and pipetted onto the designated glass cover slips to allow for spreading. After the respective time points (5 min, 15 min and 30 min) were reached, spreading was halted by adding PBS 4% PFA. Glass slides were mounted onto the cover slips and platelet spreading was analyzed by a Zeiss Axiovert 200 inverted microscope (x100) using differential interference contrast (DIC) microscopy. Images were captured by a CoolSNAP-

EZ camera (Visitron, Munich, Germany) using MetaVue online software and readout was conducted with the ImageJ cell counter plugin.

2.2.10.2 Platelet spreading on von Willebrand Factor (vWF)

Glass cover slips were coated with 200µl of polyclonal rabbit-α-human vWF-antibody (A0082, DAKO) diluted in 50mM carbonate-bicarbonate buffer (1:500) and were incubated in a damp chamber at 4°C overnight. Cover slips were rinsed with PBS and blocking was conducted with PBS 3% BSA at 37°C for 2h.
To obtain mouse plasma, wild-type mice were bled from the retroorbital plexus and blood was collected as described in 2.2.8. Blood was centrifuged at 2800 rpm for 10 min, the supernatant transferred to a new tube and centrifuged at 14000 rpm. Incubation of slides with mouse plasma for 2h at 37°C followed.
Washed platelets were obtained as described in 2.2.8 and aliquots of 0,3x10^6 plts/µl produced. Platelets were left to incubate at 37°C for 30 min before addition of integrilin (60 µg/ml) to the suspension and renewed incubation for 10 min.
Glass cover slips were rinsed after incubation with sterile PBS multiple times and as a last step Tyrode's buffer with Ca^{2+}. Platelets were then activated by addition of Ca^{2+}-containing Tyrode's buffer and high-dose Botrocetin (50 U/ml) and pipetted onto the designated glass cover slips to allow for spreading. In case of the vWF spreading assay, time spans analyzed were 10 min, 20 min and 30 min. The reaction was stopped and platelets were analyzed as described in 2.2.10.1.

2.2.11 Data analysis

All data were explored for normality by Shapiro-Wilk test, including homogenous variances by Levene-test. Student's t-test was performed when parametric conditions were fulfilled and variance was homogenous. The Welch-test (modified t-test) was used when unequal variances occurred. In case of GP blockade experiments, in-group comparisons were performed using the t-test for paired samples. Under non-parametric conditions, the Mann Whitney U-test was applied to test for statistical significant difference between two groups and exact significance was calculated (n<30 fulfilled). For comparison of more than two

groups, one-way analysis of variance (ANOVA) was used, followed by post-hoc Tukey-test. SPSS 23 (IBM SPSS Statistics, New York, USA) was used for statistical analysis. Results are displayed as mean $\pm$ SD and usually represent three individual experiments, if not stated otherwise. Knock-out and littermate wild-type mice were used for experiments, if not stated otherwise.

3. Results

3.1 MK localization upon deficiency of different cytoskeletal regulatory proteins

3.1.1. Findings from bone marrow and spleen sections of *RhoA^{-/-}* mice

3.1.1.1 RhoA^{-/-} mice exhibit an altered distribution of MKs compared to the wild-type

Upon platelet activation, the small GTPase RhoA plays a pivotal role in mediating shape change, the release of α- and dense granules and outside-in signaling through integrin $\alpha IIb\beta 3$. RhoA has also been identified as an important actor in the formation of focal adhesions during cell migration[79]. Platelet studies revealed a macrothrombocytopenia with upregulated megakaryopoiesis in the bone marrow (BM) in RhoA deficient mice[18], but RhoA had not been studied in the highlight of MK migration or localization in the BM.

Mice were created by crossing animals carrying a RhoA gene flanked by loxP sites – so-called floxed (fl) mice (*RhoA^{fl/fl}*)[232] – with transgenic mice expressing Cre recombinase downstream of the MK- and platelet-specific platelet factor 4 (PF4) promoter[233], leading to loss of the gene product. Floxed, PF4-Cre positive (*RhoA[fl/fl,PF4-Cre+/-]*) RhoA deficient mice are further referred to as *RhoA^{-/-}* and *RhoA[fl/fl,PF4-Cre-/-]* as wild-type (wt) mice.

Michael Popp kindly provided and genotyped *RhoA^{-/-}* mice. Mice femura were harvested, decalcified, embedded in paraffin and then cut by microtome. Hematoxylin and eosin staining (HE staining) was performed and a microscopic readout of the localization of MKs of 20 visual fields per bone section conducted (see Materials and Methods chapter). MKs were assigned to the three groups intraluminal, adjacent to vessel wall (vessel wall) and stroma.

Strikingly, *RhoA^{-/-}* mice exhibited a significantly higher number of MKs inside of BM sinusoids and adjacent to the blood vessel as compared to wt MKs (Fig. 1).

In contrast, MKs were found only very rarely intraluminally in wt mice. Fig. 2 depicts representative images of this so far unreported observation in *RhoA*$^{-/-}$ mice. The divergence in the percentage of intrasinusoidal MKs in the BM could potentially be explained by an increase in MK numbers in the BM of *RhoA*$^{-/-}$ mice, however, as Fig. 3 shows, no statistically significant difference was found in comparison to the wt.
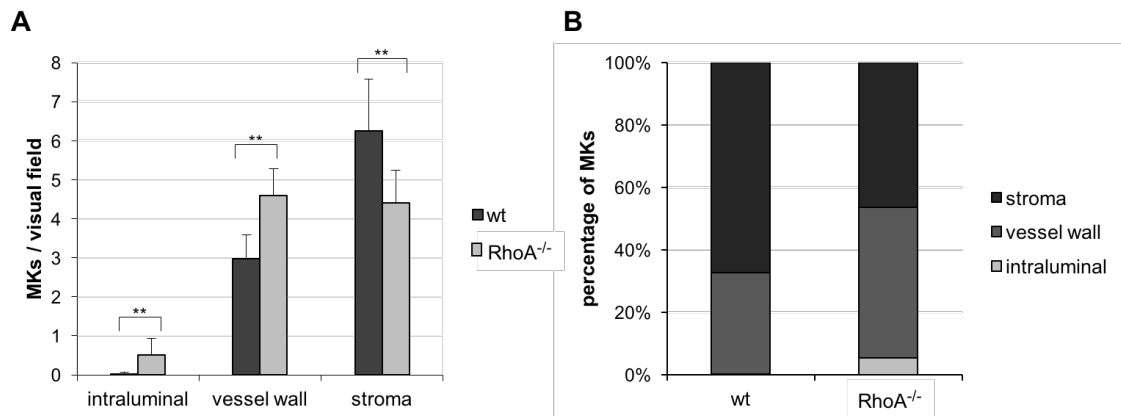

Fig. 1. Alterations of MK localization in the BM of *RhoA*$^{-/-}$ mice. (A) The table depicts the mean numbers of MKs per visual field resting intraluminally, adjacent to the vessel wall (vessel wall) and in the stroma of the BM for *RhoA*$^{-/-}$ and wt mice in total numbers. (B) Presentation of MK numbers as percentages for *RhoA*$^{-/-}$ and wt. Representative experiment with n=7 (*RhoA*$^{-/-}$) and n=8 (wt) mice. ** p < 0.01.
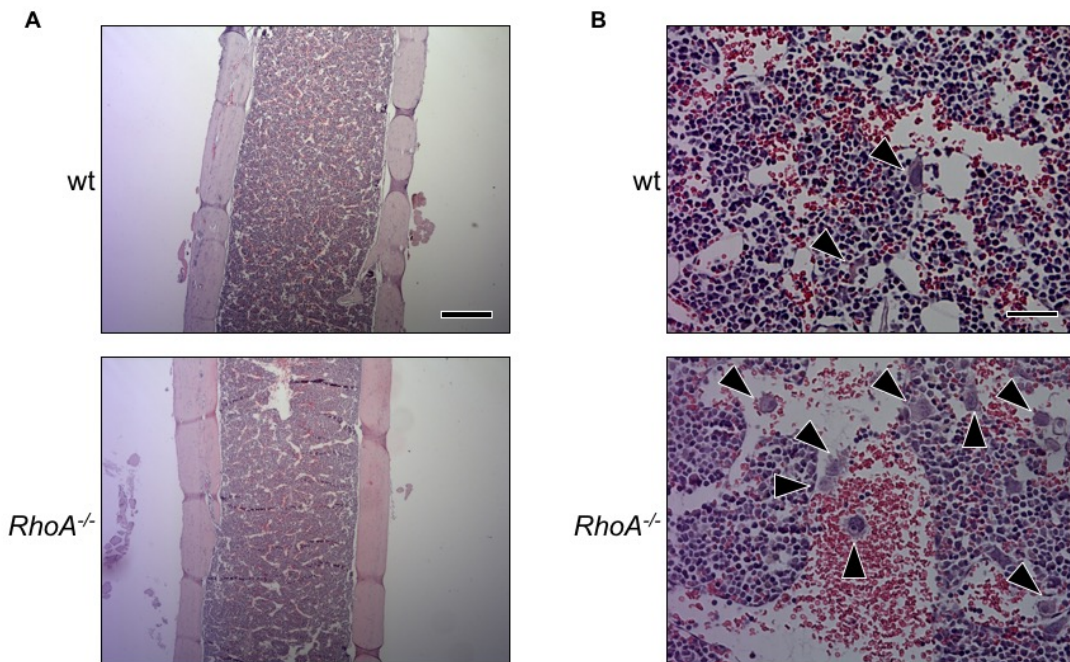
Fig. 2. Intraluminal localization of MKs in *RhoA*$^{-/-}$ mice. (A) Overview at 5x magnification: the left panel demonstrates preservation quality of the analyzed BM in both the *RhoA*$^{-/-}$ and the wt mice. Scale bar: 480 µm. (B) Close-up view at 40x magnification: the lower picture of the right panel displays representative pictures of *RhoA*$^{-/-}$ MKs within the lumen of well-preserved BM sinusoids. The upper picture provides a detailed view of comparable wt BM in which MK transmigration occurs much less frequently. Arrows depict MKs. Scale bar: 60 µm.
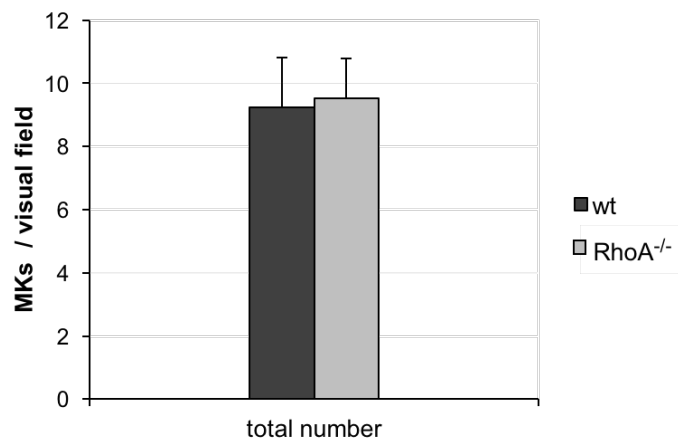

Fig. 3. MK counts in the BM of *RhoA*$^{-/-}$ and wt mice are similar. Total counts of MKs correspond to the experiment depicted in Fig. 1, n=7 (*RhoA*$^{-/-}$) and n=8 (wt) mice.

This indicates a distinct and potentially defective compartmentalization of MKs in the BM in *RhoA*$^{-/-}$ mice which suggests RhoA is needed in physiological MK

localization or migration and might account at least in part for the markedly reduced platelet count observed in *RhoA*^{-/-} mice[18].

3.1.1.2 MK number in the spleen is unaltered in RhoA^{-/-} mice

Another natural site of hematopoiesis and consequently megakaryopoiesis in mice is the spleen which is why investigation of potential distinct knock-out features in this organ was performed. Only the total number of MKs was determined, as an assignment of MK localization to the aforementioned three groups remained elusive by conventional microscopy owing to the fact of much smaller sinusoids and a very densely populated red pulp in the spleen.

Fig. 4 shows that, while a trend towards increased MK numbers was observed in *RhoA*^{-/-} mice, it did not reach a statistically significant difference. Notably, the overall spleen architecture and MK morphology was similar in *RhoA*^{-/-} and corresponding wt mice (Fig. 5).
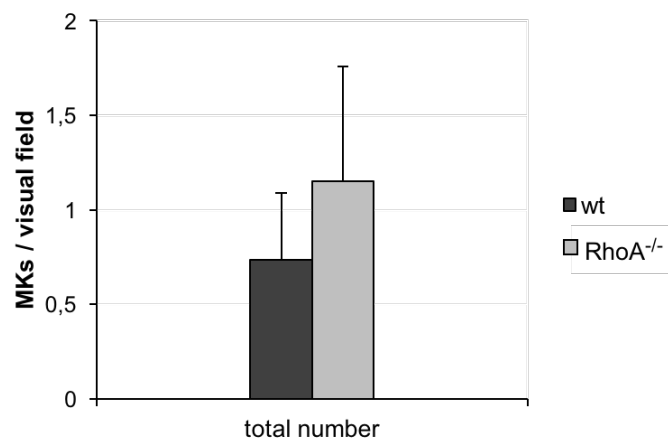

Fig. 4. A trend towards increased MK numbers in spleens from *RhoA*^{-/-} mice. The number of MKs per visual field in *RhoA*^{-/-} mice is moderately increased, but not significantly different compared to the wt. Representative experiment with n=8 mice per group.
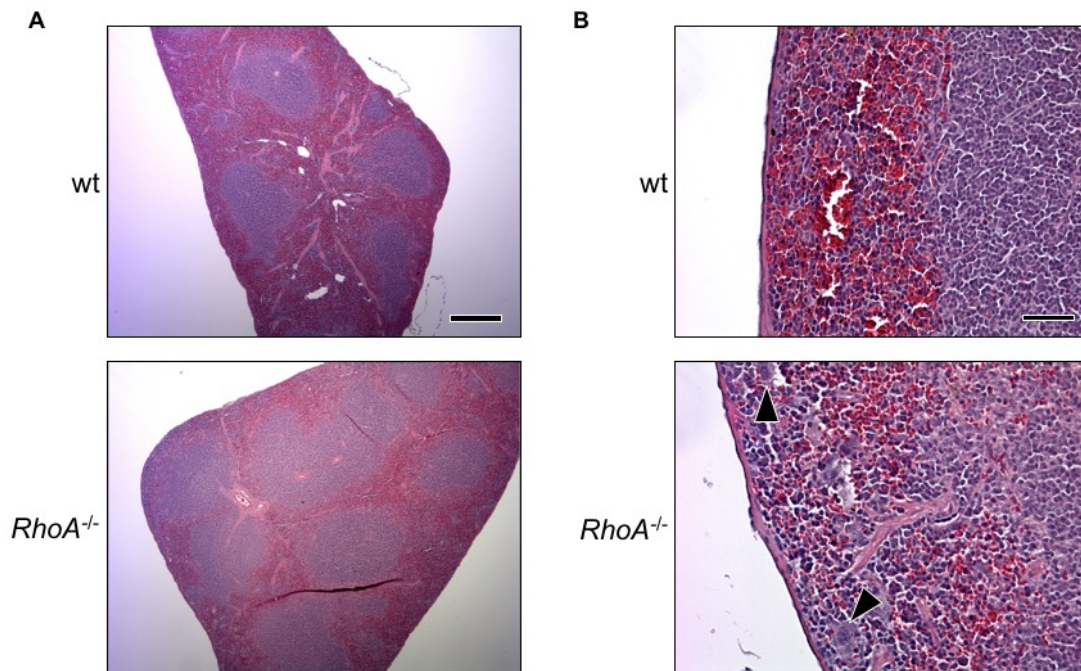
Fig. 5. Similar MK counts in *RhoA*$^{-/-}$ and wt spleens. (A) Left panel, overview at 5x magnification: *RhoA*$^{-/-}$ and wt mice exhibit no obvious morphological differences regarding configuration of the organ as a whole and the red pulp. Scale bar: 480 μm. (B) Right panel, close-up view at 40x magnification: observed MKs were similar in size and morphology. Arrows depict MKs. Scale bar: 60 μm.

These findings point out that MK localization in the spleen is not obviously affected by the knock-out of RhoA. They also indicate that there is no major shift of megakaryopoiesis from the BM to the spleen as a secondary site of hematopoiesis, owing to the macrothrombocytopenia reported in *RhoA*$^{-/-}$ mice.

3.1.2 Increased MK counts in the BM and the spleen of *RhoA/Cdc42*$^{-/-}$ mice

Cdc42$^{-/-}$ single knock-out mice display mild macrothrombocytopenia which is associated with a decreased platelet life span[149]. Circulating platelet numbers and megakaryocytic replenishment are linked by a negative feedback loop to be kept in a steady-state[234]. *Cdc42*$^{-/-}$ mice also exhibit higher MK numbers in the BM. In addition, *Cdc42*$^{-/-}$ MKs derived from murine fetal liver cells showed impaired proplatelet formation which was even more pronounced upon Rac1/Cdc42 double-deficiency, revealing redundant functions of these two GTPases in platelet production[52]. To investigate whether also RhoA and Cdc42 might have

overlapping function in MK localization or migration, MK numbers were analyzed in BM and spleen of *RhoA/Cdc42*$^{-/-}$ mice. Deya Cherpokova generously provided and genotyped mice for the following experiments.

Due to insufficient preservation of BM sinusoids in this mouse strain, compartmental read-out was not possible to conduct and thus only overall MK counts were established. *RhoA/Cdc42*$^{-/-}$ mice exhibited significantly higher numbers of MKs in the BM than wt mice, in line with results of the *Cdc42*$^{-/-}$ single knock-out (Fig. 6). This may be the result of an upregulation in megakaryopoiesis in response to the observed thrombocytopenia. The overall morphology of *RhoA/Cdc42*$^{-/-}$ and wt MKs was similar (Fig. 7).
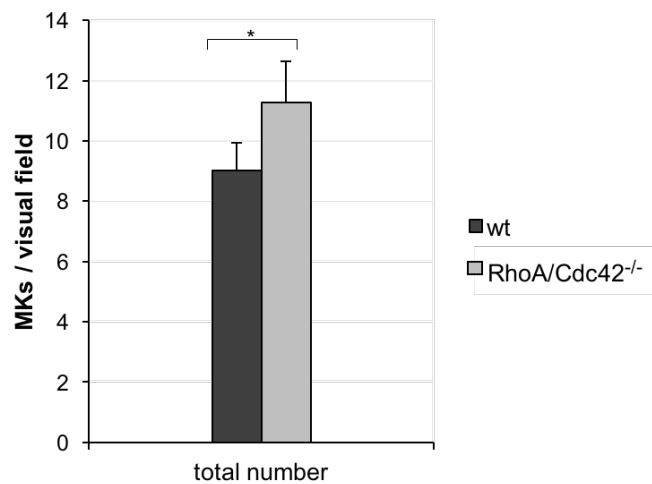

Fig. 6. *RhoA/Cdc42*$^{-/-}$ mice have increased MK numbers in the BM. The BM of *RhoA/Cdc42*$^{-/-}$ mice contains more MKs compared to the wt. Representative experiment with n=4 mice per group. * p < 0.05.
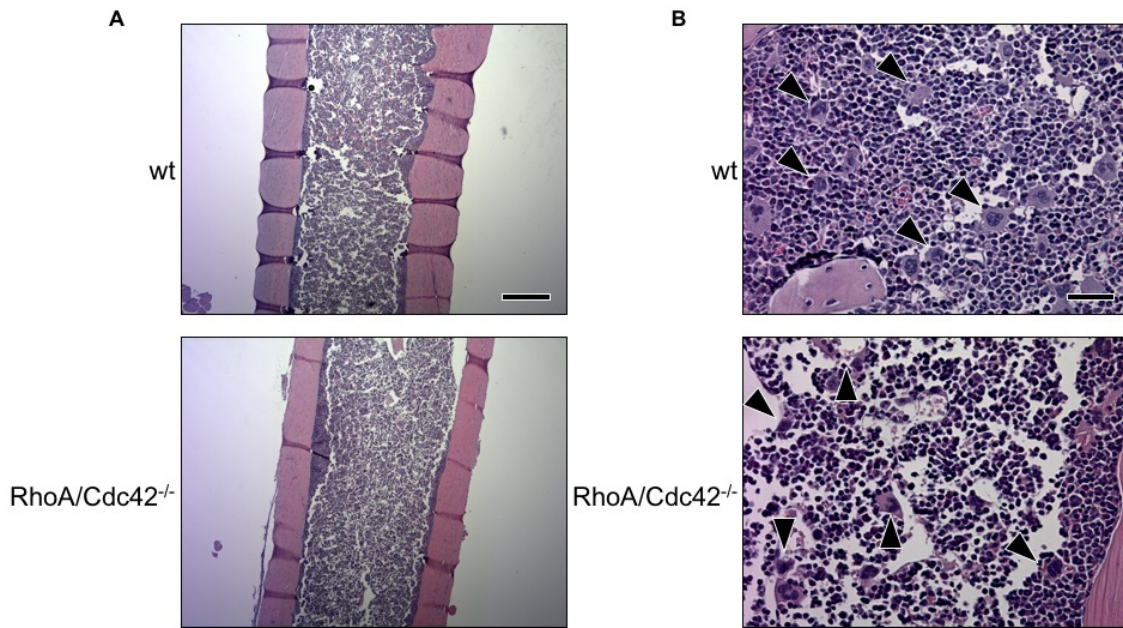
Fig. 7. BM comparison of *RhoA/Cdc42*-/- with wt mice. (A) The left panel displays an overview at 5x magnification of both *RhoA/Cdc42*-/- and wt BM. Scale bar: 480 μm. (B) The right panel with a closer view at 40x magnification of both *RhoA/Cdc42*-/- and wt MKs. Sinusoid preservation was not sufficient for compartmental read-out. *RhoA/Cdc42*-/- MKs do not show an altered morphology compared to their wt counterparts. Arrows depict MKs. Scale bar: 60 μm.

Interestingly, splenic MK numbers were strongly increased in *RhoA/Cdc42*-/- mice and exceeded wt counts threefold (Fig. 8). No observable changes neither concerning spleen architecture nor MK morphology could be observed compared to the wt. Representative images of spleen sections are depicted in Fig. 9.
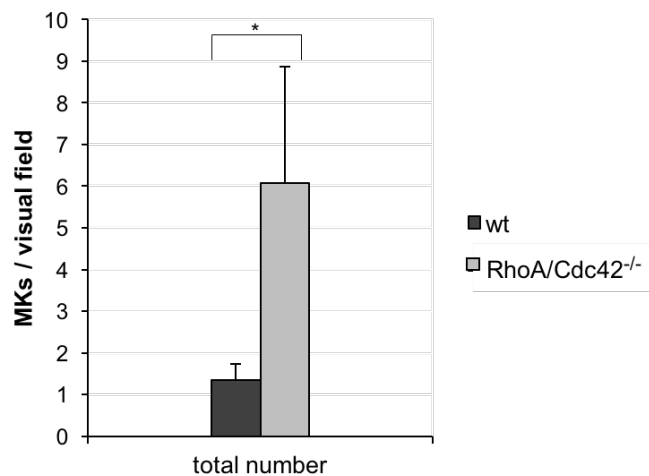

Fig. 8. *RhoA/Cdc42*-/- mice display drastically increased counts of MKs in the spleen. The

sum of MKs in *RhoA/Cdc42*$^{-/-}$ mice is greatly increased related to wt mice. Representative experiment with n=4 mice per group. * p < 0.05.
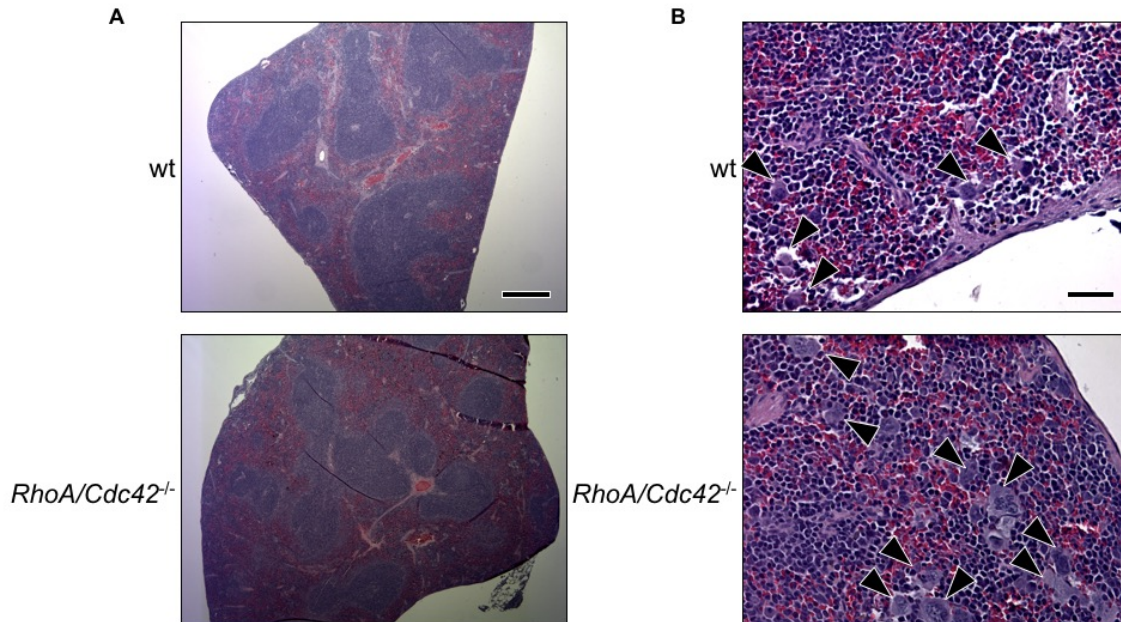

Fig. 9. Spleen architecture and MK morphology are similar in *RhoA/Cdc42*$^{-/-}$ compared to wt mice. (A) Overview of spleens at 5x magnification does not see a major difference in setup regarding, e.g. organ shape or the red pulp/ white pulp ratio between *RhoA/Cdc42*$^{-/-}$ and wt mice. Scale bar: 480µm. (B) The right panel at 40x magnification shows a similar phenotype of *RhoA/Cdc42*$^{-/-}$ and wt MKs. Arrows depict some MKs. Scale bar: 60 µm.

Having observed drastically elevated MK counts in *RhoA/Cdc42*$^{-/-}$ spleens, total spleen weight was measured to check for splenomegaly as a sign of a shift of megakaryopoiesis from the bone marrow to this site of secondary hematopoiesis. Indeed, spleen weight of *RhoA/Cdc42*$^{-/-}$ mice was increased by 30% compared to wt counterparts, compare Fig. 10, indicating a mild splenomegaly. Although this study lacks the inclusion of *Cdc42*$^{-/-}$ mice to be compared with *RhoA*$^{-/-}$ and *RhoA/Cdc42*$^{-/-}$ mice, together these findings support the observation that the defect thrombopoiesis is considerably aggravated upon RhoA/Cdc42 double-deficiency compared to single-deficiency of either RhoA or Cdc42.
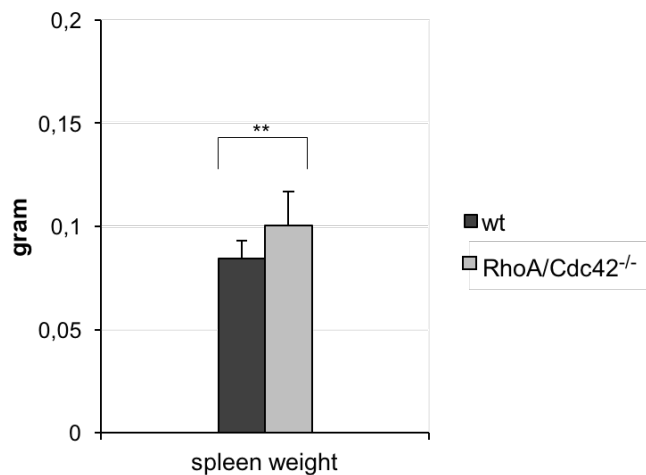
Fig. 10. *RhoA/Cdc42*$^{-/-}$ mice show increased spleen weight. *RhoA/Cdc42*$^{-/-}$ mice compared to wt mice display a significantly increased her spleen weight, indicating a shift of megakaryopoiesis to this secondary hematopoietic organ. Results are given as spleen weight/ body weight of the respective mice. Representative experiment with n=4 mice per group. ** $p < 0.01$.

3.1.3 Analysis of MK localization in BM of $G_{12/13}$ double knock-out mice

Signaling through the G_{12} and more importantly G_{13} protein is one of the two major axes of RhoA activation. RhoA can also be activated downstream of G_q protein-mediated signaling, especially in the setting of high agonist doses[155]. In platelets, G_{12} and G_{13} of the stimulating type G_s are activated downstream of protease activated receptors (PARs) and the thromboxane-prostanoid (TP) receptor upon stimulation with agonists, e.g. thrombin, thromboxane A2 (TxA2) and the TxA2 mimetic U-46619 (U-46)[154,155].

A mouse strain double deficient of G_{12} and G_{13} (encoded by the genes *Gna12* and *Gna13*) was used to investigate whether RhoA activation/signaling might also involve these G proteins in MKs. Mice were generously provided and genotyped by Ina Thielmann. Notably, however, the MK phenotype of *RhoA*$^{-/-}$ mice was not observed in $G_{12/13}$$^{-/-}$ mice resulting in unaltered MK distributions in the BM compared to the wt (Fig. 11).
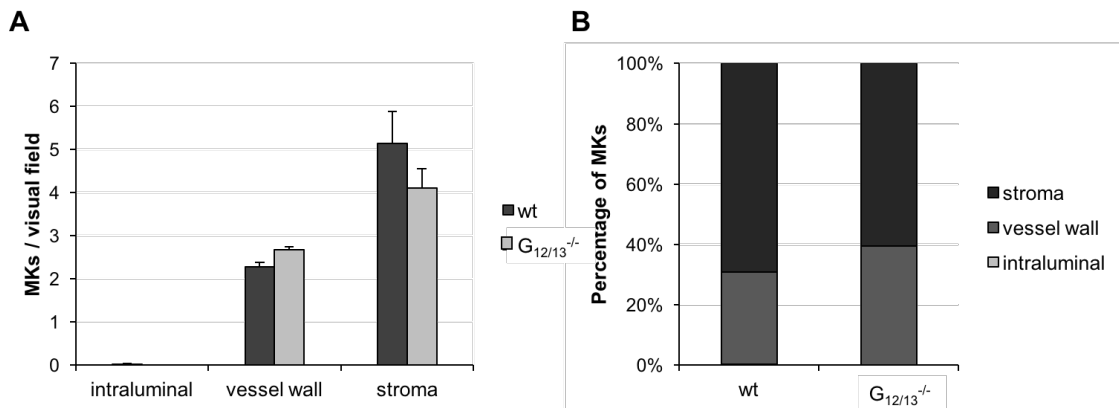
Fig. 11. $G_{12/13}^{-/-}$ mice and their wt counterparts show a similar MK distribution in the BM. Representative experiment with n=3 ($G_{12/13}^{-/-}$) and n=2 (wt) per group.

Studies of the total numbers of MKs in the BM were performed as well and showed a similar number of MKs in mice from both genotypes (Fig. 12). It has to be noted though that the genetic background and the knock-out strategy of mice were different in $G_{12/13}^{-/-}$ mice, compared to $RhoA^{-/-}$ mice with creation of a *Gna13* allele, *Gna13*^ta^ which contains three loxP sites, along with a cassette of the neomycin resistance (*neo*^r^) and thymidine kinase gene (*tk*). After conversion into a floxed allele (*Gna13*^flox^), mice were crossed with the Cre-deleter mouse strain EIIa-Cre to allow generation of a *Gna13*^-^ null allele[154].
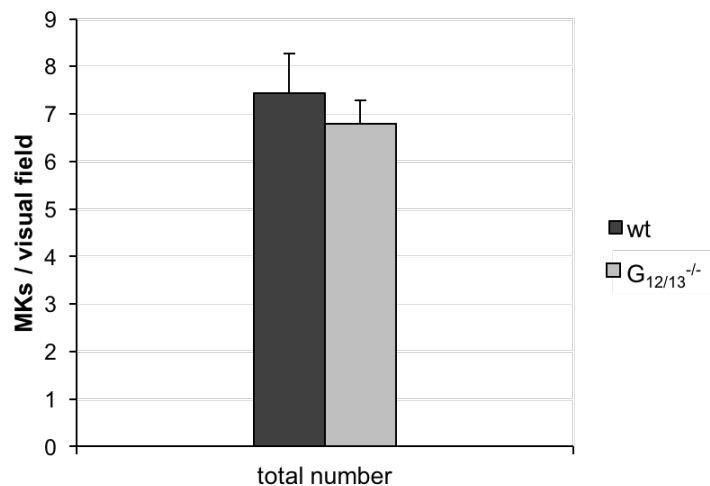

Fig. 12. Total MK numbers in the BM are similar in $G_{12/13}^{-/-}$ and wt. Representative experiment with n=3 ($G_{12/13}^{-/-}$) and n=2 (wt) mice per group.
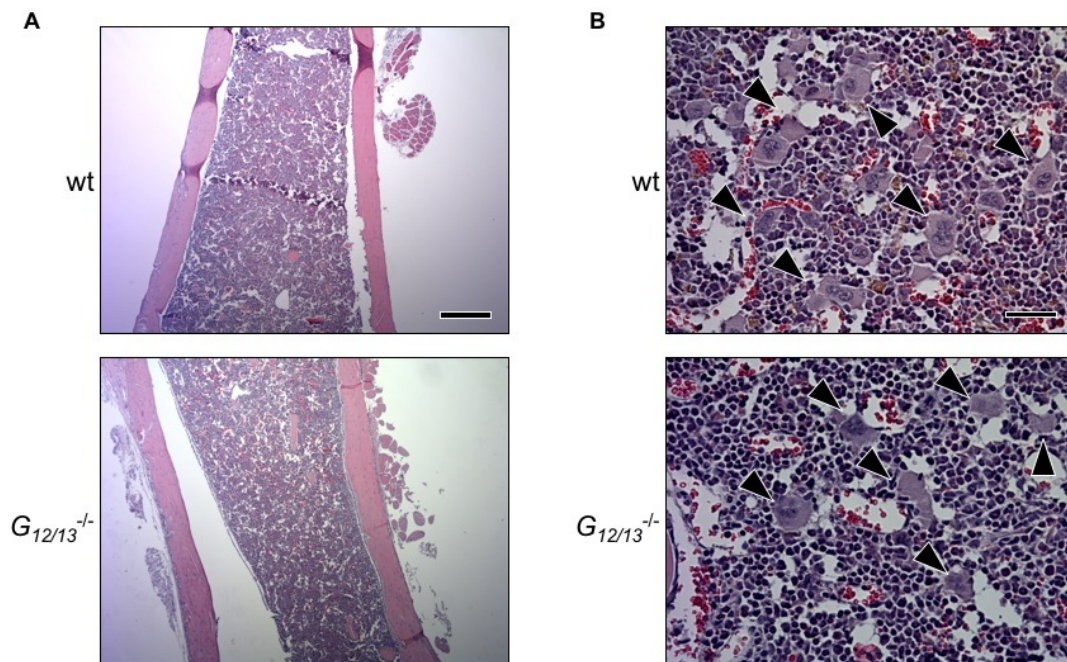
Fig. 13. BM and MK morphology are identical in $G_{12/13}^{-/-}$ and wt mice. (A) Overview at 5x magnification shows the configuration of the BM for $G_{12/13}^{-/-}$ and wt mice respectively. Scale bar: 480 µm. (B) Close up-view at higher magnification (40x) for analysis of MK morphology yielding no obvious divergence in structure. Arrows depict MKs. Scale bar: 60 µm.

No substantial difference in BM architecture or MK morphology could be observed during analysis of the BM sections (Fig. 13). In line with these observations, MK numbers and spleen architecture were similar in spleen sections from $G_{12/13}^{-/-}$ mice and wt mice (Fig. 14, 15.)
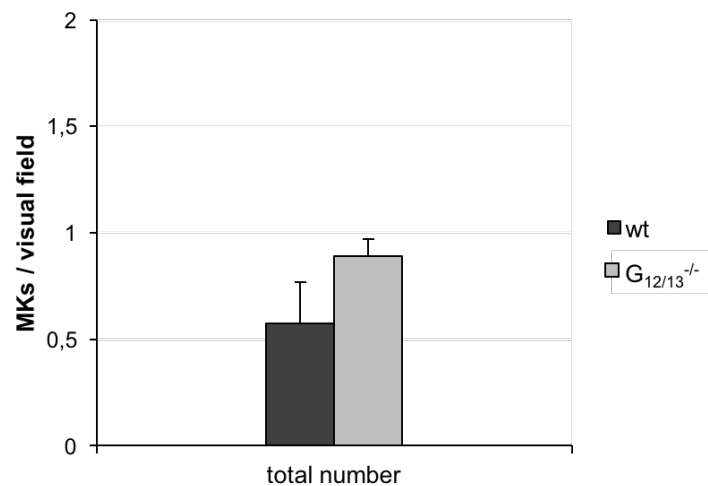
Fig. 14. Spleens of $G_{12/13}^{-/-}$ and wt mice display similar MK numbers. Representative experiment with n=3 mice per group.
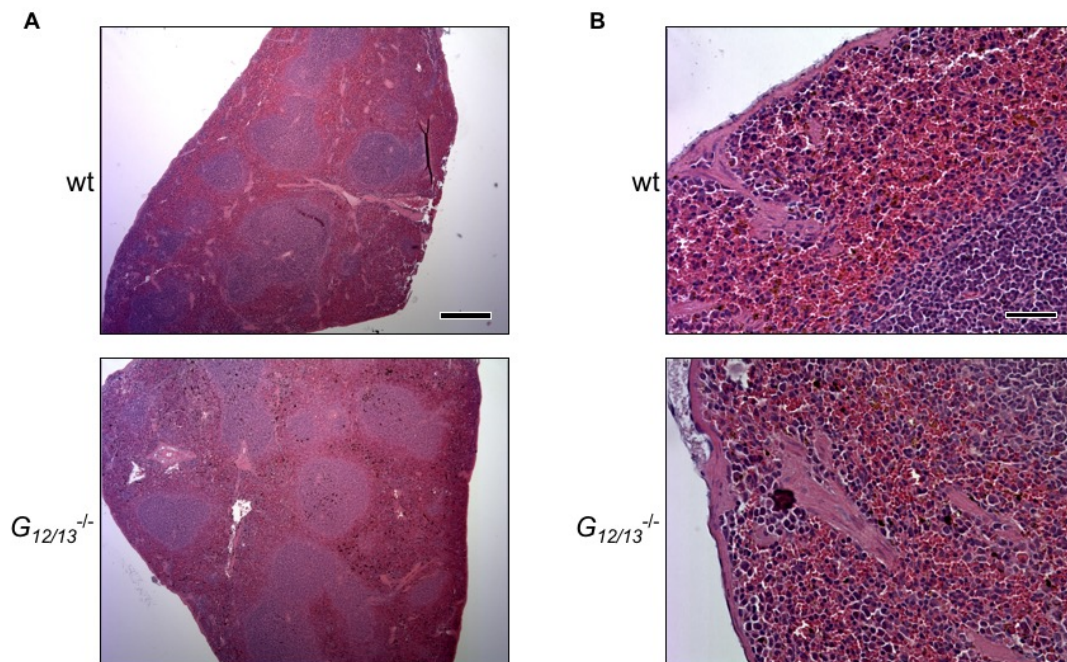
Fig. 15. $G_{12/13}^{-/-}$ mice do not show an altered spleen morphology. (A) Upper panel at 5x magnification demonstrates comparable organ morphology of $G_{12/13}^{-/-}$ and wt mice. Scale bar: 480 µm. (B) Lower panel depicts a close-up view at 40x magnification of the spleen architecture. No MKs visible on this picture. Scale bar: 60 µm.

Together, these results show that $G_{12/13}^{-/-}$ mice do not reproduce the MK phenotype observed in the RhoA knock-out, suggesting RhoA-controlled MK

compartmentalization takes place independently of signaling through G_{12} and G_{13} proteins.

3.2. Investigation of signaling pathways involving RhoA in MKs

3.2.1 GPIb-mediated platelet depletion and effects on MK localization in *RhoA^{-/-}* mice

3.2.1.1 Findings one day after platelet depletion in RhoA^{-/-} mice

The finding that the *RhoA^{-/-}* phenotype shows a significantly higher percentage of intraluminal MKs entails the question which signaling events might contribute to that phenomenon. First, investigation of megakaryopoiesis under stress was conducted by antibody mediated platelet depletion in order to assess possible influences. Michael Popp kindly provided, genotyped and performed antibody injection on the mice. Depletion was achieved by injection of polyclonal rat anti-mouse GPIb antibody binding to circulating platelets and leading to consecutive clearance from the blood stream. Preservation and analysis of bone marrow sections was carried out as laid out before.

Compartmentalization readout had to be omitted due to technical difficulties which is why only total numbers of MKs were established. As Fig. 16 shows, femura of *RhoA^{-/-}* mice harvested one day after (t=1d) platelet depletion showed no alteration in their MK counts compared to the wt. Likewise, MK morphology was similar as compared to BM from the respective non-treated genotype (Fig. 17).
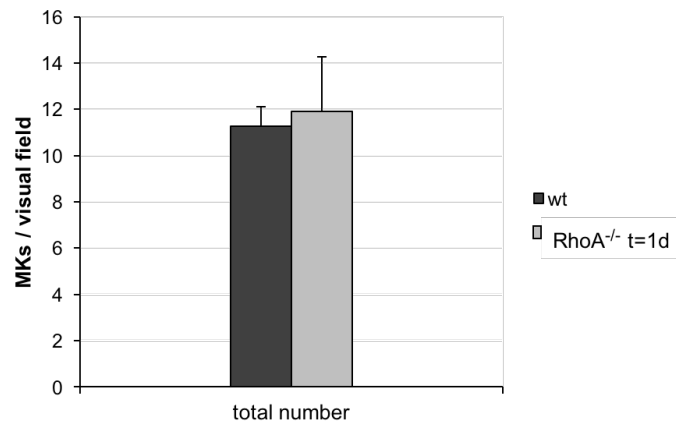
Fig. 16. GPIb antibody injected *RhoA*$^{-/-}$ mice show comparable MK numbers on t=1d. BM of *RhoA*$^{-/-}$ mice one day after antibody injection (t=1d) exhibit similar MK numbers compared to the wt. Single experiment with n=4 mice per group.
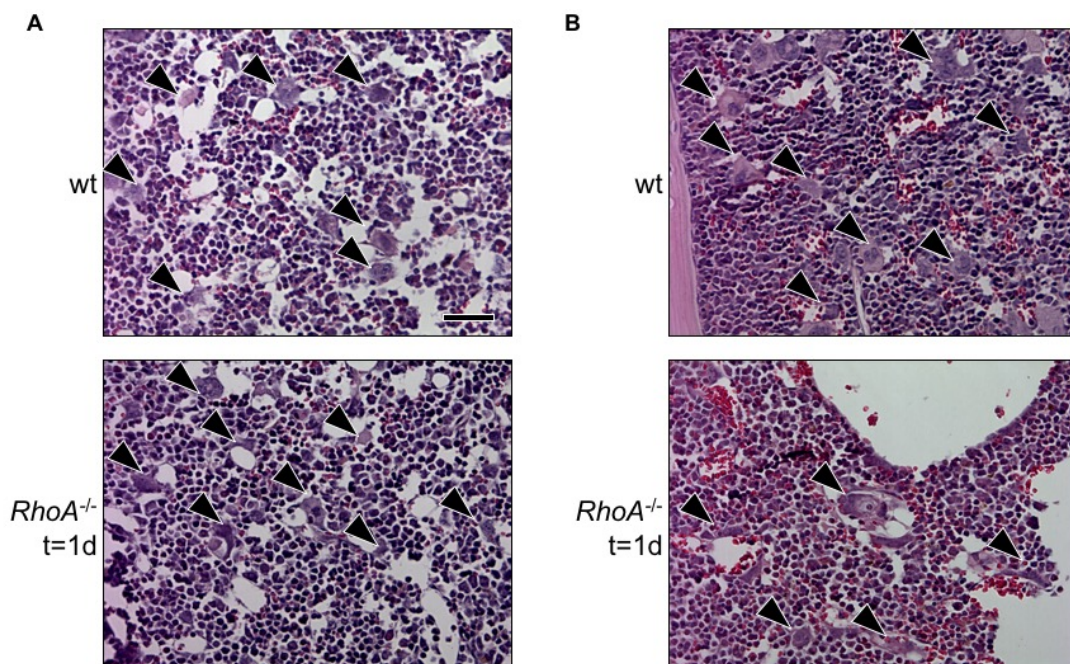
Fig. 17. Unaltered MK morphology in *RhoA*$^{-/-}$ mice one day after antibody. (A) Left and (B) right panels from different animals with close-up views at 40x magnification detail similar morphology of MKs of *RhoA*$^{-/-}$ and wt mice one day after GPIb antibody injection and platelet depletion. Arrows depict MKs. Scale bar: 60 µm.
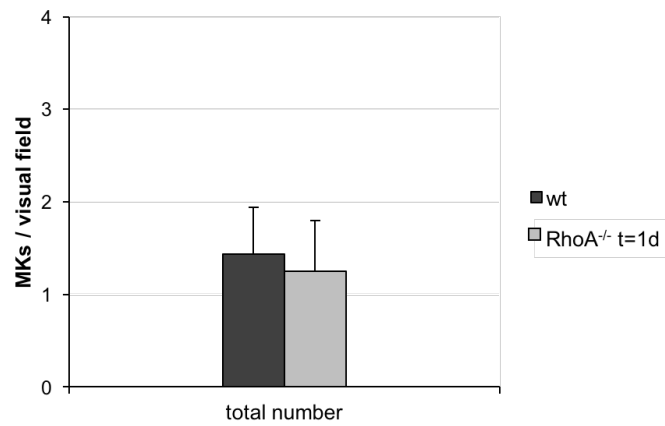
Fig. 18. Antibody injection of *RhoA*^{-/-} mice leaves counts of MKs unaltered in the spleen after one day. GPIb mediated platelet depletion of *RhoA*^{-/-} and wt mice yield comparable MK numbers one day (t=1d) after injection. Single experiment with n=4 mice per group.

In line with this, splenic MK numbers were similar in *RhoA*^{-/-} and wt mice, see Fig. 18. Also MK morphology in the spleen was not affected by sustained megakaryopoietic stress (Fig. 19).
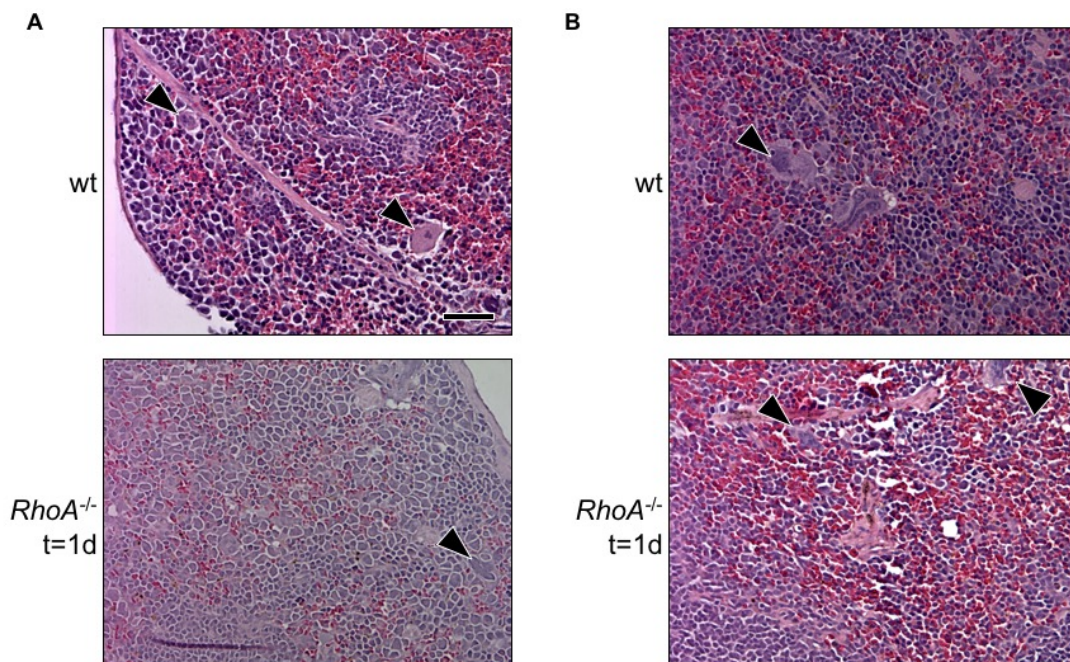
Fig. 19. Spleens of platelet-depleted *RhoA*^{-/-} and wt mice exhibit similar architecture. Both panels (A) and (B) depicting *RhoA*^{-/-} and corresponding wt MKs at a high magnification (40x) in the spleen. Arrows depict MKs. Scale bar: 60 μm.

These findings illustrate that short-term stress on megakaryopoiesis does not become visible in a change of MK numbers in the bone in either *RhoA^{-/-}* or wt mice.

3.2.1.2 Similar recovery of MK counts in RhoA^{-/-} and wt mice at day 10 after platelet depletion

Analysis of BM sections from *RhoA^{-/-}* mice 10 days after platelet depletion was performed in order to investigate longer term effects on MKs. At this time point, experiments by Michael Popp showed that the platelet numbers in both *RhoA^{-/-}* and wt mice had returned to their original levels, respectively (data not shown). In this experiment, *RhoA^{-/-}* mice exhibited results similar to the phenotype of wt mice 10 days after platelet depletion with regard to total MK numbers in the BM (Fig. 20). Studied sections of bone marrow did not show an altered architecture of the bone marrow itself, nor at the cellular level regarding MKs (Fig. 21).
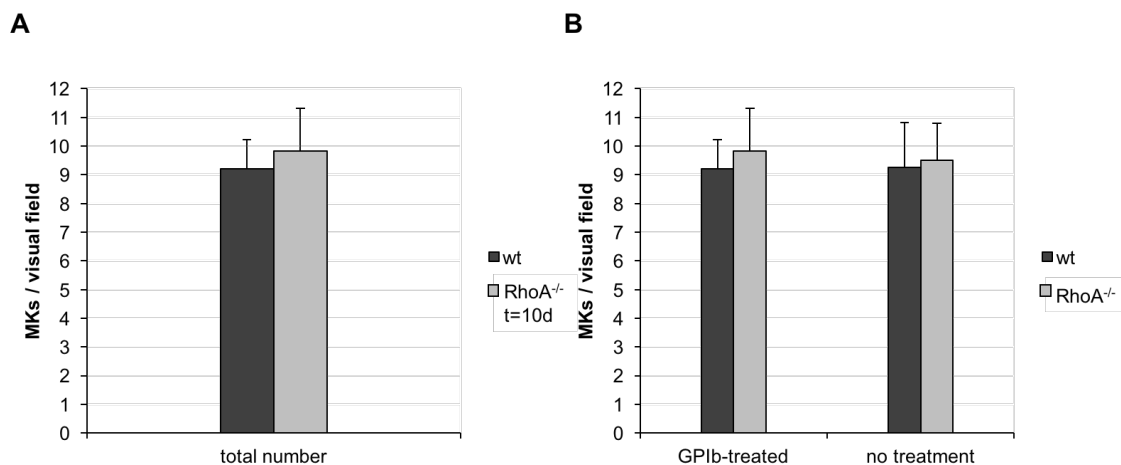
Fig. 20. *RhoA^{-/-}* and wt mice do not show increased totals of MKs at t=10d after platelet depletion. (A) MK numbers in platelet-depleted *RhoA^{-/-}* and wt mice are comparable to one another. (B) Comparison of *RhoA^{-/-}* and wt mice at t=10d with untreated mice exhibits similar results. Data for control group taken from experiment depicted in Fig. 2. Single experiment with n=6 mice per group.
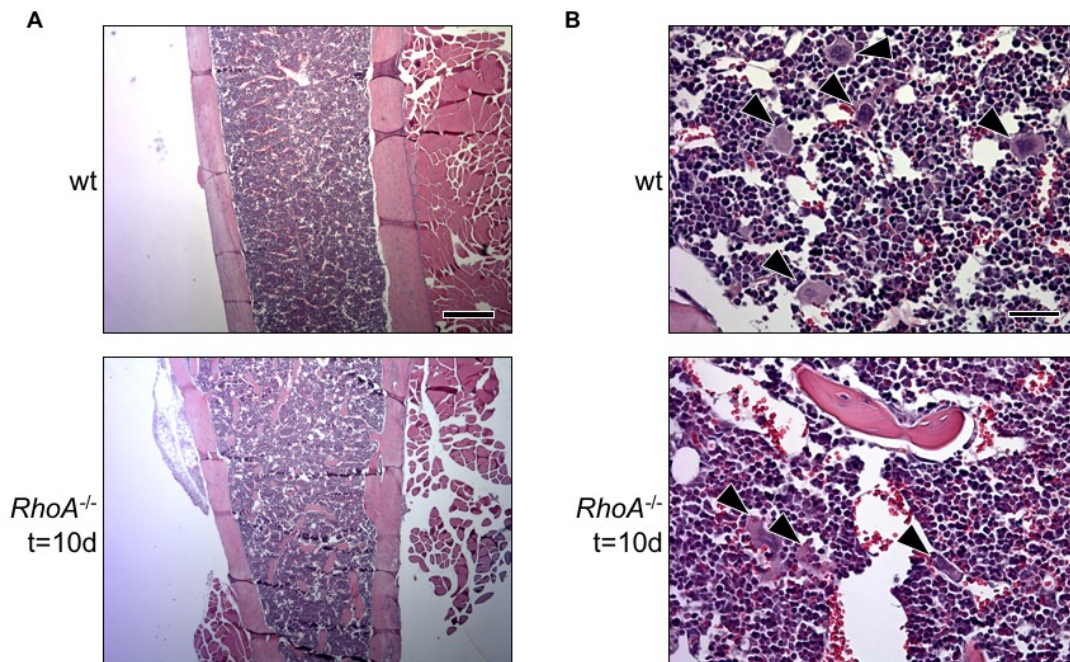
Fig. 21. Bone marrow sections of *RhoA⁻/⁻* and wt mice obtained at day 10 after platelet depletion show similar morphology. (A) An overview at 5x magnification does not reveal major differences between *RhoA⁻/⁻* (t=10d) and the wt (t=10d) regarding BM structure. Scale bar: 480µm. (B) Detailed view at 40x magnification: *RhoA⁻/⁻* and wt MKs exhibit similar morphologies. Arrows depict MKs. Scale bar: 60 µm.

Examination of the spleen was additionally performed in order to investigate potential changes elsewhere in the murine hematopoietic system. Comparison of antibody-injected *RhoA⁻/⁻* and wt mice revealed no divergence in MK numbers in this organ, neither regarding organ architecture, nor MK appearance (Fig. 22, 23). Together, these findings indicate that RhoA does not play a major role for the recovery of megakaryopoiesis under acute stress.
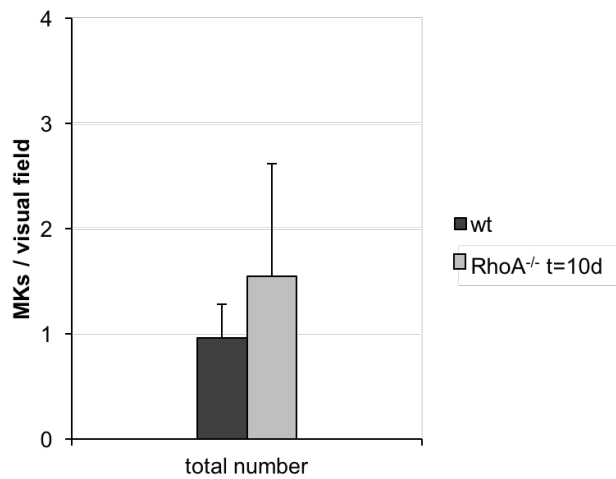
Fig. 22. MK numbers are on an equal level 10 days after antibody injection in *RhoA*^{-/-} and wt mice spleens. *RhoA*^{-/-} and wt spleens exhibit similar counts of MKs in the spleen (t=10d) after GPIb antibody injection. Single experiment with n=6 mice per group.
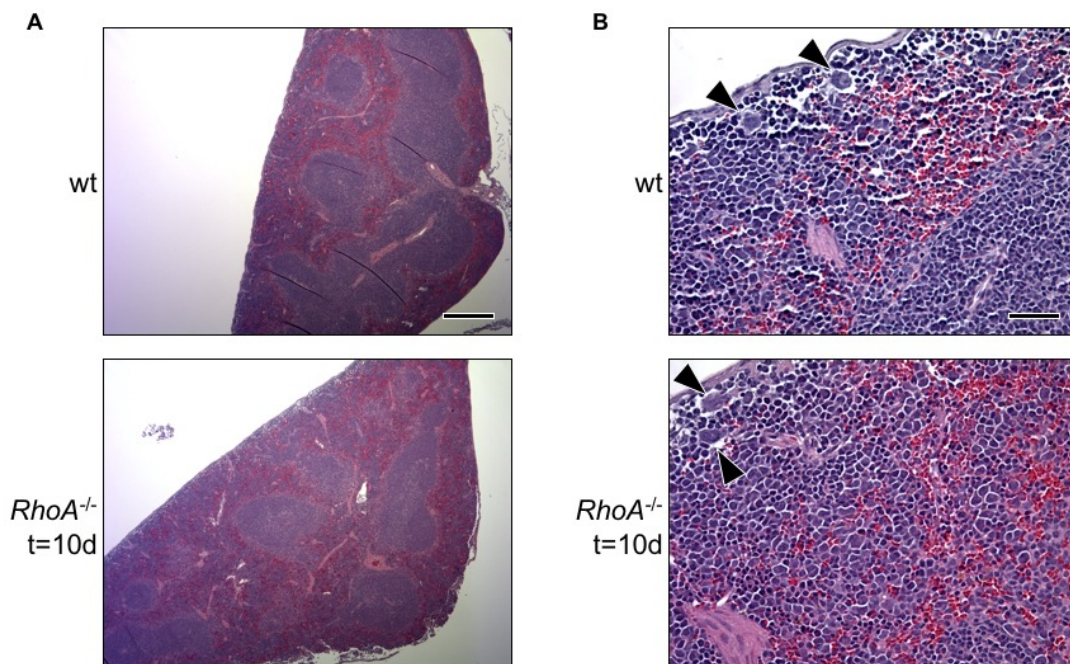
Fig. 23. Comparable spleen morphology 10 days after platelet depletion in *RhoA*^{-/-} and wt mice. (A) Left panel depicting spleen morphologies at a lower magnification (5x) of both *RhoA*^{-/-} (t=10d) and wt (t=10d) mice. Scale bar: 480 µm. (B) Right panel with a detailed view (40x magnification) of MK morphology in the spleen. Arrows depict MKs. Scale bar: 60 µm.

3.2.2 Effect of blockade of important MK surface receptors on MK localization in *RhoA*^{-/-} mice

3.2.2.1 Integrin αIIbβ3 blockade does not alter MK compartmentalization in RhoA^{-/-} mice

Integrin αIIbβ3 is instrumental in platelet activation and mediates a great variety of effects required for physiological hemostasis such as firm adhesion to the ECM and cross-linking of platelets to allow a growing platelet plug. Functioning as adhesion molecules[32,87], MKs might likely depend on their function during BM egress from the stroma towards the lumen of BM sinusoids.

Therefore, investigation of the effect of in vivo blockade of integrin αIIbβ3 was conducted with special focus on the intraluminal compartment, being best accessible and susceptible to antibody injection.

RhoA^{-/-} and wt mice were injected intravenously (i.v.) into the retroorbital plexus three times with 100µl of 4H5 F(ab)$_2$ fragments (IgG2b) on consecutive days and bones were harvested on day 5. Michael Popp kindly provided, genotyped and injected mice according to protocol.

Analysis of integrin αIIbβ3 blocked-*RhoA*^{-/-} (*RhoA*^{-/-} 4H5 F(ab)$_2$) mice showed that the RhoA knock-out phenotype was preserved and a significantly higher number of MKs were located intraluminally and adjacent to the endothelial lining of BM sinusoids compared to likewise treated wt (wt 4H5 F(ab)$_2$), see Fig. 24. Stimulating effects on megakaryopoiesis could not be observed, as total numbers of MKs remained constant compared with non-injected *RhoA*^{-/-} and wt mice (Fig. 25). Consistently, histological study of the BM of the dissected femura did not reveal an alteration in BM architecture (Fig. 26).
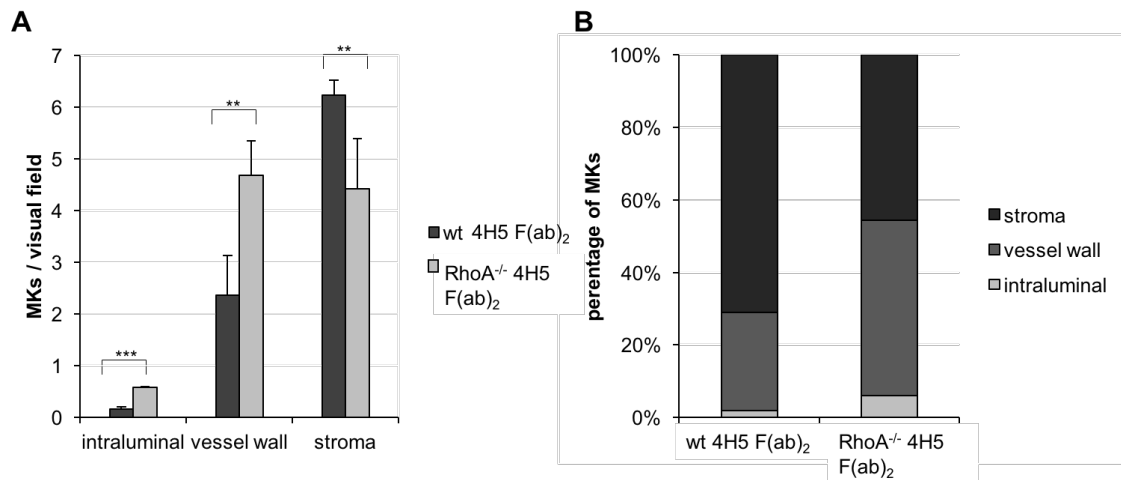
Fig. 24. MKs of *RhoA*^{-/-} 4H5 F(ab)₂ mice show similar compartmentalization as compared to *RhoA*^{-/-} mice. (A) MKs of *RhoA*^{-/-} 4H5 F(ab)₂ mice rest intraluminally and adjacent to the vessel wall more often than in the stroma related to wt 4H5 F(ab)₂ mice. (B) Percentagewise depiction of MKs for better comparison. Single experiment with n=4 mice per group (*RhoA*^{-/-}/wt 4H5 F(ab)₂). *** p < 0.001, ** p < 0.01.
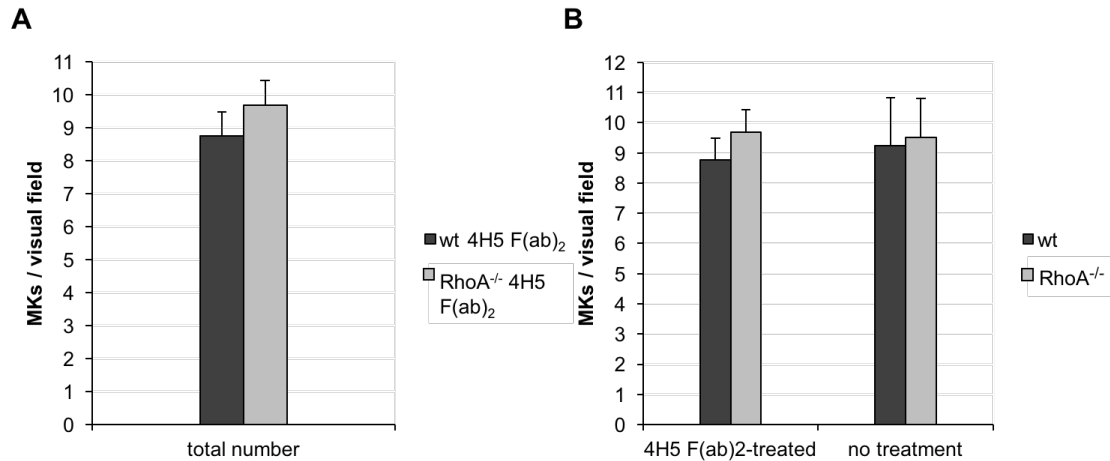
Fig. 25. Total numbers of MKs of 4H5 F(ab)₂-injected *RhoA*^{-/-} and wt mice are comparable to non-injected mice. (A) Depiction of *RhoA*^{-/-} and wt mice receiving antibody-mediated integrin αIIbβ3 blockade. Similar MK counts were found in both groups. (B) Comparison of 4H5 F(ab)₂-injected mice to non-injected *RhoA*^{-/-} and wt mice. Data for *RhoA*^{-/-} mice are taken from Fig. 2. n=4 mice per group (*RhoA*^{-/-}/wt 4H5 F(ab)₂).
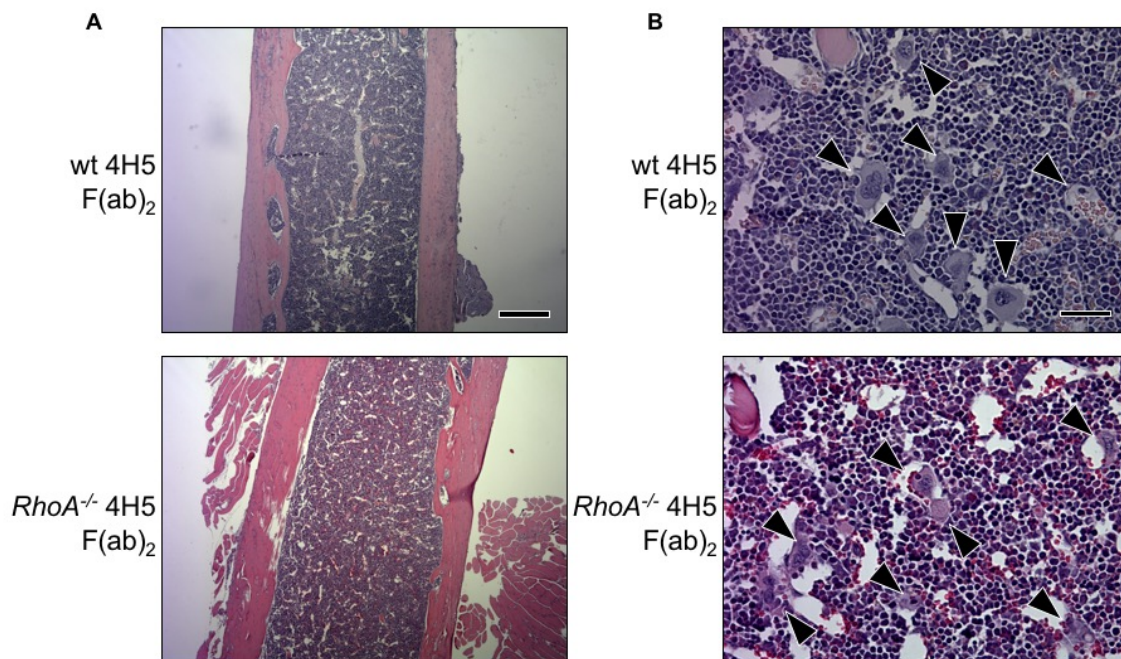
Fig 26. BM architecture and MK morphology is similar in _RhoA_^{-/-} 4H5 F(ab)₂ and treated wt mice. (A) 5x magnified overview of BM sections does not reveal differences in morphology of integrin αIIbβ3-attenuated _RhoA_$^{-/-}$ and wt mice. Scale bar: 480µm. (B) Close-up view at 40x magnification shows unaltered MK structure for injected _RhoA_$^{-/-}$ and wt mice. Arrows depict some MKs. Scale bar: 60 µm.

Although of major importance in platelet signaling, blockade of integrin αIIbβ3 did not lead to changes in the phenotype of _RhoA_$^{-/-}$ mice with regard to MK localization in the BM. Thus integrin αIIbβ does not seem to be required for neither the transmigration of deficient MKs into BM sinusoids, nor the adhesion to the vessel wall once inside.

3.2.2.2 Blockade of GPVI does not substantially alter intraluminal localization of RhoA$^{-/-}$ MKs

Glycoprotein VI (GPVI) is the central platelet collagen receptor[235] which might also indicate a role for GPVI in MK interaction with elements of the extracellular matrix. To address the effects of a GPVI blockade, _RhoA_$^{-/-}$ and littermate wt mice were injected with 100µl of JAQ-1 IgG2a antibody on day 1 and 3. Mice were generously provided, genotyped and injected by Michael Popp.

Although no statistical significant difference in intraluminal MKs could be

observed in *RhoA*$^{-/-}$ GPVI blocked (*RhoA*$^{-/-}$ JAQ-1) mice compared to likewise treated wt JAQ-1 mice, the phenotype of an increased number of MKs inside of BM sinusoids persisted. Taking into account the stromal and vessel-wall adjacent distribution of MKs, it can be concluded that GPVI blockade does not influence the ability of *RhoA*$^{-/-}$ to transmigrate into BM sinusoids (Fig. 27). An effect of GPVI blockade on total MK numbers in the BM could not be found (Fig. 28). Furthermore, BM examination showed no obvious alterations in MK morphology (Fig. 29).
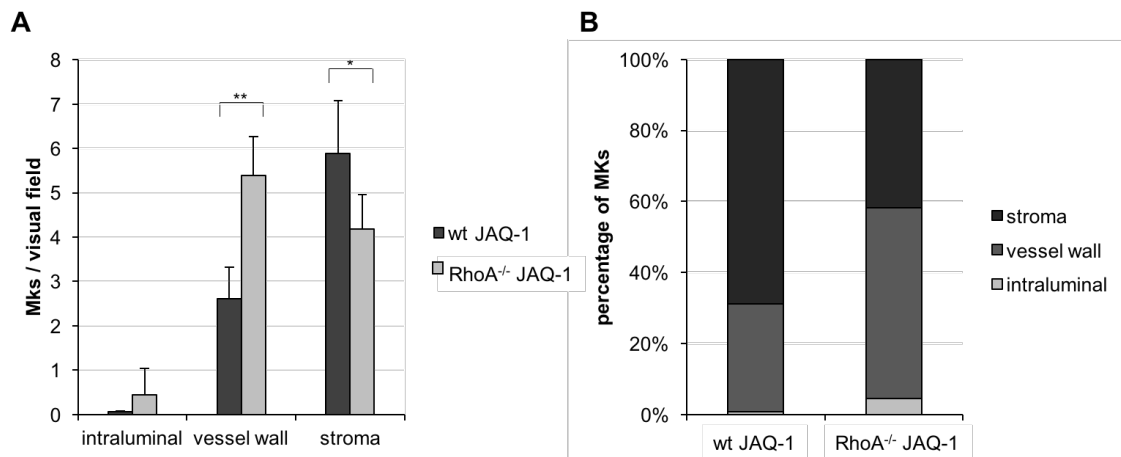
Fig. 27. JAQ-1-treated *RhoA*$^{-/-}$ and wt mice display similar levels of intraluminal MKs. (A) BM sections of JAQ-1-injected *RhoA*$^{-/-}$ and wt mice show a similar distribution of MKs, compared to non-injected *RhoA*$^{-/-}$ and wt mice with intraluminal and vessel-adjacent populations being increased under *RhoA*$^{-/-}$ conditions. (B) Percentagewise depiction of MKs for better comparison. Data for *RhoA*$^{-/-}$ mice are taken from Fig.2. Single experiment with n=3 (*RhoA*$^{-/-}$ JAQ-1) and n=4 (wt JAQ-1) per group. ** $p < 0.01$, * $p < 0.05$.
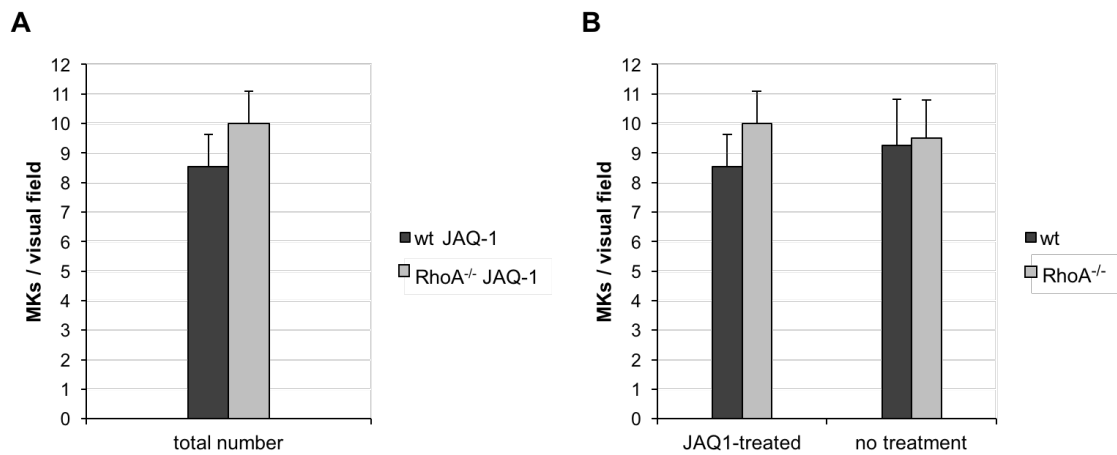
Fig. 28. Total MK numbers in BM of *RhoA*$^{-/-}$ JAQ-1 and injected wt mice are similar. (A) *RhoA*$^{-/-}$ JAQ-1 and wt JAQ-1 mice exhibit no significant difference in MK numbers. (B) The BM of *RhoA*$^{-/-}$ JAQ-1 and comparable wt mice contains a similar number of MKs compared to non-injected mice. Data for *RhoA*$^{-/-}$ mice are taken from Fig. 2. n=3 (*RhoA*$^{-/-}$ JAQ-1) and n=4 (wt JAQ-1) mice per group.
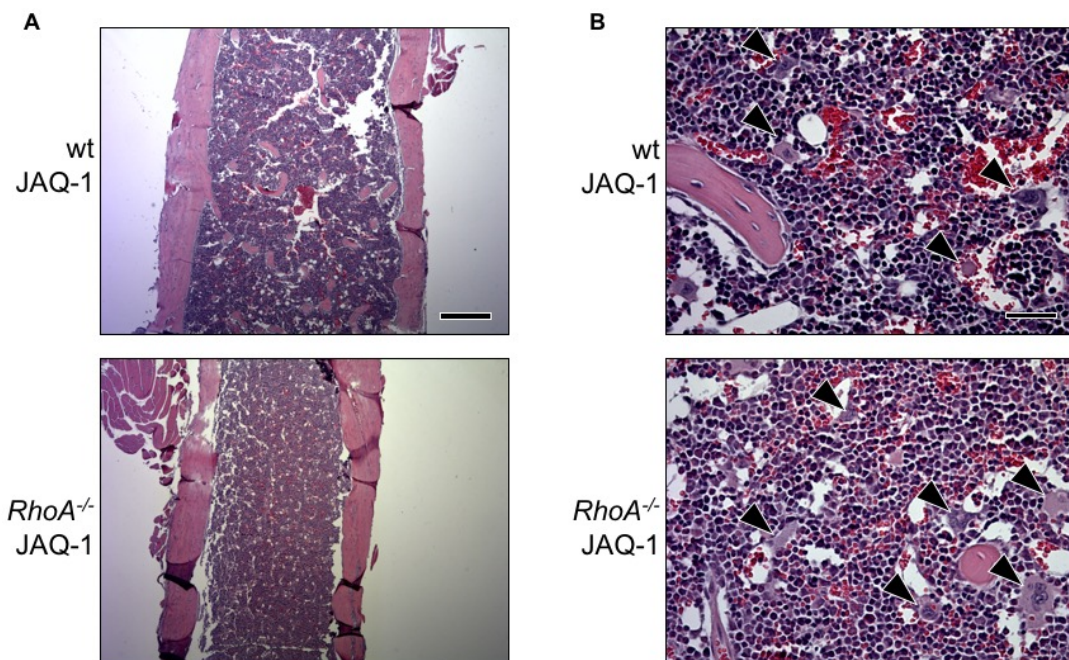
Fig. 29. Histological evaluation of *RhoA*$^{-/-}$ JAQ-1 and injected wt mice exhibit physiological phenotypes. (A) Overview at 5x magnification displays BM morphology for both *RhoA*$^{-/-}$ JAQ-1 and wt JAQ-1 mice. Scale bar: 480 μm. (B) Detailed view at 40x magnification showing regularly configured MKs in GPVI blocked mice. Arrows depict MKs. Scale bar: 60 μm.

These findings suggest that transmigration and adherence to the vessel wall of MKs happens independently of GPVI and might involve signaling through

different receptors and ECM proteins.

3.2.2.3 Blockade of the Clec-2 receptor does not have a major influence on MK compartmentalization in RhoA$^{-/-}$ mice

The C-type lectin-like receptor 2 (Clec-2) is physiologically activated by podoplanin and has been studied with regard to antithrombotic and antimetastatic therapy in hematology and cancer medicine[236]. Signaling occurs through a hemi immunoreceptor tyrosine-based activation motif (ITAM) and is hereby similar to GPVI-mediated signaling via the double YxxL ITAM.

Analogous to injection of a GPVI depleting antibody, treatment with the INU1 antibody results in the transient loss of the Clec-2 receptor from the platelet and MK surface, yielding a knock-out like phenotype.

Both *RhoA$^{-/-}$* and wt mice were injected with 100µl INU1 (IgG1) antibody on days 1 and 3 with bone dissection following on day 5. Michael Popp kindly provided, genotyped and injected mice according to protocol.

RhoA$^{-/-}$ INU1 mice showed slightly non-significantly increased numbers of intraluminal MKs, while MKs adjacent to the vessel wall were significantly increased compared to injected wt INU1 mice, reproducing the results of the *RhoA$^{-/-}$* JAQ1 mice (Fig. 30). The total number of MKs in BM sections of *RhoA$^{-/-}$* INU1 mice differed from non-injected *RhoA$^{-/-}$* mice, as they exhibited a higher number of MKs (Fig. 31). Morphology of the analyzed BM and MKs were not found to diverge in *RhoA$^{-/-}$* INU1 and likewise treated wt mice (Fig. 32).
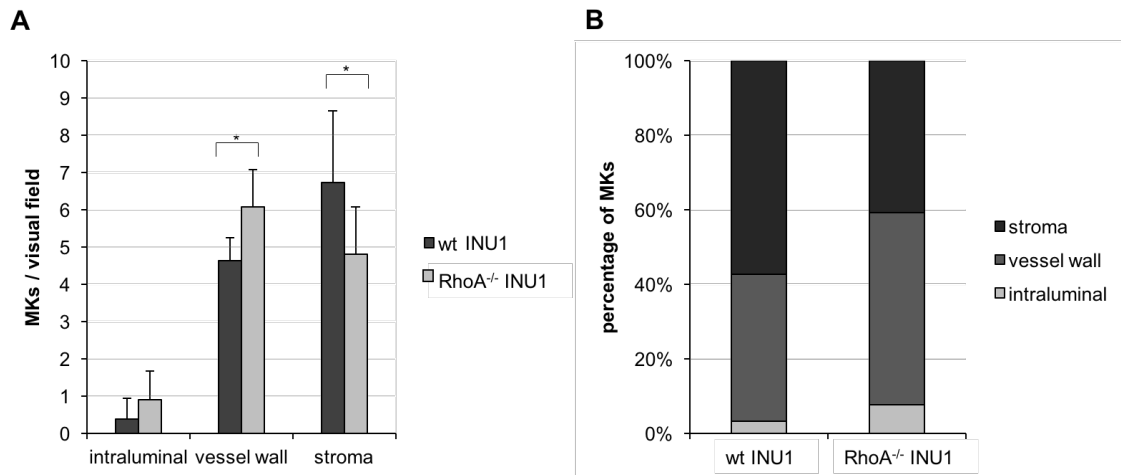
Fig. 30. *RhoA*^{-/-} **and wt INU1 mice exhibit similar numbers of intraluminal MKs in the BM.** (A) *RhoA*^{-/-} INU1 and wt INU1 controls do not differ from in intraluminal MK localization from their untreated counterparts. Vessel wall MKs were thus increased in *RhoA*^{-/-} INU1 mice, whereas the stromal population was elevated in the wt INU1 mice. (B) Depiction as percentages for better comparison. Single experiment with n=5 (*RhoA*^{-/-} INU1) and n=6 (wt INU1) mice per group. * p < 0.05.
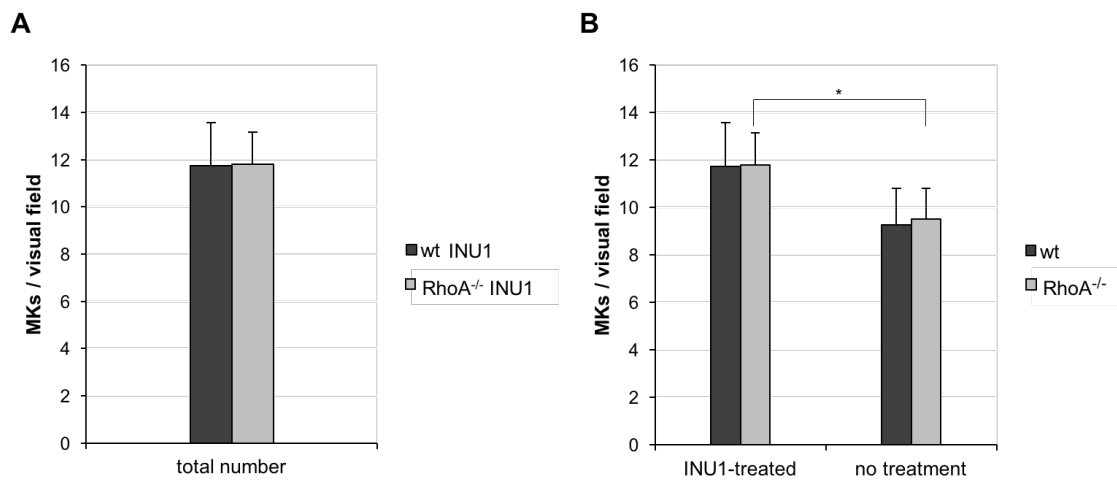
Fig. 31. The total number of MKs of *RhoA*^{-/-} INU1 and antibody-treated wt mice in the BM is equal, but totals of *RhoA*^{-/-} INU1 mice were higher compared to non-treated mice. (A) Blockade of the Clec-2 receptor does not lead to different MK levels in *RhoA*^{-/-} INU1 and wt INU1 mice. (B) Attenuation of Clec-2 leads to an increase of MK totals in the BM of *RhoA*^{-/-} mice, compared to uninjected *RhoA*^{-/-} mice. Data for *RhoA*^{-/-} mice are taken from Fig. 2. n=5 (*RhoA*^{-/-} INU1) and n=6 (wt INU1) mice per group. * p < 0.05.
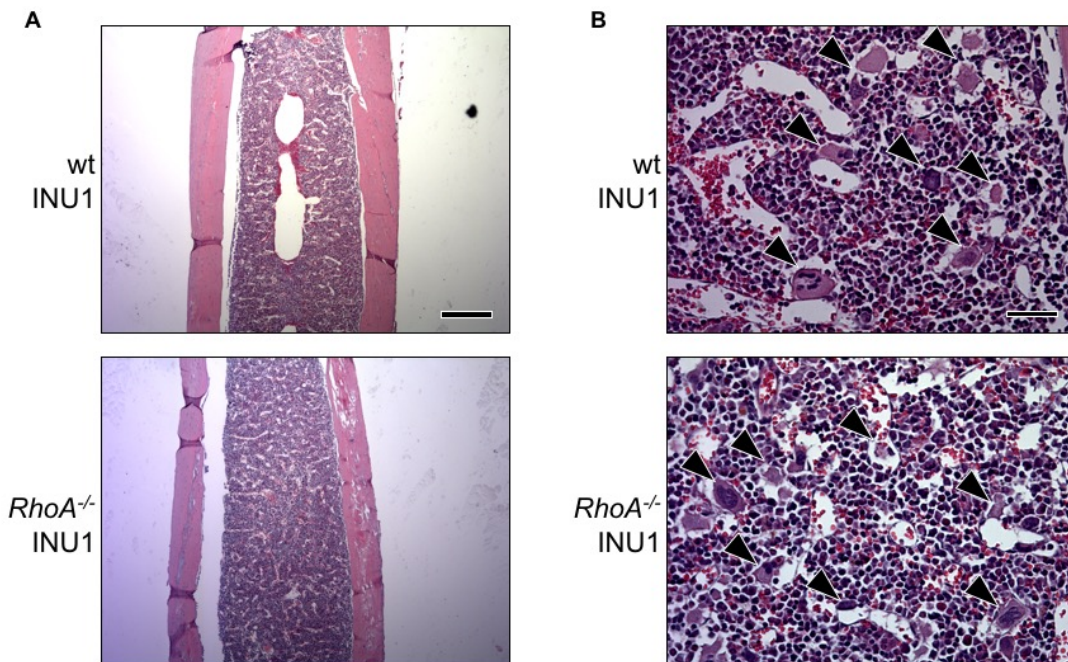
Fig. 32. BM sections reveal similar morphology of *RhoA*$^{-/-}$ INU1 and injected wt mice. (A) Left panel depicts an overview at 5x magnification exhibiting equal BM structure of *RhoA*$^{-/-}$ INU1 and corresponding wt INU1 mice. Scale bar: 480µm. (B) Right panel with a higher magnification (40x) highlighting comparable MK morphology between the injected mice. Arrows depict MKs. Scale bar: 60 µm.

In summary, these results show that after blockade of the Clec-2 receptor the compartmentalization effect of RhoA deficiency is unaltered and therefore suggests signaling through (hem)ITAM-independent pathways. With respect to MK numbers in the BM, blockade of Clec-2 has a slight effect in terms of an increase of total numbers of MKs in *RhoA*$^{-/-}$ mice, although this needs to be validated in further experiments with introduction of a non-injected control group.

3.2.2.4. Blockade of GPV in RhoA$^{-/-}$ mice does not affect compartmentalization deficit of MKs in the BM

GPV is closely associated with the GPIb-IX complex through a transmembrane domain and takes part in GPIb-mediated signaling in the presence of von Willebrand factor (vWF), thrombin or factors XI and XII[237]. The GPIb-IX-V receptor complex mediates adhesion of platelets during coagulation and therefore might be of importance already during migration and adhesion of MKs in the BM. In this regard, defective GPV could constitute signaling changes which

is why GPV antibody-injected $RhoA^{-/-}$ ($RhoA^{-/-}$ 89F12) and comparable wt (wt 89F12) mice were investigated accordingly.

Mice were kindly provided, genotyped and injected by Michael Popp. On day 1 through 3, 100µl of DOM1/89F12 (IgG2a) antibody were injected into the retroorbital plexus and dissection of bones was performed on day 5.

Compartmentalization analysis of $RhoA^{-/-}$ 89F12 resulted in a significant increase in vessel wall adjacent MKs in $RhoA^{-/-}$ 89F12 mice. In addition, the intraluminal population was higher in GPV antibody-treated $RhoA^{-/-}$ than in equally injected wt mice, whereas the stromal population was lower (Fig. 33). Of note, total numbers of MKs in the BM were increased in $RhoA^{-/-}$ 89F12 compared to treated wt mice, whereas MK counts were on a comparable level between injected wt and non-injected mice (Fig. 34). Analysis of BM sections and MKs did not show altered architecture and MK morphology in $RhoA^{-/-}$ 89F12 or equally injected wt mice (Fig. 35).
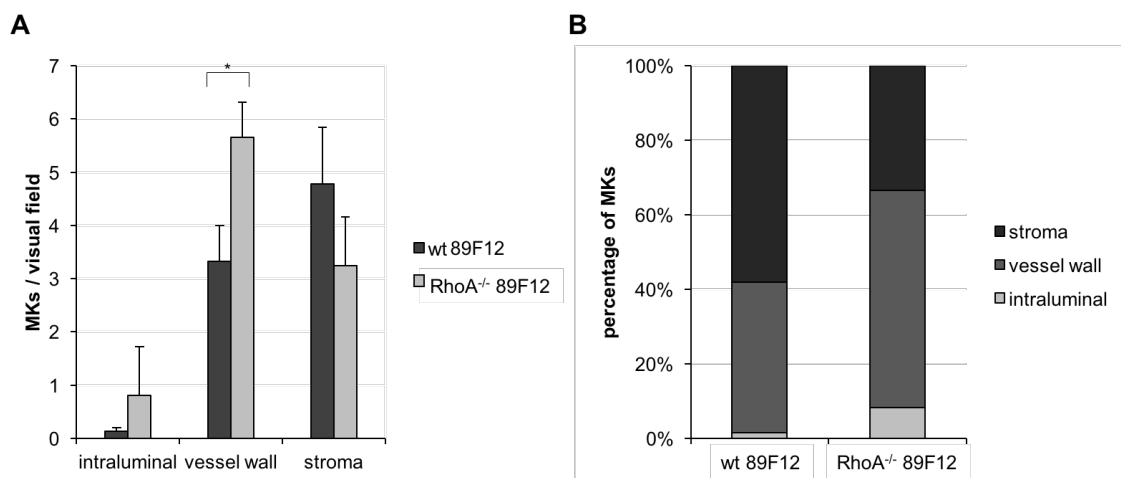
Fig. 33. $RhoA^{-/-}$ 89F12 mice and antibody-injected wt controls differ in the totals of MKs adjacent to the vessel wall. (A) The table depicts the number of MKs in the GPV blockade condition for $RhoA^{-/-}$ 89F12 and wt 89F12 mice respectively, according to BM compartment. Counts are significantly different in MKs adjacent to the vessel. (B) Percentagewise depiction for better comparison. Single experiment with n=3 ($RhoA^{-/-}$ 89F12) and n=4 (wt 89F12) mice per group. * $p < 0.05$.
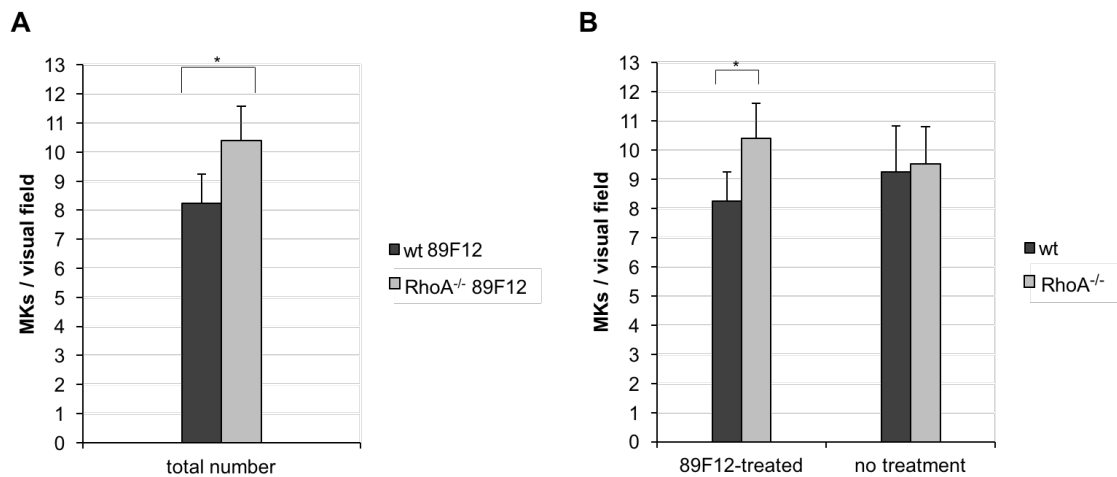
Fig. 34. *RhoA^{-/-}* 89F12 mice show increased MK numbers compared to equally treated wt mice. (A) Total counts of MKs were found to be higher in *RhoA^{-/-}* 89F12 mice than equally injected wt 89F12 mice. (B) MK numbers were on a comparable level with untreated mice. Data for *RhoA^{-/-}* mice are taken from Fig. 2. n=3 (*RhoA^{-/-}* 89F12) and n=4 (wt 89F12) mice per group. * p < 0.05.
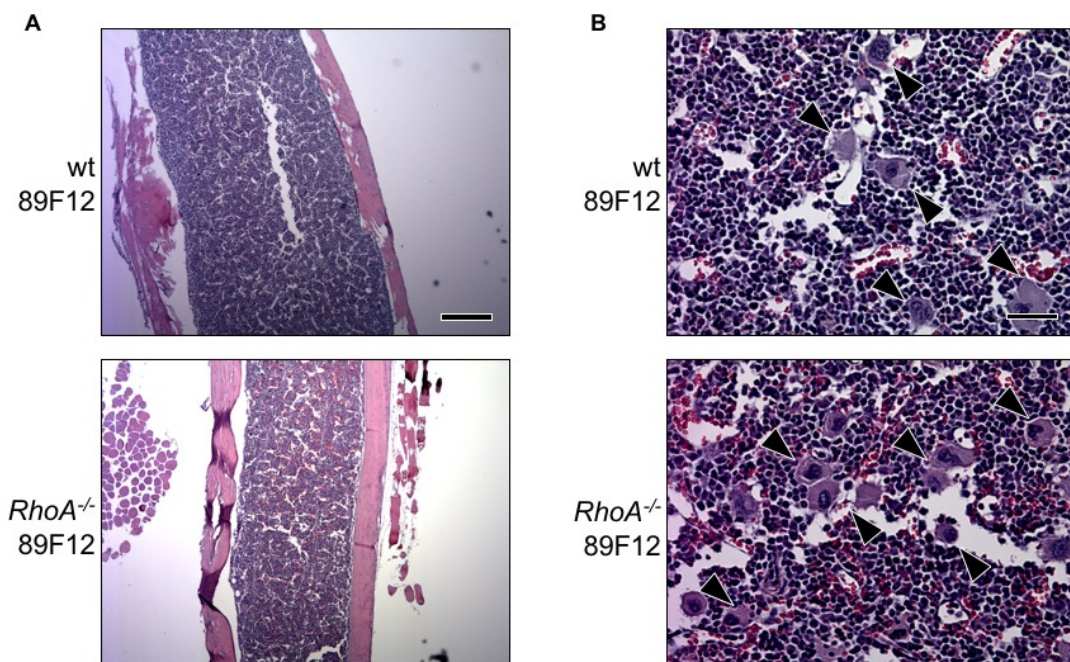
Fig. 35. BM structure and MK morphology are not affected by injection of GPV antibody in *RhoA^{-/-}* and wt mice. (A) Overview at 5x magnification displays equivalent BM configuration of both injected *RhoA^{-/-}* 89F12 and corresponding wt 89F12 mice. Scale bar: 480µm. (B) Close-up view at 40x magnification depicts unaltered MK morphology between *RhoA^{-/-}* 89F12 and wt 89F12 mice. Arrows depict MKs. Scale bar: 60 µm.

Together *RhoA^{-/-}* 89F12 mice show a similar phenotype as observed in non-

treated $RhoA^{-/-}$ mice, but GPV blockade in $RhoA^{-/-}$ mice might lead to a moderate increase in megakaryopoiesis. This finding needs to be validated in subsequent studies including a control group.

3.3 Characterization of the role of RhoF deficient in platelets using conditional knock-out mice

The small GTPase RhoF has been a more recent addition to the Rho family of small GTPases and it is presumed to play a role in filopodia formation[156]. There is evidence that RhoF-generated filopodia are longer and thinner than filopodia induced by Cdc42, raising the questions if different subtypes of filopodia exist[70,123]. Aim of this study was to characterize the role of RhoF in platelets to complement recently published results[161] and to study $RhoF^{-/-}$ platelets extensively in their behavior regarding filopodia formation. For this purpose, mice containing loxP sites introduced into the RhoF gene ($RhoF^{fl/fl}$) were successfully generated and crossed with PF-4 Cre transgenic mice, creating $RhoF^{fl/fl,PF-4Cre+/-}$ (further referred to as $RhoF^{-/-}$) mice, thereby eliminating RhoF expression in MKs and platelets. Mice were kindly provided and genotyped by Sebastian Dütting and Sylvia Hengst.

3.3.1 Analysis of platelet activation in $RhoF^{-/-}$ mice by flow cytometry

3.3.1.1 Platelet count and size and glycoprotein expression in $RhoF^{-/-}$ and wt mice

Flow cytometric and Sysmex® analysis of $RhoF^{-/-}$ platelets showed ko and wt platelets were similar in count and size (data not shown).

These findings suggest that megakaryopoiesis is not affected in $RhoF^{-/-}$ deficiency. This was later supported by investigation of the platelet life span in vivo which was found to be unaltered in $RhoF^{-/}$ mice compared to the wt[161].

Differences in glycoprotein surface expression levels have to be considered in diverging signaling responses upon agonist stimulation in platelets. To address this issue, GP expression in $RhoF^{-/-}$ platelets was studied. Components of the

GPIb-IX-V complex were similar in quantitative expression in $RhoF^{-/-}$ platelets compared to the wt. Glycoprotein CD9 also exhibited same expression levels in both groups. Integrins αIIbβ3, α2 and β1 were neither found to differ in the knock-out nor the wt, constituting regular integrin expression in $RhoF^{-/-}$ mice. The collagen receptor GPVI and Clec-2 receptor were equally expressed in $RhoF^{-/-}$ and wt mice (Fig. 36). In summary, RhoF deficiency was not associated with altered platelet surface receptor expression levels.
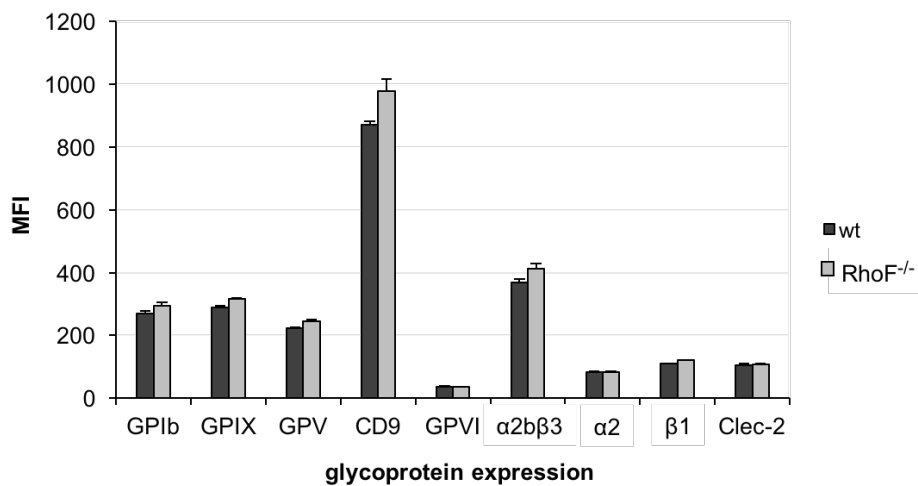
Fig 36. Expression of important platelet surface receptors as determined by flow cytometry.
No alterations could be found between $RhoF^{-/-}$ and wt mice for all glycoproteins. Results depicted as means ± SD. Representative experiment with n=4 mice per group.

3.3.1.2 Unaltered integrin αIIbβ3 activation in RhoF$^{-/-}$ platelets

Measurement of platelet activation in $RhoF^{-/-}$ mice was conducted through evaluation of levels of active integrin αIIbβ3 levels upon agonist stimulation, with integrin αIIbβ3 constituting the most abundant platelet integrin[238,239].

Platelet activation assays showed no major difference in $RhoF^{-/-}$ platelets compared to the wt in integrin αIIbβ3 activation. Upon stimulation with the agonists ADP and the TxA2 mimetic, U-46619 (U-46) $RhoF^{-/-}$ and wt platelets showed only moderate signs of activation, visible in a slight increase in mean fluorescence intensity (MFI). ADP and U-46 combined function as a strong activator of platelets, but no differences in the response of $RhoF^{-/-}$ and wt platelets

were observed. Thrombin signaling, irrespective of the used concentration, was likewise found to be unaltered in both *RhoF*^{-/-} compared to wt platelets. Taken together, activation of *RhoF*^{-/-} platelets through G_{13} and G_q receptors seems unaltered. Epinephrine as an agonist of the G_z receptor did not induce different responses in *RhoF*^{-/-} and wt platelets either. ITAM and (hem)ITAM mediated pathways of platelet activation represented by signaling via the agonists collagen-related peptide (CRP), convulxin (CVX) and rhodocytin (RC) overall elicited a higher response in *RhoF*^{-/-} than wt platelets for almost all tested concentrations (Fig. 37), but this finding could not reproduced in following experiments, suggesting technical problems in the activation setting with the wt. Therefore, we conclude that these results indicate that RhoF deficiency has no impact on platelet activation, at least under in vitro conditions.
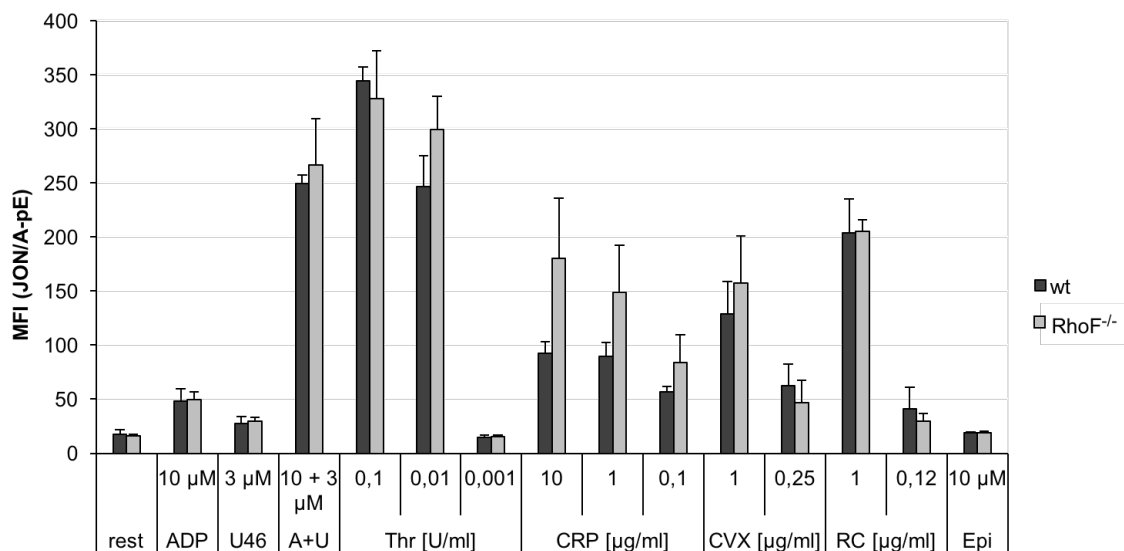
Fig. 37. Integrin αIIbβ3 activation assay shows comparable results in *RhoF*^{-/-} and wt mice. Signaling through major platelet receptors is similar and also unaffected by concentration in *RhoF*^{-/-} platelets. Binding of JON/A-PE antibody constitutes mean fluorescence intensity (MFI). Results presented as means ± SD. n=4 mice per group.

3.3.1.3 α granule release is not impaired in RhoF^{-/-} platelets

Another component of great significance in platelet activation is the ability to release stored granules, thereby sustaining platelet activation through autocrine signaling[87]. Investigation of α granule release can be studied by assessment of

P-Selectin levels, as it can be found on platelet α granules[18]. Granule release is mediated by fusion of platelet granules with the platelet surface membrane, thus making P-Selectin accessible for antibody binding and subsequent analysis by flow cytometry.

P-Selectin surface exposure as a marker of degranulation effectiveness upon stimulation was shown to be equal in $RhoF^{-/-}$ and wt platelets, regarding ADP, U-46 or combined stimulation. Thrombin stimulation yielded comparable results for knock-out and wt mice at all studied concentrations and precludes major defects in G_{13} and G_q signaling. Stimulation with the agonists CRP, CVX and RC through receptors GPVI and Clec-2 exhibited similar results in both groups. Finally, also G_z signaling assessed by the weak agonist epinephrine completed analysis of degranulation potency and was unaltered in both $RhoF^{-/-}$ and wt platelets (Fig. 38).
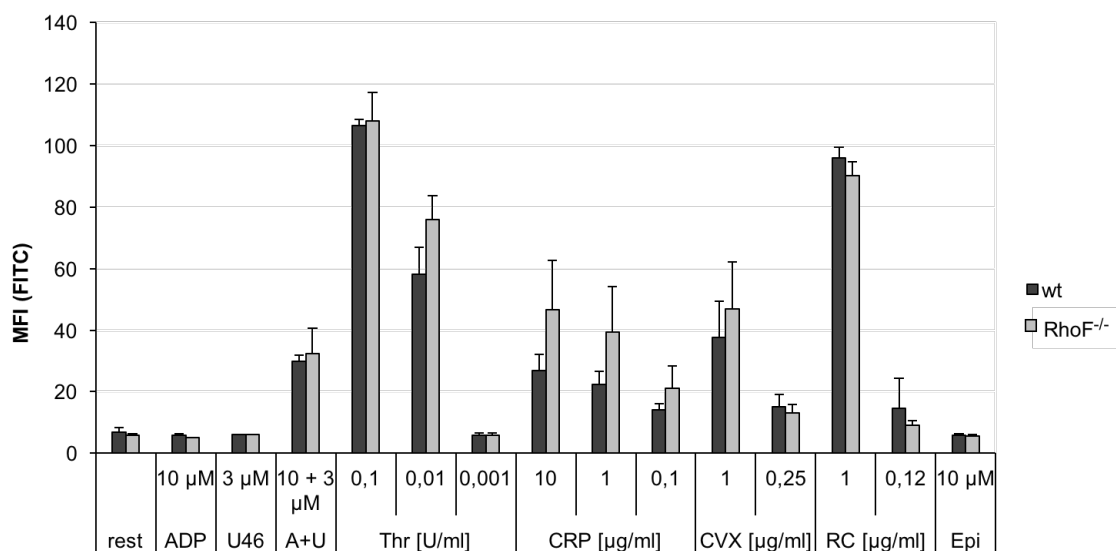
Fig. 38. Granule release is fully functional in $RhoF^{-/-}$ mice. P-Selectin exposure as a marker for platelet degranulation is equal in knock-out and wt mice, precluding signaling defects in major platelet receptors and is not affected by concentrations of the studied agonists either. Binding of anti P-Selectin-FITC antibody constitutes mean fluorescence intensity (MFI). Results given as means ± SD. n=4 mice per group.

The findings of sections 3.3.1.2 and 3.3.1.3 suggest that RhoF is dispensable in platelet activation and granule release in response to agonist stimulation, reproducing results of a similar study[161].

3.3.2 Platelet spreading of *RhoF^{-/-}* mice evaluated by two different agonists

3.3.2.1 RhoF^{-/-} platelets spread normally on fibrinogen

The extracellular matrix component and agonist surface fibrinogen is commonly used to assess platelet spreading. Fibrinogen is recognized by integrin αIIbβ3 and induces outside-in signaling leading to cytoskeletal rearrangements necessary for platelet spreading[240,241]. RhoF has been proposed to be essential for filopodia formation in various cell lines.

To investigate a potential involvement of RhoF in platelet spreading, *RhoF^{-/-}* and wt platelets were allowed to adhere to and spread on fibrinogen-treated glass cover slips and studied at three different time points upon thrombin stimulation.

RhoF^{-/-} platelets were found to spread similarly in comparison to their wt counterparts at all studied time points. Most interestingly, filopodia formation was not impaired in *RhoF^{-/-}* platelets (Fig. 39).
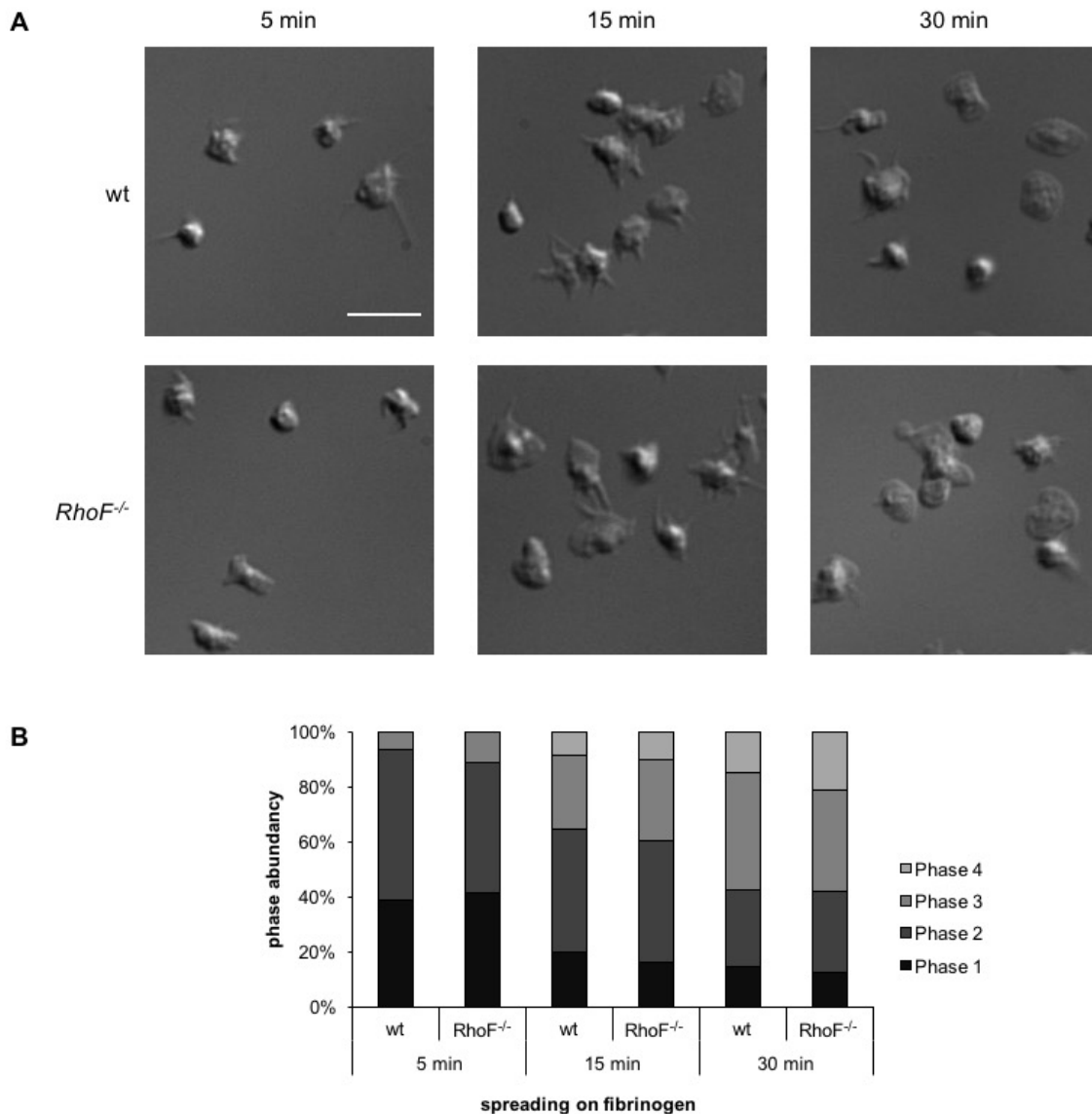
Fig. 39. Spreading of platelets on fibrinogen is unaffected by knockout of RhoF. (A) *RhoF^{-/-}* and wt platelets spread similarly on fibrinogen at 5 min, 15 min and 30 minutes. Upon activation, platelets start forming filopodia, later lamellipodia, before they become fully spread. Representative images of wt and *RhoF^{-/-}* platelets. Scale bar: 5 µm. (B) Results are displayed as stacked bars representing the mean percentage of platelets in each spreading phase. Notably, filopodia formation is not impaired in *RhoF^{-/-}* platelets. Phase1: Unspread platelets, phase 2: filopodia formation, phase 3: lamellipodia formation, phase 4: fully spread platelets. Representative experiment with n=3 mice per group.

3.3.2.2 Adhesion of RhoF^{-/-} platelets on immobilized vWF is similar to the wt

vWF binds to the GPIb-IX-V complex and this interaction helps platelets adhere at sites of vessel injuries, especially under high-shear conditions[239]. Platelet

spreading on immobilized vWF is attenuated with platelets only reaching the filopodial stage of spreading[242]. By use of this method subtle changes in spreading ability, especially regarding filopodia formation can be assessed.

RhoF$^{-/-}$ platelets were allowed to adhere to vWF immobilized on glass cover slips upon incubation with botrocetin to induce GPIb-IX-V signaling under static conditions. Integrilin which inhibits integrin αIIbβ3 was added additionally to prevent integrin activation. Three different time points were studied. In contrast to fibrinogen-mediated spreading, only three spreading stages were defined. Phase 1 comprised quiescent discoid platelets, phase 2 platelets forming 1-3 filopodia and phase 3 platelets with more than 3 filopodia. *RhoF*$^{-/-}$ platelets demonstrated unaltered filopodia formation compared to the wt at all studied time points. Thus, RhoF loss can be compensated effectively during platelet spreading (Fig. 40).
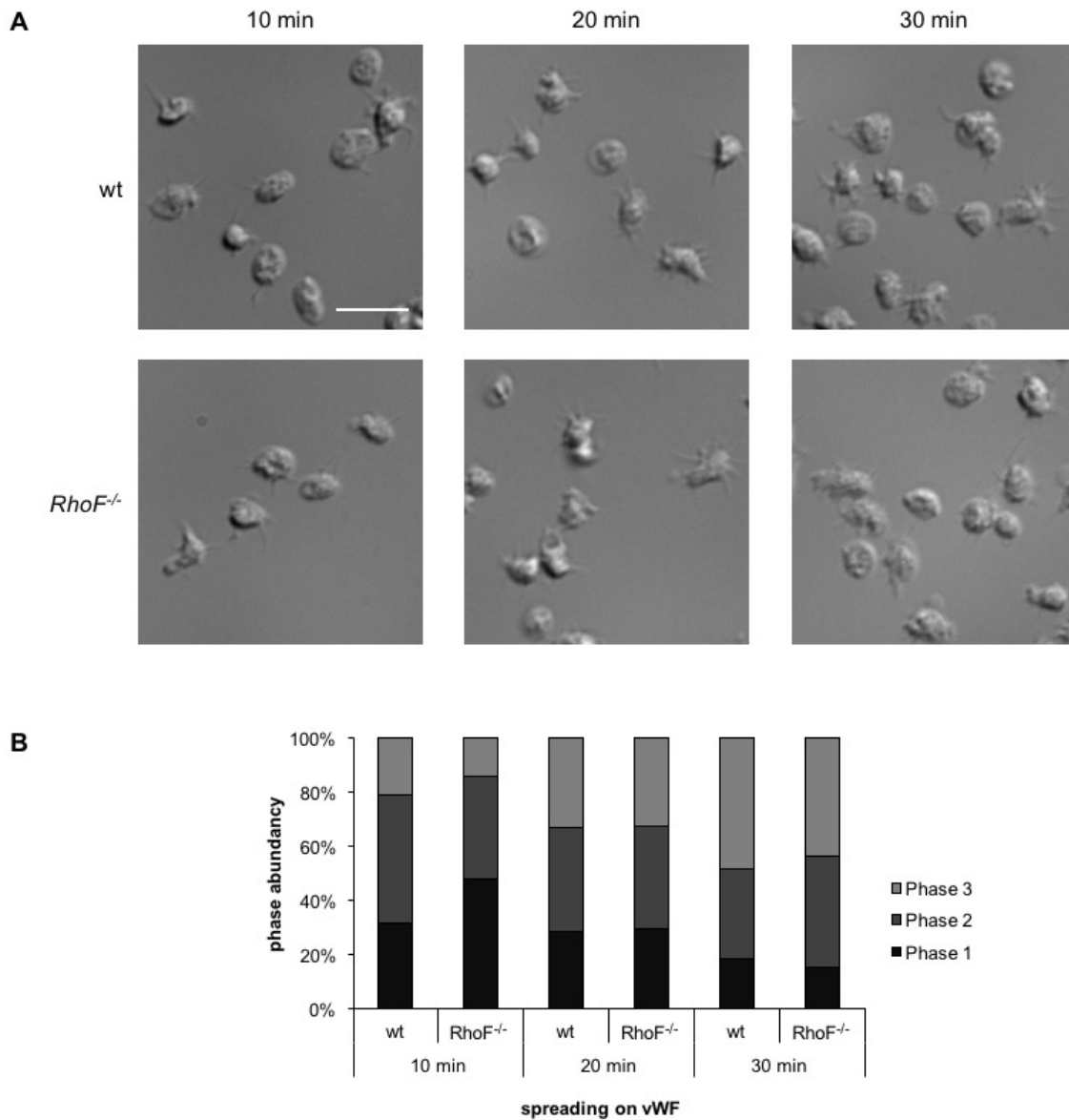
Fig. 40. Adhesion and filopodia formation of platelets on immobilized vWF is unaffected by knockout of RhoF. (A) *RhoF*^{-/-} and wt platelets spread similarly on vWF at 10 min, 20 min and 30 minutes. In vWF-mediated adhesion, only 3 phases of spreading are discriminated. Representative images of wt and *RhoF*^{-/-} platelets. Scale bar: 5 µm. (B) Results are displayed as stacked bars representing the mean percentage of platelets in each spreading phase. No significant difference in phase abundancy in *RhoF*^{-/-} and wt platelets can be detected. Representative experiment with n=3 mice per group.

In summary, platelet spreading of *RhoF*^{-/-} platelets on fibrinogen was not impaired and filopodia formation upon adhesion on VWF proceeded with no apparent defect. As mentioned earlier, Cdc42 has been described as another member of the Rho family significantly contributing to filopodia formation[72]. However, studies from our group performed after the completion of this thesis showed that filopodia

76

formation was unaffected in *RhoF/Cdc42* double-deficient platelets (unpublished results). Thus, other protein(s) seem to be required to facilitate filopodia formation in platelets.

4. Discussion

4.1 RhoA is a crucial regulator of MK localization and platelet biogenesis

The small GTPase RhoA plays an important role in actin cytoskeleton-driven remodeling processes in platelets including shape change, spreading and clot retraction[18,79,87]. This study focused on the role of RhoA in megakaryopoiesis and MK localization. Strikingly, a significant proportion of *RhoA*^{-/-} MKs was found inside BM sinusoids, ascribing a crucial role to RhoA in the transendothelial migration process. It is known that MKs extend proplatelets through gaps in the endothelial lining of BM sinusoids which accounts for the biggest proportion of produced platelets[3]. Additionally, whole MKs themselves can migrate into the intraluminal compartment through endothelial cells[4], but the cellular machinery and the physiological conditions under which this might preferentially occur have not been clarified. Fostering this observation, MKs can be found in the capillary bed of the lung which has been shown to be the result of migration, not of edaphic development[243,244,245,246].

Interestingly, proplatelet formation was shown to be regulated by RhoA through nonmuscular myosin II (NMII) activity. Myosin II consists of 2 heavy and 4 light chains and is the gene product of the MYH9 gene. Inhibition of MLC phosphorylation or absence of MYH9 increases proplatelet formation from MKs[19,247]. RhoA typically enhances MLC phosphorylation through ROCK which diminishes proplatelet formation in vitro[51], indicating that RhoA is a negative regulator of proplatelet formation. Therefore, the observed macrothrombocytopenia seems to be linked to the localization defect, rather than to deficiencies in proplatelet formation.

Recently, an additional model of platelet production through MK rupture was proposed under conditions of stress, such as acute thrombocytopenia or inflammation[248]. This research stems from the observation that MK maturation and platelet production can occur independently from TPO[249]. Moreover, in settings of acute hematopoietic/ megakaryocytic stress, e.g. irradiation or acute thrombocytopenia, HSCs were able to give rise to MKs and platelets directly without intermediaries[248,250,251,252]. The finding presented in this thesis that RhoA is crucial for MK localization at steady state indicated that it might also be an important regulator of megakaryopoiesis under stress conditions. However, the number of MKs at both early (1 day) and late (10 days) after experimentally induced thrombocytopenia was similar in BM of $RhoA^{-/-}$ and wt mice, not fostering the role of RhoA in this setting. At the same time, studies of time points in between day 1 and 10 seem warranted, as the platelet trough is most pronounced through the first few days and changes in MK numbers might occur only then, also with regard to the rupture model.

It is also relevant to discuss limitations of this part of the study. Conventional histological analysis of the compartmentalization of MKs in the BM using hematoxylin eosin stained sections can make the identification of knock-out MKs difficult, as they may be morphologically altered as for example $Cdc42^{-/-}$ MKs exhibit reduced invaginations and demarcation from the surrounding BM stromal cells [149]. Or they might undergo transmigration through the endothelial lining which could result in aberrant morphology as well. This might explain why in this work no increase of total MK numbers in the BM of $RhoA^{-/-}$ mice was observed, in contrast to published results[18]. $RhoA/Cdc42^{-/-}$ MKs exhibited higher numbers of MKs in the BM (see section 3.1.3), similar to findings from the Cdc42 single knock-out[149]. Additionally, MK numbers in the spleen were increased threefold, likely indicating severe stress and/ or inefficient megakaryopoiesis. Gross phenotypical assessment of BM structure and MKs themselves yielded comparable findings in $RhoA/Cdc42^{-/-}$ and wt MKs, but potentially left many structurally altered MKs unidentified. Due to this fact, MK counts in the $RhoA/Cdc42^{-/-}$ mice might be underreported by methods used in this work.

Indeed, after the completion of this thesis, analysis of immunofluorescently

stained cryo sections of whole femura enabled Sebastian Dütting and other members of the group[253] to show that *RhoA/Cdc42$^{-/-}$* MKs were almost completely clustered around BM sinusoids, while being unable to transmigrate into the vessel lumen. Dütting et al.[253] could demonstrate a regulatory circuit where RhoA functions as a stop-signal regarding MK transmigration while GPIb/Cdc42 signaling forms a go-signal. The observed macrothrombocytopenia is thus in part a direct result of the altered MK distribution and subsequently defective platelet biogenesis in vivo.

In this thesis, several potential signaling pathways regulating RhoA in MKs were investigated with the G-proteins G_{12} and G_{13} being obvious candidates, as they have been shown to be situated upstream of RhoA signaling in platelets[154]. While $G_{12/13}^{-/-}$ mice do not exhibit macrothrombocytopenia, redundant functions of the proteins in MK localization cannot not be excluded. However, the MK distribution was similar in $G_{12/13}^{-/-}$ mice compared to the wt, making a major contribution to RhoA signaling in MKs via these G proteins unlikely.

Integrin $\alpha IIb\beta 3$ is the most abundant platelet surface receptor, essential in platelet outside-in signaling, mediating stable adhesion and being crucial for platelet aggregation via binding of vWF and fibrinogen. Surprisingly, integrin $\alpha IIb\beta 3$ does not seem to be involved in the regulation of MK localization in the BM since its blockade in *RhoA$^{-/-}$* mice could not revert the MK mislocalization observed in non-injected *RhoA$^{-/-}$* mice. Whether other integrins, such as integrin $\beta 1$ are involved in the regulation of MK localization, remains elusive.

The platelet collagen receptor GPVI is a type I transmembrane protein of the Ig superfamily and transduces signals through its transmembrane region which interacts with the Fc receptor (FcR) γ-chain[235]. Inhibitory signaling via GPVI was recently proposed to be involved the spatial regulation of proplatelet formation in vivo[254]. However, transiently GPVI-deficient *RhoA$^{-/-}$* mice (treated by JAQ1 antibody) exhibited a similar MK mislocalization in the BM as observed in non-injected *RhoA$^{-/-}$* mice.

Similar to findings from JAQ1 treated *RhoA$^{-/-}$* mice, the MK mislocalization in *RhoA$^{-/-}$* mice could not be reverted by transient knock-out of Clec-2 by injection

of the INU1 antibody. Notably, INU1-treated $RhoA^{-/-}$ mice exhibited a statistically significant higher number of BM MKs than non-injected $RhoA^{-/-}$ mice. This effect could be due to the transient thrombocytopenia upon INU1 antibody injection[182] and the subsequent stimulation of megakaryopoiesis.

Taken together, the selective inhibition of (hem)-ITAM signaling pathways does not influence RhoA signaling in terms of MK migration and compartmentalization in the BM. While these findings are consistent with normal platelet counts and thus most probably normal thrombopoiesis in GPVI- or Clec-2 knock-out mice, they do not exclude a redundant function of the pathways in the process of platelet production.

Finally, also antibody (89F12)-mediated GPV-blockade in $RhoA^{-/-}$ mice was not able to revert the MK mislocalization observed in untreated mice. Thus, despite association of GPV with GPIb, GPV does not seem to be directly involved in the regulation of MK localization in the BM. This stands in contrast to in vivo blockade of GPIbα by treatment of mice with p0p/B Fab fragments, which after the completion of this thesis was shown to revert intrasinusoidal localization of $RhoA^{-/-}$ MKs. Nonetheless, the results presented in this part of the thesis were confirmed later by using immunofluorescently stained cryo sections[253], suggesting downstream signaling of the GPIb subunit of the GPIb-IX-V complex occurs irrespective of the functional state of GPV.

Limitations of all the conducted antibody blockade experiments include that i.v. injection regimen guarantees high availability of the antibody in the circulation and for intraluminal MKs, but tissue penetration capabilities are not easy to determine and may depend on the respective antibody.

4.2 RhoF is redundant in filopodia formation

A second part of this thesis focused on the investigation of RhoF, as $Cdc42^{-/-}$ mice were macrothrombocytopenic, while demonstrating regular filopodia formation[149]. With RhoF being hypothesized to be an important (independent) driver of filopodia formation[101], also associated changes of megakaryopoiesis were imaginable. In contrast to this speculation, platelet indices and platelet size

were comparable in *RhoF^-/-* and wt mice indicating that there is no major defect in megakaryopoiesis upon RhoF deletion. Additionally, activation and degranulation assays showed no overt phenotype for RhoF-deficient mice. Lastly, upon adherence to ECM proteins, i.e. vWF and fibrinogen RhoF-deficient platelets adhered and spread similar as compared to the wt. Together with the published work by Goggs et al.[161], these findings indicate a redundant role for RhoF in platelet biogenesis and function.

4.3 Concluding remarks and outlook

This work was targeted at studying the effects of various small GTPase single and double knock-outs on megakaryopoiesis, MK migration and subsequent compartmentalization in the BM. The observation that RhoA deficiency alters MK localization might be of relevance for other cell types, too which depend on locomotion in response to stimuli to fulfill their functions, e.g. immune cells.

As Dütting et al.[253] showed, the regulation of MK localization and transendothelial platelet biogenesis involves a Cdc42/RhoA regulatory circuit downstream of GPIb. Following up on this work, further detailed studies of potential up- and downstream regulators of the two GTPases in MKs will be required to decipher the signaling mechanism regulating platelet biogenesis in vivo.

In the future, a three dimensional (3D) matrix in vitro model of MK maturation and migration in the BM niche could be helpful, too, next to in vivo experiments, to monitor the localization/migration of MKs in response to various stimuli and help clarify which further small GTPases are involved in the process and what their spatiotemporal regulation might be. Notably, a recent study from David Stegner and colleagues using 3D in vivo imaging revealed that a distinction between an osteal and vascular niche is not conceivable in vivo. Their results show that MK progenitors and mature MKs are always in close contact with the BM sinusoids [34] leading to the revised model that thrombopoiesis is spatially regulated by the BM vasculature.

Regarding studies on RhoF in platelets and MKs, it could prove useful to create

a double knock-out of Cdc42 and RhoF in mice to investigate potential redundant functions of the two GTPases in thrombopoiesis and filopodia formation.

5. Summary

Platelets constitute the cellular component in hemostasis and play a crucial role in the physiological response to injuries the vessel wall to limit potential blood loss, but at the same time in pathological processes like plaque rupture due to atherosclerosis, where their activation and aggregation facilitates arterial thrombosis leading to ischemic stroke or myocardial infarction.

This work focuses on megakaryocyte physiology with a special interest in the description of the localization of MKs in the bone marrow in mice single-deficient of the small Rho GTPase RhoA or double-deficient for RhoA and Cdc42 – another important Rho GTPase in transgenic mice. The importance of Rho GTPases in platelet and megakaryocyte physiology has already been extensively investigated with RhoA being responsible for creation of focal adhesions and actomyosin contractions in platelets, whereas Cdc42 has been shown to be important for microtubule rearrangements in megakaryocytes in conjunction with Rac1. RhoA ko mice were generated and studied with regard to compartmentalization of megakaryocytes in the bone marrow, revealing the intraluminal presence of megakaryocytes in bone marrow sinusoids. In a next step, aggravation, confirmation or abolishment of this finding was studied in related mouse strains, namely a RhoA/Cdc42 and G_{12}/G_{13} (upstream regulators of RhoA activity) dko. Finally, RhoA ko mice treated with antibodies that block different specific surface receptors were studied in regard to MK compartmentalization.

In the second and smaller part of this thesis the role of RhoF, a Rho GTPase which has been postulated to be of importance in filopodia formation in addition to Cdc42, in platelet function was investigated by analyzing a RhoF ko mouse strain. Receptor expression, platelet activation, granule release and filopodia formation in response to various stimuli in RhoF-deficient platelets was studied, showing no significant difference compared to the wild-type.

Zusammenfassung

Blutplättchen stellen die zelluläre Komponente der Blutgerinnung und spielen eine entscheidende Rolle in der physiologischen Antwort auf Verletzungen der Gefäßwand, um etwaigen Blutverlust zu vermindern, aber gleichzeitig auch in pathologischen Prozessen wie durch Atherosklerose vermittelter Plaqueruptur bei denen ihre Aktivierung und Aggregation zu ischämischem Schlaganfall oder Myokardinfarkt führen kann.

Diese Arbeit beschäftigt sich mit Megakaryozyten, den Vorläuferzellen der Thrombozyten, mit besonderem Fokus auf der Beschreibung ihrer Verteilung im Knochenmark in Abhängigkeit von der Defizienz der kleinen Rho GTPase RhoA und der kombinierten Defizienz von RhoA und Cdc42 – einer anderen bedeutenden Rho GTPase in transgenen Mauslinien. Die Bedeutung der Rho GTPasen in der Megakaryopoiese und Thrombozytenphysiologie wurde bereits ausgiebig untersucht. So ist RhoA verantwortlich für die Schaffung fokaler Adhäsionen und die Kontraktilität des Aktin-Myosinapparates, wohingegen für Cdc42 zusammen mit Rac1 eine Bedeutung im Mikrotubuli Re-Arrangement in Megakaryozyten gezeigt werden konnte. RhoA defiziente Mäuse wurden generiert und die megakaryozytäre Kompartimentalisierung innerhalb des Knochenmarkssinusoide analysiert mit dem erfolgreichen Nachweis intraluminal gelegener Megakaryozyten. In einem nächsten Schritt wurden eine RhoA/Cdc42 doppeldefiziente und eine Mauslinie mit Doppeldefizienz in G_{12}/G_{13} (in der Signalkaskade oberhalb gelegene Regulatoren der RhoA Aktivität) auf eine Verstärkung, Bestätigung oder einen Verlust intraluminal gelegener Megakaryozyten untersucht. Letztlich wurden RhoA defiziente Mäuse mit verschiedenen, bestimmte Oberflächenrezeptorproteine blockierenden Antikörpern behandelt und der Einfluss auf die megakaryozytäre Kompartimentalisierung untersucht.

Ein zweiter, kleinerer Teil dieser Arbeit beschäftigte sich mit der Funktion von RhoF, einer kleinen Rho GTPase, von der angenommen wird neben Cdc42 für die Filopodienausbildung verantwortlich zu sein. Hierzu wurde eine RhoF-defiziente Mauslinie analysiert. Die Oberflächenrezeptorexpression, Aktivierung, Granulafreisetzung und Filopodienausbildung RhoF defizienter Blutplättchen in

Abhängigkeit verschiedener Stimuli wurde entsprechend untersucht, allerdings ohne Nachweis signifikanter Unterschiede zum Wildtyp.

6. References

1.   Nakeff A, Maat B. Separation of megakaryocytes from mouse bone marrow by velocity sedimentation. *Blood* 1974;43:591-595.

2.   Hartwig J, Italiano J, Jr. The birth of the platelet. *J Thromb Haemost* 2003;1:1580-1586.

3.   Machlus KR, Italiano JE, Jr. The incredible journey: From megakaryocyte development to platelet formation. *The Journal of cell biology* 2013;201:785-796.

4.   Bluteau D*, et al.* Regulation of megakaryocyte maturation and platelet formation. *J Thromb Haemost* 2009;7 Suppl 1:227-234.

5.   Hirata S*, et al.* Congenital amegakaryocytic thrombocytopenia iPS cells exhibit defective MPL-mediated signaling. *J Clin Invest* 2013;123:3802-3814.

6.   Dore LC, Crispino JD. Transcription factor networks in erythroid cell and megakaryocyte development. *Blood* 2011;118:231-239.

7.   Eto K, Kunishima S. Linkage between the mechanisms of thrombocytopenia and thrombopoiesis. *Blood* 2016;127:1234-1241.

8.   Kuvardina ON*, et al.* RUNX1 represses the erythroid gene expression program during megakaryocytic differentiation. *Blood* 2015;125:3570-3579.

9.   Nakamura S*, et al.* Expandable megakaryocyte cell lines enable clinically applicable generation of platelets from human induced pluripotent stem cells. *Cell Stem Cell* 2014;14:535-548.

10.   Zimmet J, Ravid K. Polyploidy: occurrence in nature, mechanisms, and significance for the megakaryocyte-platelet system. *Exp Hematol* 2000;28:3-16.

11.   Geddis AE, Fox NE, Tkachenko E, Kaushansky K. Endomitotic megakaryocytes that form a bipolar spindle exhibit cleavage furrow ingression followed by furrow regression. *Cell Cycle* 2007;6:455-460.

12.   Lordier L*, et al.* Megakaryocyte endomitosis is a failure of late cytokinesis

related to defects in the contractile ring and Rho/Rock signaling. *Blood* 2008;112:3164-3174.

13. Roy A*, et al.* Activity of nonmuscle myosin II isoforms determines localization at the cleavage furrow of megakaryocytes. *Blood* 2016;128:3137-3145.

14. Lordier L*, et al.* RUNX1-induced silencing of non-muscle myosin heavy chain IIB contributes to megakaryocyte polyploidization. *Nat Commun* 2012;3:717.

15. Pleines I, Nieswandt B. RhoA/ROCK guides NMII on the way to MK polyploidy. *Blood* 2016;128:3025-3026.

16. Melendez J*, et al.* RhoA GTPase is dispensable for actomyosin regulation but is essential for mitosis in primary mouse embryonic fibroblasts. *The Journal of biological chemistry* 2011;286:15132-15137.

17. Gao Y*, et al.* Role of RhoA-specific guanine exchange factors in regulation of endomitosis in megakaryocytes. *Dev Cell* 2012;22:573-584.

18. Pleines I*, et al.* Megakaryocyte-specific RhoA deficiency causes macrothrombocytopenia and defective platelet activation in hemostasis and thrombosis. *Blood* 2012;119:1054-1063.

19. Chen Z*, et al.* The May-Hegglin anomaly gene MYH9 is a negative regulator of platelet biogenesis modulated by the Rho-ROCK pathway. *Blood* 2007;110:171-179.

20. Leon C*, et al.* Megakaryocyte-restricted MYH9 inactivation dramatically affects hemostasis while preserving platelet aggregation and secretion. *Blood* 2007;110:3183-3191.

21. Kiel MJ, Yilmaz OH, Iwashita T, Yilmaz OH, Terhorst C, Morrison SJ. SLAM family receptors distinguish hematopoietic stem and progenitor cells and reveal endothelial niches for stem cells. *Cell* 2005;121:1109-1121.

22. Mendez-Ferrer S*, et al.* Mesenchymal and haematopoietic stem cells form a unique bone marrow niche. *Nature* 2010;466:829-834.

23. Calvi LM*, et al.* Osteoblastic cells regulate the haematopoietic stem cell niche. *Nature* 2003;425:841-846.

24. Greenbaum A*, et al.* CXCL12 in early mesenchymal progenitors is required for haematopoietic stem-cell maintenance. *Nature* 2013;495:227-230.

25. Kunisaki Y*, et al.* Arteriolar niches maintain haematopoietic stem cell

quiescence. *Nature* 2013;502:637-643.

26.   Pallotta I, Lovett M, Rice W, Kaplan DL, Balduini A. Bone marrow osteoblastic niche: a new model to study physiological regulation of megakaryopoiesis. *PLoS One* 2009;4:e8359.

27.   Malara A, Abbonante V, Di Buduo CA, Tozzi L, Currao M, Balduini A. The secret life of a megakaryocyte: emerging roles in bone marrow homeostasis control. *Cellular and molecular life sciences : CMLS* 2015;72:1517-1536.

28.   Niswander LM, Fegan KH, Kingsley PD, McGrath KE, Palis J. SDF-1 dynamically mediates megakaryocyte niche occupancy and thrombopoiesis at steady state and following radiation injury. *Blood* 2014;124:277-286.

29.   Avecilla ST*, et al.* Chemokine-mediated interaction of hematopoietic progenitors with the bone marrow vascular niche is required for thrombopoiesis. *Nat Med* 2004;10:64-71.

30.   Riviere C*, et al.* Phenotypic and functional evidence for the expression of CXCR4 receptor during megakaryocytopoiesis. *Blood* 1999;93:1511-1523.

31.   Berthebaud M*, et al.* RGS16 is a negative regulator of SDF-1-CXCR4 signaling in megakaryocytes. *Blood* 2005;106:2962-2968.

32.   Nurden A, Nurden P. Advances in our understanding of the molecular basis of disorders of platelet function. *J Thromb Haemost* 2011;9 Suppl 1:76-91.

33.   Sabri S*, et al.* Deficiency in the Wiskott-Aldrich protein induces premature proplatelet formation and platelet production in the bone marrow compartment. *Blood* 2006;108:134-140.

34.   Stegner D*, et al.* Thrombopoiesis is spatially regulated by the bone marrow vasculature. *Nat Commun* 2017;8:127.

35.   Yamada E. The fine structure of the megakaryocyte in the mouse spleen. *Acta Anat (Basel)* 1957;29:267-290.

36.   Radley JM, Haller CJ. The demarcation membrane system of the megakaryocyte: a misnomer? *Blood* 1982;60:213-219.

37.   Schulze H*, et al.* Characterization of the megakaryocyte demarcation membrane system and its role in thrombopoiesis. *Blood* 2006;107:3868-3875.

38.   Haddad E*, et al.* The thrombocytopenia of Wiskott Aldrich syndrome is not related to a defect in proplatelet formation. *Blood* 1999;94:509-518.

39. Chen Y, *et al.* Loss of the F-BAR protein CIP4 reduces platelet production by impairing membrane-cytoskeleton remodeling. *Blood* 2013;122:1695-1706.

40. Eckly A, *et al.* Biogenesis of the demarcation membrane system (DMS) in megakaryocytes. *Blood* 2014;123:921-930.

41. Italiano JE, Jr., Patel-Hett S, Hartwig JH. Mechanics of proplatelet elaboration. *J Thromb Haemost* 2007;5 Suppl 1:18-23.

42. Choi ES, Nichol JL, Hokom MM, Hornkohl AC, Hunt P. Platelets generated in vitro from proplatelet-displaying human megakaryocytes are functional. *Blood* 1995;85:402-413.

43. Italiano JE, Jr., Lecine P, Shivdasani RA, Hartwig JH. Blood platelets are assembled principally at the ends of proplatelet processes produced by differentiated megakaryocytes. *The Journal of cell biology* 1999;147:1299-1312.

44. Tablin F, Castro M, Leven RM. Blood platelet formation in vitro. The role of the cytoskeleton in megakaryocyte fragmentation. *J Cell Sci* 1990;97 (Pt 1):59-70.

45. Machlus KR, Thon JN, Italiano JE, Jr. Interpreting the developmental dance of the megakaryocyte: a review of the cellular and molecular processes mediating platelet formation. *British journal of haematology* 2014;165:227-236.

46. Patel SR, *et al.* Differential roles of microtubule assembly and sliding in proplatelet formation by megakaryocytes. *Blood* 2005;106:4076-4085.

47. Patel-Hett S, *et al.* Visualization of microtubule growth in living platelets reveals a dynamic marginal band with multiple microtubules. *Blood* 2008;111:4605-4616.

48. Kaushansky K. Determinants of platelet number and regulation of thrombopoiesis. *Hematology Am Soc Hematol Educ Program* 2009:147-152.

49. Suzuki A, *et al.* RhoA is essential for maintaining normal megakaryocyte ploidy and platelet generation. *PLoS One* 2013;8:e69315.

50. Gobbi G, *et al.* Proplatelet generation in the mouse requires PKCepsilon-dependent RhoA inhibition. *Blood* 2013;122:1305-1311.

51. Chang Y, *et al.* Proplatelet formation is regulated by the Rho/ROCK pathway. *Blood* 2007;109:4229-4236.

52. Pleines I*, et al.* Defective tubulin organization and proplatelet formation in murine megakaryocytes lacking Rac1 and Cdc42. *Blood* 2013;122:3178-3187.

53. Schwertz H*, et al.* Anucleate platelets generate progeny. *Blood* 2010;115:3801-3809.

54. Thon JN, Devine MT, Jurak Begonja A, Tibbitts J, Italiano JE, Jr. High-content live-cell imaging assay used to establish mechanism of trastuzumab emtansine (T-DM1)--mediated inhibition of platelet production. *Blood* 2012;120:1975-1984.

55. Howell WH, Donahue DD. The Production of Blood Platelets in the Lungs. *The Journal of experimental medicine* 1937;65:177-203.

56. Xiao da W, Yang M, Yang J, Hon KL, Fok FT. Lung damage may induce thrombocytopenia. *Platelets* 2006;17:347-349.

57. Fuentes R*, et al.* Infusion of mature megakaryocytes into mice yields functional platelets. *J Clin Invest* 2010;120:3917-3922.

58. Aspenstrom P, Fransson A, Saras J. Rho GTPases have diverse effects on the organization of the actin filament system. *The Biochemical journal* 2004;377:327-337.

59. Barbacid M. ras genes. *Annu Rev Biochem* 1987;56:779-827.

60. Madaule P, Axel R. A novel ras-related gene family. *Cell* 1985;41:31-40.

61. Ridley AJ. Rho family proteins: coordinating cell responses. *Trends Cell Biol* 2001;11:471-477.

62. Hall A. *Frontiers in Molecular Biology: GTPases* 2001. Oxford University Press.

63. Takai Y, Sasaki T, Matozaki T. Small GTP-binding proteins. *Physiol Rev* 2001;81:153-208.

64. Etienne-Manneville S, Hall A. Rho GTPases in cell biology. *Nature* 2002;420:629-635.

65. Ridley AJ. Rho GTPases and cell migration. *J Cell Sci* 2001;114:2713-2722.

66. Ridley AJ. Rho GTPase signalling in cell migration. *Current opinion in cell biology* 2015;36:103-112.

67. Sadok A, Marshall CJ. Rho GTPases: masters of cell migration. *Small GTPases* 2014;5:e29710.

68. Ridley AJ, Paterson HF, Johnston CL, Diekmann D, Hall A. The small GTP-binding protein rac regulates growth factor-induced membrane ruffling. *Cell* 1992;70:401-410.

69. Ridley AJ, Hall A. The small GTP-binding protein rho regulates the assembly of focal adhesions and actin stress fibers in response to growth factors. *Cell* 1992;70:389-399.

70. Nobes CD, Hall A. Rho, rac, and cdc42 GTPases regulate the assembly of multimolecular focal complexes associated with actin stress fibers, lamellipodia, and filopodia. *Cell* 1995;81:53-62.

71. Fransson A, Ruusala A, Aspenstrom P. Atypical Rho GTPases have roles in mitochondrial homeostasis and apoptosis. *The Journal of biological chemistry* 2003;278:6495-6502.

72. Heasman SJ, Ridley AJ. Mammalian Rho GTPases: new insights into their functions from in vivo studies. *Nat Rev Mol Cell Biol* 2008;9:690-701.

73. Aspenstrom P, Ruusala A, Pacholsky D. Taking Rho GTPases to the next level: the cellular functions of atypical Rho GTPases. *Exp Cell Res* 2007;313:3673-3679.

74. Rossman KL, Der CJ, Sondek J. GEF means go: turning on RHO GTPases with guanine nucleotide-exchange factors. *Nat Rev Mol Cell Biol* 2005;6:167-180.

75. Dovas A, Couchman JR. RhoGDI: multiple functions in the regulation of Rho family GTPase activities. *The Biochemical journal* 2005;390:1-9.

76. Tcherkezian J, Lamarche-Vane N. Current knowledge of the large RhoGAP family of proteins. *Biol Cell* 2007;99:67-86.

77. Chardin P. Function and regulation of Rnd proteins. *Nat Rev Mol Cell Biol* 2006;7:54-62.

78. Sorrentino S, Studt JD, Medalia O, Tanuj Sapra K. Roll, adhere, spread and contract: structural mechanics of platelet function. *Eur J Cell Biol* 2015;94:129-138.

79. Aslan JE, McCarty OJ. Rho GTPases in platelet function. *J Thromb Haemost* 2013;11:35-46.

80. Lannan KL*, et al.* Breaking the mold: transcription factors in the anucleate platelet and platelet-derived microparticles. *Front Immunol* 2015;6:48.

81. Lindsay CR, Edelstein LC. MicroRNAs in Platelet Physiology and Function. *Semin Thromb Hemost* 2016;42:215-222.

82. Schoenwaelder SM*, et al.* RhoA sustains integrin alpha IIbbeta 3 adhesion contacts under high shear. *The Journal of biological chemistry* 2002;277:14738-14746.

83. Martens L*, et al.* The human platelet proteome mapped by peptide-centric proteomics: a functional protein profile. *Proteomics* 2005;5:3193-3204.

84. Rowley JW*, et al.* Genome-wide RNA-seq analysis of human and mouse platelet transcriptomes. *Blood* 2011;118:e101-111.

85. Chardin P, Boquet P, Madaule P, Popoff MR, Rubin EJ, Gill DM. The mammalian G protein rhoC is ADP-ribosylated by Clostridium botulinum exoenzyme C3 and affects actin microfilaments in Vero cells. *EMBO J* 1989;8:1087-1092.

86. Sekine A, Fujiwara M, Narumiya S. Asparagine residue in the rho gene product is the modification site for botulinum ADP-ribosyltransferase. *The Journal of biological chemistry* 1989;264:8602-8605.

87. Stegner D, Nieswandt B. Platelet receptor signaling in thrombus formation. *J Mol Med (Berl)* 2011;89:109-121.

88. Klages B, Brandt U, Simon MI, Schultz G, Offermanns S. Activation of G12/G13 results in shape change and Rho/Rho-kinase-mediated myosin light chain phosphorylation in mouse platelets. *The Journal of cell biology* 1999;144:745-754.

89. Hart MJ*, et al.* Direct stimulation of the guanine nucleotide exchange activity of p115 RhoGEF by Galpha13. *Science (New York, NY)* 1998;280:2112-2114.

90. Li Z, Delaney MK, O'Brien KA, Du X. Signaling during platelet adhesion and activation. *Arterioscler Thromb Vasc Biol* 2010;30:2341-2349.

91. Suzuki Y*, et al.* Agonist-induced regulation of myosin phosphatase activity in human platelets through activation of Rho-kinase. *Blood* 1999;93:3408-3417.

92. Bauer M*, et al.* Dichotomous regulation of myosin phosphorylation and shape change by Rho-kinase and calcium in intact human platelets. *Blood* 1999;94:1665-1672.

93. Bodie SL, Ford I, Greaves M, Nixon GF. Thrombin-induced activation of RhoA in platelet shape change. *Biochem Biophys Res Commun*

2001;287:71-76.

94. Gong H*, et al.* G protein subunit Galpha13 binds to integrin alphaIIbbeta3 and mediates integrin "outside-in" signaling. *Science (New York, NY)* 2010;327:340-343.

95. Calaminus SD, Auger JM, McCarty OJ, Wakelam MJ, Machesky LM, Watson SP. MyosinIIa contractility is required for maintenance of platelet structure during spreading on collagen and contributes to thrombus stability. *J Thromb Haemost* 2007;5:2136-2145.

96. Didsbury J, Weber RF, Bokoch GM, Evans T, Snyderman R. rac, a novel ras-related family of proteins that are botulinum toxin substrates. *The Journal of biological chemistry* 1989;264:16378-16382.

97. Boureux A, Vignal E, Faure S, Fort P. Evolution of the Rho family of ras-like GTPases in eukaryotes. *Mol Biol Evol* 2007;24:203-216.

98. Jaffe AB, Hall A. Rho GTPases: biochemistry and biology. *Annual review of cell and developmental biology* 2005;21:247-269.

99. Montell DJ, Yoon WH, Starz-Gaiano M. Group choreography: mechanisms orchestrating the collective movement of border cells. *Nat Rev Mol Cell Biol* 2012;13:631-645.

100. Faroudi M*, et al.* Critical roles for Rac GTPases in T-cell migration to and within lymph nodes. *Blood* 2010;116:5536-5547.

101. Goggs R, Williams CM, Mellor H, Poole AW. Platelet Rho GTPases-a focus on novel players, roles and relationships. *The Biochemical journal* 2015;466:431-442.

102. Ridley AJ. Historical overview of Rho GTPases. *Methods Mol Biol* 2012;827:3-12.

103. Vidal C, Geny B, Melle J, Jandrot-Perrus M, Fontenay-Roupie M. Cdc42/Rac1-dependent activation of the p21-activated kinase (PAK) regulates human platelet lamellipodia spreading: implication of the cortical-actin binding protein cortactin. *Blood* 2002;100:4462-4469.

104. Bernard O. Lim kinases, regulators of actin dynamics. *The international journal of biochemistry & cell biology* 2007;39:1071-1076.

105. Vega FM, Fruhwirth G, Ng T, Ridley AJ. RhoA and RhoC have distinct roles in migration and invasion by acting through different targets. *The Journal of cell biology* 2011;193:655-665.

106. McCarty OJ*, et al.* Rac1 is essential for platelet lamellipodia formation and

aggregate stability under flow. *The Journal of biological chemistry* 2005;280:39474-39484.

107. Bialkowska K, Zaffran Y, Meyer SC, Fox JE. 14-3-3 zeta mediates integrin-induced activation of Cdc42 and Rac. Platelet glycoprotein Ib-IX regulates integrin-induced signaling by sequestering 14-3-3 zeta. *The Journal of biological chemistry* 2003;278:33342-33350.

108. Gratacap MP, Payrastre B, Nieswandt B, Offermanns S. Differential regulation of Rho and Rac through heterotrimeric G-proteins and cyclic nucleotides. *The Journal of biological chemistry* 2001;276:47906-47913.

109. Soulet C*, et al.* A differential role of the platelet ADP receptors P2Y1 and P2Y12 in Rac activation. *J Thromb Haemost* 2005;3:2296-2306.

110. Akbar H*, et al.* Genetic and pharmacologic evidence that Rac1 GTPase is involved in regulation of platelet secretion and aggregation. *J Thromb Haemost* 2007;5:1747-1755.

111. Aslan JE, Tormoen GW, Loren CP, Pang J, McCarty OJ. S6K1 and mTOR regulate Rac1-driven platelet activation and aggregation. *Blood* 2011;118:3129-3136.

112. Offermanns S, Toombs CF, Hu YH, Simon MI. Defective platelet activation in G alpha(q)-deficient mice. *Nature* 1997;389:183-186.

113. Welch HC, Coadwell WJ, Stephens LR, Hawkins PT. Phosphoinositide 3-kinase-dependent activation of Rac. *FEBS Lett* 2003;546:93-97.

114. McCarty OJ, Calaminus SD, Berndt MC, Machesky LM, Watson SP. von Willebrand factor mediates platelet spreading through glycoprotein Ib and alpha(IIb)beta3 in the presence of botrocetin and ristocetin, respectively. *J Thromb Haemost* 2006;4:1367-1378.

115. Pleines I*, et al.* Rac1 is essential for phospholipase C-gamma2 activation in platelets. *Pflugers Arch* 2009;457:1173-1185.

116. Nonne C*, et al.* Importance of platelet phospholipase Cgamma2 signaling in arterial thrombosis as a function of lesion severity. *Arterioscler Thromb Vasc Biol* 2005;25:1293-1298.

117. Li J, Luo R, Kowluru A, Li G. Novel regulation by Rac1 of glucose- and forskolin-induced insulin secretion in INS-1 beta-cells. *Am J Physiol Endocrinol Metab* 2004;286:E818-827.

118. Li Q*, et al.* Facilitation of Ca(2+)-dependent exocytosis by Rac1-GTPase in bovine chromaffin cells. *J Physiol* 2003;550:431-445.

119. Johnson DI, Pringle JR. Molecular characterization of CDC42, a Saccharomyces cerevisiae gene involved in the development of cell polarity. *The Journal of cell biology* 1990;111:143-152.

120. Polakis PG, Snyderman R, Evans T. Characterization of G25K, a GTP-binding protein containing a novel putative nucleotide binding domain. *Biochem Biophys Res Commun* 1989;160:25-32.

121. Tao W, Pennica D, Xu L, Kalejta RF, Levine AJ. Wrch-1, a novel member of the Rho gene family that is regulated by Wnt-1. *Genes Dev* 2001;15:1796-1807.

122. Neudauer CL, Joberty G, Tatsis N, Macara IG. Distinct cellular effects and interactions of the Rho-family GTPase TC10. *Curr Biol* 1998;8:1151-1160.

123. Kozma R, Ahmed S, Best A, Lim L. The Ras-related protein Cdc42Hs and bradykinin promote formation of peripheral actin microspikes and filopodia in Swiss 3T3 fibroblasts. *Mol Cell Biol* 1995;15:1942-1952.

124. Yang L, Wang L, Zheng Y. Gene targeting of Cdc42 and Cdc42GAP affirms the critical involvement of Cdc42 in filopodia induction, directed migration, and proliferation in primary mouse embryonic fibroblasts. *Mol Biol Cell* 2006;17:4675-4685.

125. Akbar H*, et al.* Gene targeting implicates Cdc42 GTPase in GPVI and non-GPVI mediated platelet filopodia formation, secretion and aggregation. *PLoS One* 2011;6:e22117.

126. Pula G, Poole AW. Critical roles for the actin cytoskeleton and cdc42 in regulating platelet integrin alpha2beta1. *Platelets* 2008;19:199-210.

127. Czuchra A*, et al.* Cdc42 is not essential for filopodium formation, directed migration, cell polarization, and mitosis in fibroblastoid cells. *Mol Biol Cell* 2005;16:4473-4484.

128. Goh WI, Sudhaharan T, Lim KB, Sem KP, Lau CL, Ahmed S. Rif-mDia1 interaction is involved in filopodium formation independent of Cdc42 and Rac effectors. *The Journal of biological chemistry* 2011;286:13681-13694.

129. Pellegrin S, Mellor H. The Rho family GTPase Rif induces filopodia through mDia2. *Curr Biol* 2005;15:129-133.

130. Gad AK, Aspenstrom P. Rif proteins take to the RhoD: Rho GTPases at the crossroads of actin dynamics and membrane trafficking. *Cellular signalling* 2010;22:183-189.

131. Passey S, Pellegrin S, Mellor H. What is in a filopodium? Starfish versus hedgehogs. *Biochem Soc Trans* 2004;32:1115-1117.

132. Zhang X, *et al.* Cdc42 interacts with the exocyst and regulates polarized secretion. *The Journal of biological chemistry* 2001;276:46745-46750.

133. Hong-Geller E, Cerione RA. Cdc42 and Rac stimulate exocytosis of secretory granules by activating the IP(3)/calcium pathway in RBL-2H3 mast cells. *The Journal of cell biology* 2000;148:481-494.

134. Dash D, Aepfelbacher M, Siess W. Integrin alpha IIb beta 3-mediated translocation of CDC42Hs to the cytoskeleton in stimulated human platelets. *The Journal of biological chemistry* 1995;270:17321-17326.

135. Azim AC, Barkalow K, Chou J, Hartwig JH. Activation of the small GTPases, rac and cdc42, after ligation of the platelet PAR-1 receptor. *Blood* 2000;95:959-964.

136. Higgs HN, Pollard TD. Activation by Cdc42 and PIP(2) of Wiskott-Aldrich syndrome protein (WASp) stimulates actin nucleation by Arp2/3 complex. *The Journal of cell biology* 2000;150:1311-1320.

137. Rohatgi R, *et al.* The interaction between N-WASP and the Arp2/3 complex links Cdc42-dependent signals to actin assembly. *Cell* 1999;97:221-231.

138. Tomasevic N, *et al.* Differential regulation of WASP and N-WASP by Cdc42, Rac1, Nck, and PI(4,5)P2. *Biochemistry* 2007;46:3494-3502.

139. Snapper SB, *et al.* N-WASP deficiency reveals distinct pathways for cell surface projections and microbial actin-based motility. *Nat Cell Biol* 2001;3:897-904.

140. Arias-Romero LE, Chernoff J. A tale of two Paks. *Biol Cell* 2008;100:97-108.

141. Peng J, Wallar BJ, Flanders A, Swiatek PJ, Alberts AS. Disruption of the Diaphanous-related formin Drf1 gene encoding mDia1 reveals a role for Drf3 as an effector for Cdc42. *Curr Biol* 2003;13:534-545.

142. Wang W, Eddy R, Condeelis J. The cofilin pathway in breast cancer invasion and metastasis. *Nat Rev Cancer* 2007;7:429-440.

143. Ng J, Luo L. Rho GTPases regulate axon growth through convergent and divergent signaling pathways. *Neuron* 2004;44:779-793.

144. Cory GO, Cullen PJ. Membrane curvature: the power of bananas, zeppelins and boomerangs. *Curr Biol* 2007;17:R455-457.

145. Bahou WF, Scudder L, Rubenstein D, Jesty J. A shear-restricted pathway of platelet procoagulant activity is regulated by IQGAP1. *The Journal of*

biological chemistry 2004;279:22571-22577.

146. Beck S, Fotinos A, Lang F, Gawaz M, Elvers M. Isoform-specific roles of the GTPase activating protein Nadrin in cytoskeletal reorganization of platelets. *Cellular signalling* 2013;25:236-246.

147. Elvers M, Beck S, Fotinos A, Ziegler M, Gawaz M. The GRAF family member oligophrenin1 is a RhoGAP with BAR domain and regulates Rho GTPases in platelets. *Cardiovasc Res* 2012;94:526-536.

148. Malarkannan S*, et al.* IQGAP1: a regulator of intracellular spacetime relativity. *J Immunol* 2012;188:2057-2063.

149. Pleines I*, et al.* Multiple alterations of platelet functions dominated by increased secretion in mice lacking Cdc42 in platelets. *Blood* 2010;115:3364-3373.

150. Yang L, Wang L, Geiger H, Cancelas JA, Mo J, Zheng Y. Rho GTPase Cdc42 coordinates hematopoietic stem cell quiescence and niche interaction in the bone marrow. *Proceedings of the National Academy of Sciences of the United States of America* 2007;104:5091-5096.

151. Yang L*, et al.* Cdc42 critically regulates the balance between myelopoiesis and erythropoiesis. *Blood* 2007;110:3853-3861.

152. Wu X*, et al.* Cdc42 is crucial for the establishment of epithelial polarity during early mammalian development. *Dev Dyn* 2007;236:2767-2778.

153. Yang FC*, et al.* Rac and Cdc42 GTPases control hematopoietic stem cell shape, adhesion, migration, and mobilization. *Proceedings of the National Academy of Sciences of the United States of America* 2001;98:5614-5618.

154. Moers A*, et al.* G13 is an essential mediator of platelet activation in hemostasis and thrombosis. *Nat Med* 2003;9:1418-1422.

155. Offermanns S. Activation of platelet function through G protein-coupled receptors. *Circ Res* 2006;99:1293-1304.

156. Ellis S, Mellor H. The novel Rho-family GTPase rif regulates coordinated actin-based membrane rearrangements. *Curr Biol* 2000;10:1387-1390.

157. Watkins NA*, et al.* A HaemAtlas: characterizing gene expression in differentiated human blood cells. *Blood* 2009;113:e1-9.

158. Gouw LG, Reading NS, Jenson SD, Lim MS, Elenitoba-Johnson KS. Expression of the Rho-family GTPase gene RHOF in lymphocyte subsets and malignant lymphomas. *British journal of haematology* 2005;129:531-533.

159. Lammers M, Meyer S, Kuhlmann D, Wittinghofer A. Specificity of interactions between mDia isoforms and Rho proteins. *The Journal of biological chemistry* 2008;283:35236-35246.

160. Fan L, Pellegrin S, Scott A, Mellor H. The small GTPase Rif is an alternative trigger for the formation of actin stress fibers in epithelial cells. *J Cell Sci* 2010;123:1247-1252.

161. Goggs R, Savage JS, Mellor H, Poole AW. The small GTPase Rif is dispensable for platelet filopodia generation in mice. *PLoS One* 2013;8:e54663.

162. Thomas SG, Calaminus SD, Machesky LM, Alberts AS, Watson SP. G-protein coupled and ITAM receptor regulation of the formin FHOD1 through Rho kinase in platelets. *J Thromb Haemost* 2011;9:1648-1651.

163. Swieringa F, Kuijpers MJ, Heemskerk JW, van der Meijden PE. Targeting platelet receptor function in thrombus formation: the risk of bleeding. *Blood reviews* 2014;28:9-21.

164. Savage B, Saldivar E, Ruggeri ZM. Initiation of platelet adhesion by arrest onto fibrinogen or translocation on von Willebrand factor. *Cell* 1996;84:289-297.

165. Li R, Emsley J. The organizing principle of the platelet glycoprotein Ib-IX-V complex. *J Thromb Haemost* 2013;11:605-614.

166. Ruggeri ZM, Orje JN, Habermann R, Federici AB, Reininger AJ. Activation-independent platelet adhesion and aggregation under elevated shear stress. *Blood* 2006;108:1903-1910.

167. Nesbitt WS*, et al.* A shear gradient-dependent platelet aggregation mechanism drives thrombus formation. *Nat Med* 2009;15:665-673.

168. Elvers M*, et al.* Impaired alpha(IIb)beta(3) integrin activation and shear-dependent thrombus formation in mice lacking phospholipase D1. *Sci Signal* 2010;3:ra1.

169. Ware J, Russell S, Ruggeri ZM. Generation and rescue of a murine model of platelet dysfunction: the Bernard-Soulier syndrome. *Proceedings of the National Academy of Sciences of the United States of America* 2000;97:2803-2808.

170. Kato K*, et al.* Genetic deletion of mouse platelet glycoprotein Ibbeta produces a Bernard-Soulier phenotype with increased alpha-granule size. *Blood* 2004;104:2339-2344.

171. Wu D, *et al.* Inhibition of the von Willebrand (VWF)-collagen interaction by an antihuman VWF monoclonal antibody results in abolition of in vivo arterial platelet thrombus formation in baboons. *Blood* 2002;99:3623-3628.

172. Kleinschnitz C, Pozgajova M, Pham M, Bendszus M, Nieswandt B, Stoll G. Targeting platelets in acute experimental stroke: impact of glycoprotein Ib, VI, and IIb/IIIa blockade on infarct size, functional outcome, and intracranial bleeding. *Circulation* 2007;115:2323-2330.

173. Kleinschnitz C, *et al.* Deficiency of von Willebrand factor protects mice from ischemic stroke. *Blood* 2009;113:3600-3603.

174. Nieswandt B, Watson SP. Platelet-collagen interaction: is GPVI the central receptor? *Blood* 2003;102:449-461.

175. Watson SP, Herbert JM, Pollitt AY. GPVI and CLEC-2 in hemostasis and vascular integrity. *J Thromb Haemost* 2010;8:1456-1467.

176. Lecut C, *et al.* Principal role of glycoprotein VI in alpha2beta1 and alphaIIbbeta3 activation during collagen-induced thrombus formation. *Arterioscler Thromb Vasc Biol* 2004;24:1727-1733.

177. Massberg S, *et al.* A crucial role of glycoprotein VI for platelet recruitment to the injured arterial wall in vivo. *The Journal of experimental medicine* 2003;197:41-49.

178. Konishi H, *et al.* Platelets activated by collagen through immunoreceptor tyrosine-based activation motif play pivotal role in initiation and generation of neointimal hyperplasia after vascular injury. *Circulation* 2002;105:912-916.

179. Holtkotter O, *et al.* Integrin alpha 2-deficient mice develop normally, are fertile, but display partially defective platelet interaction with collagen. *The Journal of biological chemistry* 2002;277:10789-10794.

180. Gruner S, *et al.* Anti-glycoprotein VI treatment severely compromises hemostasis in mice with reduced alpha2beta1 levels or concomitant aspirin therapy. *Circulation* 2004;110:2946-2951.

181. Suzuki-Inoue K, *et al.* A novel Syk-dependent mechanism of platelet activation by the C-type lectin receptor CLEC-2. *Blood* 2006;107:542-549.

182. May F, *et al.* CLEC-2 is an essential platelet-activating receptor in hemostasis and thrombosis. *Blood* 2009;114:3464-3472.

183. Lewandrowski U, *et al.* Platelet membrane proteomics: a novel repository for functional research. *Blood* 2009;114:e10-19.

184. Wong C*, et al.* CEACAM1 negatively regulates platelet-collagen interactions and thrombus growth in vitro and in vivo. *Blood* 2009;113:1818-1828.

185. Murugappa S, Kunapuli SP. The role of ADP receptors in platelet function. *Front Biosci* 2006;11:1977-1986.

186. Hechler B*, et al.* The P2Y1 receptor is necessary for adenosine 5'-diphosphate-induced platelet aggregation. *Blood* 1998;92:152-159.

187. Leon C*, et al.* Defective platelet aggregation and increased resistance to thrombosis in purinergic P2Y(1) receptor-null mice. *J Clin Invest* 1999;104:1731-1737.

188. Hechler B*, et al.* A role of the fast ATP-gated P2X1 cation channel in thrombosis of small arteries in vivo. *The Journal of experimental medicine* 2003;198:661-667.

189. Oury C, Toth-Zsamboki E, Vermylen J, Hoylaerts MF. P2X(1)-mediated activation of extracellular signal-regulated kinase 2 contributes to platelet secretion and aggregation induced by collagen. *Blood* 2002;100:2499-2505.

190. Holmsen H. Prostaglandin endoperoxide--thromboxane synthesis and dense granule secretion as positive feedback loops in the propagation of platelet responses during "the basic platelet reaction". *Thrombosis and haemostasis* 1977;38:1030-1041.

191. Thomas DW*, et al.* Coagulation defects and altered hemodynamic responses in mice lacking receptors for thromboxane A2. *J Clin Invest* 1998;102:1994-2001.

192. Nakanishi-Matsui M, Zheng YW, Sulciner DJ, Weiss EJ, Ludeman MJ, Coughlin SR. PAR3 is a cofactor for PAR4 activation by thrombin. *Nature* 2000;404:609-613.

193. Kahn ML*, et al.* A dual thrombin receptor system for platelet activation. *Nature* 1998;394:690-694.

194. Kahn ML, Nakanishi-Matsui M, Shapiro MJ, Ishihara H, Coughlin SR. Protease-activated receptors 1 and 4 mediate activation of human platelets by thrombin. *J Clin Invest* 1999;103:879-887.

195. Leger AJ*, et al.* Blocking the protease-activated receptor 1-4 heterodimer in platelet-mediated thrombosis. *Circulation* 2006;113:1244-1254.

196. Sambrano GR, Weiss EJ, Zheng YW, Huang W, Coughlin SR. Role of thrombin signalling in platelets in haemostasis and thrombosis. *Nature*

2001;413:74-78.

197.   Hamilton JR, Cornelissen I, Coughlin SR. Impaired hemostasis and protection against thrombosis in protease-activated receptor 4-deficient mice is due to lack of thrombin signaling in platelets. *J Thromb Haemost* 2004;2:1429-1435.

198.   Jackson SF, Schoenwaelder SM. Type I phosphoinositide 3-kinases: potential antithrombotic targets? *Cellular and molecular life sciences : CMLS* 2006;63:1085-1090.

199.   Puri RN. Phospholipase A2: its role in ADP- and thrombin-induced platelet activation mechanisms. *The international journal of biochemistry & cell biology* 1998;30:1107-1122.

200.   Schwarz UR, Walter U, Eigenthaler M. Taming platelets with cyclic nucleotides. *Biochem Pharmacol* 2001;62:1153-1161.

201.   Jackson SP*, et al.* PI 3-kinase p110beta: a new target for antithrombotic therapy. *Nat Med* 2005;11:507-514.

202.   Hirsch E*, et al.* Resistance to thromboembolism in PI3Kgamma-deficient mice. *FASEB J* 2001;15:2019-2021.

203.   Clayton E*, et al.* A crucial role for the p110delta subunit of phosphatidylinositol 3-kinase in B cell development and activation. *The Journal of experimental medicine* 2002;196:753-763.

204.   Senis YA*, et al.* Role of the p110delta PI 3-kinase in integrin and ITAM receptor signalling in platelets. *Platelets* 2005;16:191-202.

205.   Harbeck B, Huttelmaier S, Schluter K, Jockusch BM, Illenberger S. Phosphorylation of the vasodilator-stimulated phosphoprotein regulates its interaction with actin. *The Journal of biological chemistry* 2000;275:30817-30825.

206.   Horstrup K, Jablonka B, Honig-Liedl P, Just M, Kochsiek K, Walter U. Phosphorylation of focal adhesion vasodilator-stimulated phosphoprotein at Ser157 in intact human platelets correlates with fibrinogen receptor inhibition. *Eur J Biochem* 1994;225:21-27.

207.   Bennett JS, Zigmond S, Vilaire G, Cunningham ME, Bednar B. The platelet cytoskeleton regulates the affinity of the integrin alpha(IIb)beta(3) for fibrinogen. *The Journal of biological chemistry* 1999;274:25301-25307.

208.   Chen M, Stracher A. In situ phosphorylation of platelet actin-binding protein by cAMP-dependent protein kinase stabilizes it against proteolysis by calpain. *The Journal of biological chemistry* 1989;264:14282-14289.

209. Fox JE, Berndt MC. Cyclic AMP-dependent phosphorylation of glycoprotein Ib inhibits collagen-induced polymerization of actin in platelets. *The Journal of biological chemistry* 1989;264:9520-9526.

210. Hughan SC*, et al.* Selective impairment of platelet activation to collagen in the absence of GATA1. *Blood* 2005;105:4369-4376.

211. Chen H, Locke D, Liu Y, Liu C, Kahn ML. The platelet receptor GPVI mediates both adhesion and signaling responses to collagen in a receptor density-dependent fashion. *The Journal of biological chemistry* 2002;277:3011-3019.

212. Nieswandt B*, et al.* Glycoprotein VI but not alpha2beta1 integrin is essential for platelet interaction with collagen. *EMBO J* 2001;20:2120-2130.

213. Nurden AT. Glanzmann thrombasthenia. *Orphanet J Rare Dis* 2006;1:10.

214. Suh TT*, et al.* Resolution of spontaneous bleeding events but failure of pregnancy in fibrinogen-deficient mice. *Genes Dev* 1995;9:2020-2033.

215. Nurden AT, Pillois X, Fiore M, Heilig R, Nurden P. Glanzmann thrombasthenia-like syndromes associated with Macrothrombocytopenias and mutations in the genes encoding the alphaIIbbeta3 integrin. *Semin Thromb Hemost* 2011;37:698-706.

216. Ruggeri ZM, Dent JA, Saldivar E. Contribution of distinct adhesive interactions to platelet aggregation in flowing blood. *Blood* 1999;94:172-178.

217. Brass LF, Zhu L, Stalker TJ. Minding the gaps to promote thrombus growth and stability. *J Clin Invest* 2005;115:3385-3392.

218. Kasirer-Friede A, Ruggeri ZM, Shattil SJ. Role for ADAP in shear flow-induced platelet mechanotransduction. *Blood* 2010;115:2274-2282.

219. Lee HS, Lim CJ, Puzon-McLaughlin W, Shattil SJ, Ginsberg MH. RIAM activates integrins by linking talin to ras GTPase membrane-targeting sequences. *The Journal of biological chemistry* 2009;284:5119-5127.

220. Nieswandt B*, et al.* Loss of talin1 in platelets abrogates integrin activation, platelet aggregation, and thrombus formation in vitro and in vivo. *The Journal of experimental medicine* 2007;204:3113-3118.

221. Petrich BG*, et al.* Talin is required for integrin-mediated platelet function in hemostasis and thrombosis. *The Journal of experimental medicine* 2007;204:3103-3111.

222.   Honda A*, et al.* Phosphatidylinositol 4-phosphate 5-kinase alpha is a downstream effector of the small G protein ARF6 in membrane ruffle formation. *Cell* 1999;99:521-532.

223.   Moser M, Nieswandt B, Ussar S, Pozgajova M, Fassler R. Kindlin-3 is essential for integrin activation and platelet aggregation. *Nat Med* 2008;14:325-330.

224.   Malinin NL*, et al.* A point mutation in KINDLIN3 ablates activation of three integrin subfamilies in humans. *Nat Med* 2009;15:313-318.

225.   Svensson L*, et al.* Leukocyte adhesion deficiency-III is caused by mutations in KINDLIN3 affecting integrin activation. *Nat Med* 2009;15:306-312.

226.   Moser M*, et al.* Kindlin-3 is required for beta2 integrin-mediated leukocyte adhesion to endothelial cells. *Nat Med* 2009;15:300-305.

227.   Nieswandt B*, et al.* Long-term antithrombotic protection by in vivo depletion of platelet glycoprotein VI in mice. *The Journal of experimental medicine* 2001;193:459-469.

228.   Nieswandt B, Bergmeier W, Rackebrandt K, Gessner JE, Zirngibl H. Identification of critical antigen-specific mechanisms in the development of immune thrombocytopenic purpura in mice. *Blood* 2000;96:2520-2527.

229.   Bergmeier W, Schulte V, Brockhoff G, Bier U, Zirngibl H, Nieswandt B. Flow cytometric detection of activated mouse integrin alphaIIbbeta3 with a novel monoclonal antibody. *Cytometry* 2002;48:80-86.

230.   Gruner S*, et al.* Multiple integrin-ligand interactions synergize in shear-resistant platelet adhesion at sites of arterial injury in vivo. *Blood* 2003;102:4021-4027.

231.   Nieswandt B*, et al.* Acute systemic reaction and lung alterations induced by an antiplatelet integrin gpIIb/IIIa antibody in mice. *Blood* 1999;94:684-693.

232.   Jackson B*, et al.* RhoA is dispensable for skin development, but crucial for contraction and directed migration of keratinocytes. *Mol Biol Cell* 2011;22:593-605.

233.   Tiedt R, Schomber T, Hao-Shen H, Skoda RC. Pf4-Cre transgenic mice allow the generation of lineage-restricted gene knockouts for studying megakaryocyte and platelet function in vivo. *Blood* 2007;109:1503-1506.

234.   Hirayama Y*, et al.* Concentrations of thrombopoietin in bone marrow in

normal subjects and in patients with idiopathic thrombocytopenic purpura, aplastic anemia, and essential thrombocythemia correlate with its mRNA expression of bone marrow stromal cells. *Blood* 1998;92:46-52.

235. Dutting S, Bender M, Nieswandt B. Platelet GPVI: a target for antithrombotic therapy?! *Trends Pharmacol Sci* 2012;33:583-590.

236. Suzuki-Inoue K, Inoue O, Ozaki Y. Novel platelet activation receptor CLEC-2: from discovery to prospects. *J Thromb Haemost* 2011;9 Suppl 1:44-55.

237. De Candia E. Mechanisms of platelet activation by thrombin: a short history. *Thrombosis research* 2012;129:250-256.

238. Ni H, Freedman J. Platelets in hemostasis and thrombosis: role of integrins and their ligands. *Transfus Apher Sci* 2003;28:257-264.

239. Xu XR*, et al.* Platelets and platelet adhesion molecules: novel mechanisms of thrombosis and anti-thrombotic therapies. *Thrombosis journal* 2016;14:29.

240. Tao L, Zhang Y, Xi X, Kieffer N. Recent advances in the understanding of the molecular mechanisms regulating platelet integrin alphaIIbbeta3 activation. *Protein & cell* 2010;1:627-637.

241. Dai B*, et al.* Integrin-alphaIIbbeta3-mediated outside-in signalling activates a negative feedback pathway to suppress platelet activation. *Thrombosis and haemostasis* 2016;116.

242. Yuan Y*, et al.* The von Willebrand factor-glycoprotein Ib/V/IX interaction induces actin polymerization and cytoskeletal reorganization in rolling platelets and glycoprotein Ib/V/IX-transfected cells. *The Journal of biological chemistry* 1999;274:36241-36251.

243. Melamed MR, Cliffton EE, Mercer C, Koss LG. The megakaryocyte blood count. *Am J Med Sci* 1966;252:301-309.

244. Kaufman RM, Airo R, Pollack S, Crosby WH. Circulating megakaryocytes and platelet release in the lung. *Blood* 1965;26:720-731.

245. Pedersen NT. The pulmonary vessels as a filter for circulating megakaryocytes in rats. *Scand J Haematol* 1974;13:225-231.

246. Trowbridge EA, Martin JF, Slater DN. Evidence for a theory of physical fragmentation of megakaryocytes, implying that all platelets are produced in the pulmonary circulation. *Thrombosis research* 1982;28:461-475.

247. Eckly A*, et al.* Abnormal megakaryocyte morphology and proplatelet

formation in mice with megakaryocyte-restricted MYH9 inactivation. *Blood* 2009;113:3182-3189.

248.   Nishimura S*, et al.* IL-1alpha induces thrombopoiesis through megakaryocyte rupture in response to acute platelet needs. *The Journal of cell biology* 2015;209:453-466.

249.   Ng AP*, et al.* Mpl expression on megakaryocytes and platelets is dispensable for thrombopoiesis but essential to prevent myeloproliferation. *Proceedings of the National Academy of Sciences of the United States of America* 2014;111:5884-5889.

250.   Nakamura-Ishizu A, Takubo K, Kobayashi H, Suzuki-Inoue K, Suda T. CLEC-2 in megakaryocytes is critical for maintenance of hematopoietic stem cells in the bone marrow. *The Journal of experimental medicine* 2015;212:2133-2146.

251.   Sanjuan-Pla A*, et al.* Platelet-biased stem cells reside at the apex of the haematopoietic stem-cell hierarchy. *Nature* 2013;502:232-236.

252.   Yamamoto R*, et al.* Clonal analysis unveils self-renewing lineage-restricted progenitors generated directly from hematopoietic stem cells. *Cell* 2013;154:1112-1126.

253.   Dutting S*, et al.* A Cdc42/RhoA regulatory circuit downstream of glycoprotein Ib guides transendothelial platelet biogenesis. *Nat Commun* 2017;8:15838.

254.   Semeniak D*, et al.* Proplatelet formation is selectively inhibited by collagen type I through Syk-independent GPVI signaling. *J Cell Sci* 2016;129:3473-3484.

7. Appendix

7.1 Abbreviations

3D	three dimensional
ADP	adenosine nucleotide diphosphate
AMR	Ashwell-Morrell receptor
Arp	actin related protein
ATP	adenosine nucleotide triphosphate
BD	Becton Dickinson
BSA	bovine serum albumin
C	Celsius
c-Src	cellular Sarcoma kinase
CalDAG-GEF1	Ca^{2+} and diacylglycerol-regulated guanine nucleotide exchange factor 1
cAMP	cyclic adenosine monophosphate
CAMT	congenital amegakaryocytic thrombocytopenia
Cdc42	cell division cycle protein 42
cGMP	cyclic guanosine monophosphate
CIP4	cdc42-interacting protein 4
CRP	collagen-related peptide
CVX	convulxin
DAG	diacylglycerol
ddH$_2$O	double-distilled water
DIC	differential interference contrast
dko	double knock-out
DMS	demarcation membrane system
DNA	deoxyribonucleic acid
DOCK	dedicator of cytokinesis protein

e.g.	example given
EB3	end-binding protein 3
ECM	extracellular matrix
EDTA	ethylenediaminetetraacetic acid
et al.	et alteri
EtOH	ethanol
FACS	Fluorescence activated cell sorting
FcR	Fc receptor
fg	fibrinogen
FGF-4	fibroblast growth factor-4
fig	figure
fl	flox
FLC	fetal liver cells
FLI1	Friend leukemia virus integration 1
FOG	Friend of GATA
G6b-B	G6b-B receptor of the Immunoglobulin superfamily
GAP	GTPase-activating protein
GATA	GATA transcription factor
GDI	guanine nucleotide-dissociation inhibitor
GDP	guanine nucleotide diphosphate
GEF	guanine nucleotide triphosphate exchange factor
GP	glycoprotein
GPCR	G-protein coupled receptor
GPCR	G-Protein coupled receptor
GTP	guanine nucleotide triphosphate
GTPase	guanine nucleotide triphosphate hydrolase
H_2O_2	hydrogen peroxide

HE	hematoxylin and eosin
HRP	horse radish peroxidase
HSC	hematopoietic stem cell
i.e.	id est, that is
i.p.	intraperitoneally
i.v.	intravenously
IHC	immunohistochemistry
IL	interleukin
IL	interleukin
IP$_3$	inositol 1,4,5-triphosphate
IQGAP1/2	IQ-domain containing GAP 1/2
IRSp53	insulin-receptor substrate p53
ITIM	immunoreceptor tyrosine-based inhibition motif
IVS	invaginated membrane system
JAK	Janus kinase
KLF1	Kruppel-like factor 1
ko	knock-out
LIMK	LIM kinase
mab	monoclonal antibody
MAPK	mitogen activated protein kinase
mDia	mammalian diaphanous
ME-P	megakaryocyte/erythroid-progenitor
min	minute
MK	megakaryocyte
MK-P	megakaryocyte-progenitor
MMP	matrix metalloprotease
Mpl	Myeloproliferative Leukemia Protein
MVS	multivesicular bodies
MYH	myosin heavy chain
N-WASP	neuronal-Wiskott-Aldrich syndrome

	protein
nonmuscle myosin	NM
OPHN1	oligophrenin
P-Rex	phosphatidylinositol 3,4,5-trisphosphate-dependent Rac exchanger
PAK	p21-activated kinase
PAR	protease-activated receptor
PBS	phosphate buffered saline
PCR	polymerase chain reaction
PECAM-1	Platelet Endothelial Cell Adhesion Molecule-1
PF-4	platelet factor-4
PFA	paraformaldehyde
PGE$_1$	prostaglandin E1
PGI$_2$	prostacyclin
PI3K	phosphatidyl inositol 3 kinase
PKC	protein kinase C
plt	platelet
prp	platelet rich plasma
Rac1	Ras-related C3 botulinum toxin substrate 1
Ras	rat sarcoma
RC	rhodocytin
RhoA	Ras homologue A
RIAM	Rap1-interacting adaptor molecule
ROCK	Rho-associated protein kinase
rpm	rounds per minute
RT	room temperature
Runx	runt-related transcription factor
S1P	sphingosine 1-phosphate

Scar	suppressor of cyclic AMP receptor
SCF	stem cell factor
SDF-1	stromal cell-derived factor 1
sec	second
SFK	Src family kinase
Shp	SH2 domain-containing protein phosphatase
STAT	Signal Transducer and Activator of Transcription
TBS	Tris buffered saline
TEM	transmission electron microscopy
TIAM	T-cell Lymphoma Invasion and Metastasis protein
TP	thromboxane-prostanoid
TPO	thrombopoietin
TRAP	thrombin receptor-activating peptide
TxA2	thromboxane A2
U-46	U-46619
VASP	vasodilator-stimulated phosphoprotein
Vav	onc F proto-oncogene
VCAM	vascular cell adhesion molecule
VEGFR	vascular endothelial growth factor receptor
VLA	very late antigen
vol	volume
vWF	von Willebrand Factor
WASP	Wiskott-Aldrich syndrome protein
WAVE	WASP-family Verprolin homologous
wt	wild-type
β-PIX	Rho guanine nucleotide exchange

	factor (GEF) 7b

7.3 Publication

Kleinschmidt D, Giannou AD, McGee HM, Kempski J, Steglich B, Huber FJ, Ernst TM, Shiri AM, Wegscheid C, Tasika E, Hübener P, **Huber P**, Bedke T, Steffens N, Agalioti T, Fuchs T, Noll J, Lotter H, Tiegs G, Lohse AW, Axelrod JH, Galun E, Flavell RA, Gagliani N, Huber S. A Protective Function of IL-22BP in Ischemia Reperfusion and Acetaminophen-Induced Liver Injury. *J Immunol.* 2017 Dec 15;199(12):4078-4090.

7.4 Acknowledgements

7.5 Affidavit

I hereby confirm that my thesis entitled "Megakaryocyte localization in the bone marrow depending on the knock-out of small Rho GTPases" is the result of my own work. I did not receive any help or support from commercial consultants. All sources and/or materials applied are listed and specified in the thesis.

Furthermore, I confirm that this thesis has not yet been submitted as part of another examination process neither in identical nor in similar form.

Wuerzburg, February 2019   …………………………………………….

                                                            Philipp Huber

Eidesstattliche Erklärung

Hiermit erkläre ich an Eides statt, die Dissertation „Megakaryozytenlokalisation im Knochenmark in Abhängigkeit der Defizienz von kleinen Rho GTPasen" eigenständig, d.h. insbesondere selbständig und ohne Hilfe eines kommerziellen Promotionsberaters, angefertigt und keine anderen als die von mir angegebenen Quellen und Hilfsmittel verwendet zu haben.

Ich erkläre außerdem, dass die Dissertation weder in gleicher noch in ähnlicher Form bereits in einem anderen Prüfungsverfahren vorgelegen hat.

Würzburg, Februar 2019   …………………………………………….

                                                            Philipp Huber